Evaluating drug delivery to the lung using polyamine ion-pairs

Mohamed Sofian, Zarif Bin

Awarding institution:
King's College London

Evaluating drug delivery to the lung using polyamine ion-pairs

Zarif Mohamed Sofian

In fulfilment of the requirement
for the degree of Doctor of Philosophy (PhD)
in Pharmaceutical Science

Institute of Pharmaceutical Science
King's College London

2018

Buat abah dan arwah mak
Mohamed Sofian Talib
Sofiah Awang (1952-2014) Al-fatihah

Acknowledgement

First and foremost, I would like to express my gratitude to my supervisors for their continuous support and guidance throughout this 4-year journey. I am extremely grateful to Dr. Stuart Jones for his encouragement and constructive advice which has inspired and motivated me to achieve the projects full potential. I am very thankful to Dr. Paul Royall for his valuable advice and motivational encouragement. I would like to thank Dr. Arcadia Woods for her assistance in keeping the project's momentum going during Dr. Jones year away. I am thankful to Prof. Ben Forbes for his expert biology advise. Many thanks to Dr. David Barlow for his kind help with the 3D modelling technique. To my fellow PhD students and technical staff at Franklin-Wilkins Building, Waterloo campus (3rd and 5th floors), thank you for all the help and friendship. Many thanks to all my Malaysian friends in London for making this journey memorable. Not to forget, much love to my family for their understanding and continuous support, emotionally and financially. Last but not least, I would like to thank Majlis Amanah Rakyat (MARA), Malaysia for the PhD sponsorship.

List of publications

Journal articles

Zarif M. Sofian, Paul G. Royall, Ben Forbes, Faiza Benaouda, David Barlow, Yuan L, Wang J. T, Khuloud T. Jamal, Stuart A Jones. An improved lung targeting of polyamine ion-pair using cyclodextrin complexes: In-vitro and in-vivo assessments. Intended journal submission: Journal of Controlled Release (*in preparation*).

Zarif M. Sofian, Paul G. Royall, Ben Forbes, Stuart A. Jones. Temporally diminishing P-gp drug efflux through the formation of polyamine ion-pairs. Intended journal submission: Molecular Pharmaceutics (*in preparation*).

Abstract

Zarif M. Sofian, Arcadia Woods, Paul G. Royall, Stuart A. Jones. Polyamine ion-pairs to target drugs to the lung. Drug Delivery to the Lung (DDL 27), Edinburgh 2016.

Abstract

Specific ligand targeting has been shown to facilitate drug transport across biological membranes. The aim of this PhD was to investigate whether ion-pairing a drug (theophylline) with a polyamine transporter system (PTS) substrate (polyamine) could actively target drug delivery into the lungs from the pulmonary circulation. To try and achieve this, cyclodextrins were used in a co-solvent to engineer a physically stable cyclodextrin-ion-pair complex. FT-IR and HPLC binding assays showed that theophylline (THE) bound most tightly to spermine (SP) (THE-SP: $pK_{FT\text{-}IR} = 1.96 \pm 0.04$, $pK_{HPLC} = 2.81 \pm 0.06$) than to spermidine (SPD) (THE-SPD: $pK_{FT\text{-}IR} = 1.93 \pm 0.05$, $pK_{HPLC} = 2.79 \pm 0.065$) followed by ethylenediamine (EDA) (THE-EDA: $pK_{FT\text{-}IR} = 1.43 \pm 0.02$, $pK_{HPLC} = 2.49 \pm 0.05$) and the least with ethylamine (EA) (THE-EA: $pK_{FT\text{-}IR} = 1.32 \pm 0.04$, $pK_{HPLC} = 2.43 \pm 0.042$). Ion-pairing theophylline with the counter-ions significantly increased the drug's solubility and reduced its lipophilicity. The formation of 1:1 cyclodextrin/[theophylline-spermine] ion-pair complexes were confirmed by NMR. Reducing the dielectric constant of the vehicle was found to increase the binding affinity of theophylline to spermine ($pK_{THE\text{-}SP}$ in 70 % PG: $pK_{THE\text{-}SP} = 2.11 \pm 0.045 > pK_{THE\text{-}SP}$ in 10% EtOH: $2.05 \pm 0.053 > pK_{THE\text{-}SP}$ in water: 1.96 ± 0.06) when assayed with FT-IR. However, it was found that the ion-pair, regardless of the vehicle used or when complexed with cyclodextrins, dissociated rapidly when the pH of the solution was dropped to 7.4. The theophylline-spermine uptake in A549 showed that the PTS was involved in the membrane transport of the drug. In addition, a sustained delivery of theophylline was achieved when cyclodextrin was complexed with the ion-pair, which suggested cyclodextrins could stabilize the ion-pair association. Hence, a cyclodextrin-theophylline-spermine complex described herein represents a potential for lung targeting delivery.

Table of Contents

CHAPTER 3: CYCLODEXTRIN-THEOPHYLLINE-POLYAMINE COMPLEXES

CHAPTER 4: EFFECT OF CO-SOLVENT ON THE COMPLEX STABILITY AND pH-INDUCED DISSOCIATION OF THEOPHYLLINE-POLYAMINE ION-PAIR

List of Figures

List of Tables

List of equations

List of abbreviations

ANOVA	Analysis of variance
API	Active pharmaceutical ingredient
βCD	Beta-cyclodextrin
CDs	Cyclodextrins
D_2O	Deuterium oxide
DMSO	Dimethyl sulfoxide
DOX	Doxorubicin
EA	Ethylamine
EDA	Ethylenediamine
EtOH	Ethanol
FBS	Fetal bovine serum
FDA	Food and drug administration
FT-IR	Fourier transform infrared
γCD	Gamma-cyclodextrin
HBSS	Hank's balanced salt solution
HCl	Hydrochloric acid
HPLC	High performance liquid chromatography
HPβCD	2-hydroxypropyl beta-cyclodextrin
LOD	Limit of detection
LOQ	Limit of quantification
MTT	3-(4,5-Dimethylthiazol-2-yl)-2,5-diphenyltetrazolium bromide
MW	Molecular weight
NP	Nanoparticle
NOE	Nuclear overhauser effect
ppm	Parts per million
PG	Propylene glycol
P-gp	P-glycoprotein
PTS	Polyamine transport system
^{1}H-NMR	Proton nuclear magnetic resonance
ROESY	Rotating-frame nuclear overhauser effect correlation spectroscopy
NaCl	Sodium chloride

NaOH	Sodium hydroxide
SD	Standard deviation
SEM	Standard error mean
SPD	Spermidine
SP	Spermine
THE	Theophylline
IC_{50}	The half maximal inhibitory concentration
UV-Vis	Ultra violet visible

CHAPTER 1
INTRODUCTION

1.0 General introduction

The development of a new active pharmaceutical ingredient (API) is very expensive (estimated in excess cost of USD 1 billion) and time-consuming (Hughes et al. 2011; Fortunak et al. 2014). This can be seen in the case of acetaminophen or better known as paracetamol which is currently the most widely used drug worldwide for its painkilling properties. Paracetamol was first discovered in late 1800's but was only available commercially in the market in the mid of 1950's (Brune et al. 2015). Considering this fact, scientists often resort to reformulating the "old" drugs using different strategies with the aim to optimize their therapeutic efficacy. However, the main obstacle remains on how to deliver the active therapeutic agents effectively to the target sites with minimal or no side-effects. Drug delivery using traditional administration approaches is often characterized by non-specific biodistribution, poor selectivity and limited effectiveness (Khan et al. 2017; Kumar et al. 2017; Z. Wang et al. 2017).

A targeted drug delivery system could overcome some of the current limitations of drug development (Liu et al. 2017; Khan et al. 2017; Z. Wang et al. 2017). It can enhance drug efficacy by increasing drug accumulation at the target site which can reduce effects of off-target tissues and minimizes undesirable side-effects and improve patient compliance (Mu et al. 2018). This concept is not new, but rather it is a continuation of the "magic bullet" concept proposed by Paul Ehrlich, a German researcher back in 1906 (Bosch & Rosich 2008). After more than 100 years, the quest for a "magic bullet" continues to be a challenge to scientists around the world. In principle, the challenge lies on (i) identifying the proper target to tackle a particular state of disease, (ii) employing an effective active therapeutic agent to treat the disease and (iii) designing an efficient means to carry the active agent to the

site of interest. Passive drug targeting relies on the affinity of the drug to the endothelial cell lining whilst an active targeting is achieved through a ligand-targeted approach, i.e., attaching the drug to a specific carrier (Wang et al. 2017; Szczepanowicz et al. 2016).

If a drug carrier is used for targeted delivery, the carrier must be recognized by the target cell for cellular internalization and deposition of the drug to occur (Kim & Cochran 2017). In addition, an ideal carrier must be non-toxic, biocompatible and chemically stable in-vivo. It should also be biodegradable and easily excreted from the body (Liu et al. 2017). Over the last few decades, various materials including macromolecules, liposomes, dendrimers and most recently nanomaterials have been synthesized with the aim of drug targeting (Banerjee et al. 2017). Unfortunately, very few effective site-specific drug systems are currently used in the clinic. The subsequent sections of this chapter will focus on targeted drug delivery to the lung and the strategies which have been tested to-date. It will discuss the potential use of ion-pairing to generate targeting complexes that are labile and have the potential to deliver and dissociate from the drug to release it in a specific tissue. At the end of this chapter, the future work that is needed to evaluate ion-pair strategy is outlined and from this the aim of this PhD thesis was generated.

1.1 Targeting drug to the lungs

The major challenge for lung diseases treatment such as asthma and chronic obstructive pulmonary disease (COPD) is the limited ability of the conventional drug delivery systems to delivery drugs effectively to the target site which results in low therapeutic effect. To improve this, lung-targeted drug delivery (LTDT) could be employed to provide an efficient means to deliver therapeutic agents to the lung whilst minimizing drug distribution in off-target sites. The pulmonary system, because of its unique physiology, offers an attractive target site for the delivery bioactive compounds. This system comprises of the airways, lungs and muscles, which together facilitate the process of gaseous exchange in the body (Figure 1.1). In humans, the airways can be divided into the respiratory zone, which covers the airways and the alveoli, and the conducting zone that is made up of trachea, bronchi and bronchioles (Banerjee et al. 2017).

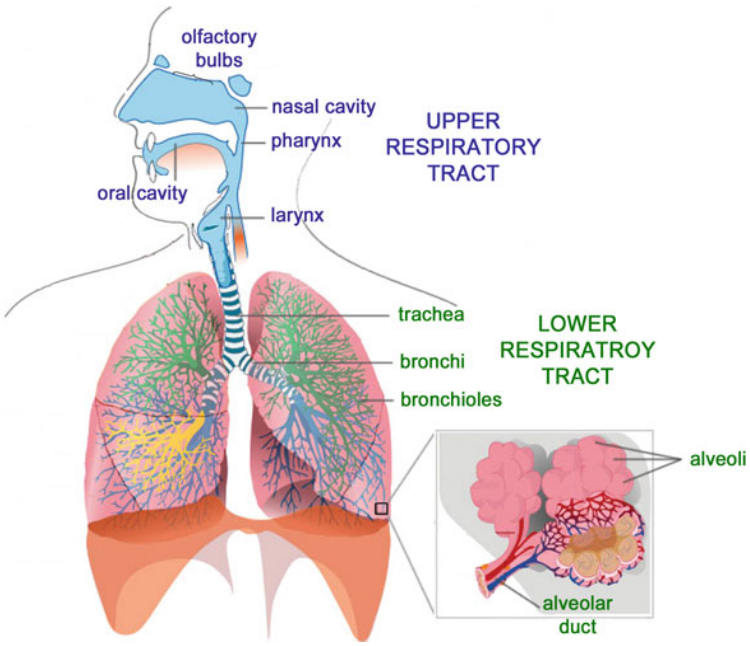

Figure 1.1 The overview of human respiratory system (Tu et al. 2013)

The human lung is estimated to contain half a billion alveoli and more than 2000 km of airways. The surface area is approximately 75-140 m^2 in adults. The carbon dioxide and oxygen exchange process removes metabolic waste and maintains the body pH (Stone et al. 1992). The alveoli are wrapped with pulmonary circulation whilst the bronchial veins bypass the pulmonary circulation and return the oxygenated blood to the heart via pulmonary veins. The alveoli are known to have a high solute permeability due to the thin epithelial barrier (alveoli epithelium is merely a single cell thick where the distance from the alveolar lumen to the bloodstream is <400 nm), an extensive vascularization and exhibits low proteolytic activity (Sahin-Yilmaz & Naclerio 2011).

Drugs can be delivered to the lungs via inhalation or from the systemic circulation. The inhalation delivery route includes nasal and oral delivery depending on the site of interest. Delivering drugs into nasal cavity is used to unblock local congestion or to ameliorate allergic conditions whilst other pulmonary-related diseases such as asthma, tuberculosis, COPD, etc., the drugs are administer via oral inhalation to target tracheobronchial and pulmonary airways (Paranjpe & Müller-Goymann 2014; Agu et al. 2001; Adjei & Gupta 1994). Although this route of drug administration for lung targeting is gaining more interest over these years, due to the highly efficient clearance mechanism of the human respiratory system, only small percentage of the emitted dose (ca. 10-15%) can be successfully deposited in the lung which results in short duration of resultant clinical effects (Labiris & Dolovich 2003). To compensate, multiple day dosing which is far from ideal is required to treat pulmonary diseases such as asthma (Sturm et al. 2002; Stuart 1976). Another route for lung targeting drug delivery is from the systemic circulation through intravenous (i.v) administration. This mode of therapeutic administration is ideal to achieve immediate

therapeutic action which is recommended in cases of life-threatening asthma (Dhand et al. 2014). This route of drug delivery is also useful when inhaled bronchodilators has failed after frequent doses. The following section will be discussed on the existing methods which have been used for lung-targeting drug delivery systems exploiting the intravenous route.

1.1.1 Nanomaterial-mediated lung-targeting

Nanoparticles (NPs) encompass structures with a size range from 1 – 100 nm (Figure 1.2). However, the prefix "nano" generally refers to particles of sizes from a few nm to 1000 nm (Cheng et al. 2017). The nanotechnology market is one of the fastest growing markets in the world. The market has increased from USD 339 billion in 2010 to more than USD 1 trillion in 2013, an average increased of 40-45% a year (National Science Foundation, 2014). For therapeutic applications, NPs are used to embed active agents e.g., drugs, imaging agents and genes. These active agents can be incorporated in the matrix of the particle or deposited on the surface of the nanomaterial (Hassan et al. 2017; Yin et al. 2017; Singh & W. 2009). This approach has been shown to provide controlled drug delivery across the membrane, improved targeting in certain cells, modify cellular transport and drug bioavailability (Bruni et al. 2017; Luk & Zhang 2015; Li et al. 2017; Kim et al. 2014; Masoudipour et al. 2017). Depending on the materials used, NPs can be categorised into soft vesicular carriers and rigid NPs. Size is an important feature that helps to determine the pharmacokinetic behaviour of the formulated NPs. In general, the small NP displays greater mobility and better cell penetration (Singh & W. 2009).

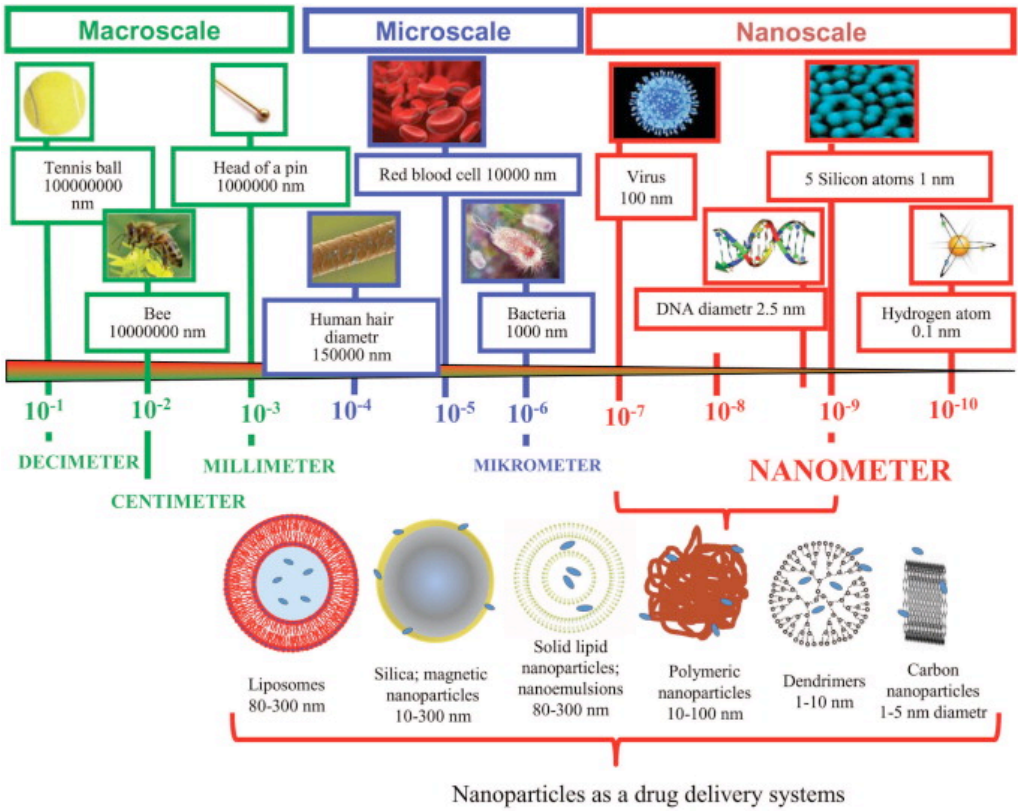

Figure 1.2 Particles categorized by size (Wilczewska et al. 2012)

For examples, Desai and colleagues noted that NPs with the size of 100 nm showed a 2.5-fold greater uptake rate than 1 µm and a 6-fold increased uptake compared to 10 µm microparticles in Caco-2 cells. In another study, Readhead et al. (2001) found that NPs penetrated throughout the submucosal layers of a rat intestinal loop model, whilst the localization of microparticles was mainly observed in the epithelial lining. When the size of particles gets smaller, it increases the area-to-volume ratio. Therefore, therapeutic agents embedded into small particles would be at or close to the particle surface which could lead to faster or immediate drug release (Singh & W. 2009). Smaller particles also have greater tendency to form aggregate during storage and upon delivery (Baalousha 2017). Hence, careful manipulation of the size of the NPs is important since this can significantly affect the

drug loading, drug release and also the stability of NPs in-vivo. NPs which are smaller than 7 nm in hydrodynamic diameter are susceptible for renal clearance whilst NPs larger than 100 nm can be excreted from the circulation by phagocytic cells (Sykes et al. 2014; Longmire et al. 2008). Apart from size, by coating the surface of NPs with biodegradable hydrophilic polymers *e.g.,* polyethylene glycol (PEG), polyethylene oxide, polyoxamer, poloxamine and polysorbate 80 (Tween 80) was reported to enhance the drug loading of NPs (Biesta et al. 2012; Qie et al. 2016). The addition of PEG to the NP surface (PEGylation) reduces the uptake of NPs by the reticuloenothelial system (RES), in which NPs are rapidly excreted out from the circulation to the liver, spleen or bone marrow, thus prolong NPs circulation time. In addition, PEGylation of NP surface decreases aggregation due to passivated surfaces (Jesse V Jokerst, Tatsiana Lobovkina 2012).

There have been a number of studies that assessed the use of NPs for lung targeted delivery via i.v administration. For example, Xiang et al., (2007) studied the biodistribution of newly developed solid lipid nanoparticle (SLN) containing dexamethanose acetate (DXM). This optimized formulation consisted of 2 % pluronic F68, 110 mg of glycerol tristearate and 60 mg DXM. After intravenous administration, DXM-SLN showed a 17.8-fold increase in the lung uptake of DXM compared to DXM alone. This study suggested that SLN modified with F68 might provide a means for lung targeting drug delivery. Another study by Krueter and co-workers assessed the biodistribution of poly(methy-2-14C-methacrylate) nanoparticles. The organ distribution of the NP was measured from 0.5 up to 7 days after i.v injection. They reported that a maximum accumulation of the NP in the lungs was after 30 min (21.8%) and decreased to 13.2% after 7 days. Löbenberg et al. (1998) showed significant lung uptake of ^{14}C-azidothymidine bound to hexylcynoacrylate nanoparticles after i.v injection in rats compared to the uptake of the drug alone. The drug concentration in the lungs was reported to

be 18 times higher than control after 8 hours of administration. Given that growing interest in the application of nanomaterials in drug delivery, concerns have been raised regarding the possible risks that they may bring. There are mixed reviews on the toxicity of NPs with some studies reported that NPs are safe to be used whilst others showed that the uptake of NPs might eventually perturb cellular pathways and induce toxicity. NPs could easily find ways to enter the human body and cross the various biological barriers due to their small size and may reach the most sensitive organs (Yildirimer et al. 2011). It has been proposed that NPs of size less than 10 nm act like gas molecule and can enter human tissues easily and may disrupt the cell normal biochemical environment. This is an area that needs more work if nanomaterials are to be used to target the lung as it is a very sensitive organ that can, if insulted will result in perturbed respiration. Apart for toxicity issue, another major obstacle for intravenous lung-targeting of nanomaterials is the massive uptake in the liver (Azarmi et al. 2008).

1.1.2 Prodrug-mediated lung targeting

Prodrugs refer to derivatives of drug molecules that can be chemically converted into their active metabolites at the specified pharmacological site (Zhang et al. 2017; Zawilska et al. 2013). This strategy relies on the unique physiological events which only occur at the site of interest (Rautio et al. 2017). This approach offers a more site-specific delivery of active molecules with a potential decrease in drug dosing requirements (Huttunen et al. 2011).

A prodrug can be classified into (i) a bio-precursor prodrug i.e., a simple compound that can be chemically or metabolically transformed into its active compound and (ii) a carrier-linked

prodrug where the active metabolite is chemically linked to a carrier through covalent bond and release through biotransformation processes (Huttunen et al. 2011; Zawilska et al. 2013). The latter type of prodrugs can be further subclassified into bipartite and tripartite prodrugs. A bipartite prodrug is formed when the bioactive agent is directly attached to the carrier whilst for tripartite prodrugs, a spacer is used to link the carrier and the parent drug (Wu 2009). Chemical groups such as carbamate, ester, phosphate, imine, carbonate amongst others are normally attached to the carrier so that a link could be formed between the active agent and the carrier (Rautio et al. 2008; Jornada et al. 2016) (Figure 1.3). A double prodrug is formed when two promoieties are attached to other and linked to the parent drug molecule. The two promoieties are usually different and normally cleaved through the non-identical mechanism. In some cases, two bioactive agents can be linked to each other forming another type of prodrug known as codrug where each molecule acts as the carrier to each other (Das et al. 2010). The use of prodrugs in drug delivery has been shown able to improve drug permeability and absorption, modify the distribution profile of active agents, provide protection from rapid metabolism and excretion as well as reducing toxicity-related problems (Huttunen et al. 2011; Rautio et al. 2017; Zawilska et al. 2013).

In 2015, of 32 new drugs approved by FDA, 7 were identified as prodrugs (Rautio et al. 2017). Fosphenytoin is a commercial product of prodrug containing an active molecule, phenytoin. Phenytoin is used clinically for anti-seizure treatment. Oxymethylene is used as a spacer to form a bridge between the phosphate ester and the amine group of phenytoin. The aqueous solubility of fosphenytoin is 7000 times greater than the drug alone and rapidly activated into phenytoin in the blood ($t_{1/2}$ < 15 min in human) (Browne et al. 1996). Another example of a commercial product of prodrugs is dabigratan etexilate (brand name: Pradaxa)

which is administered orally for the prevention of stroke. The parent drug dabigatran is very hydrophilic (log P = -2.4) that results in very poor bioavailability after administration.

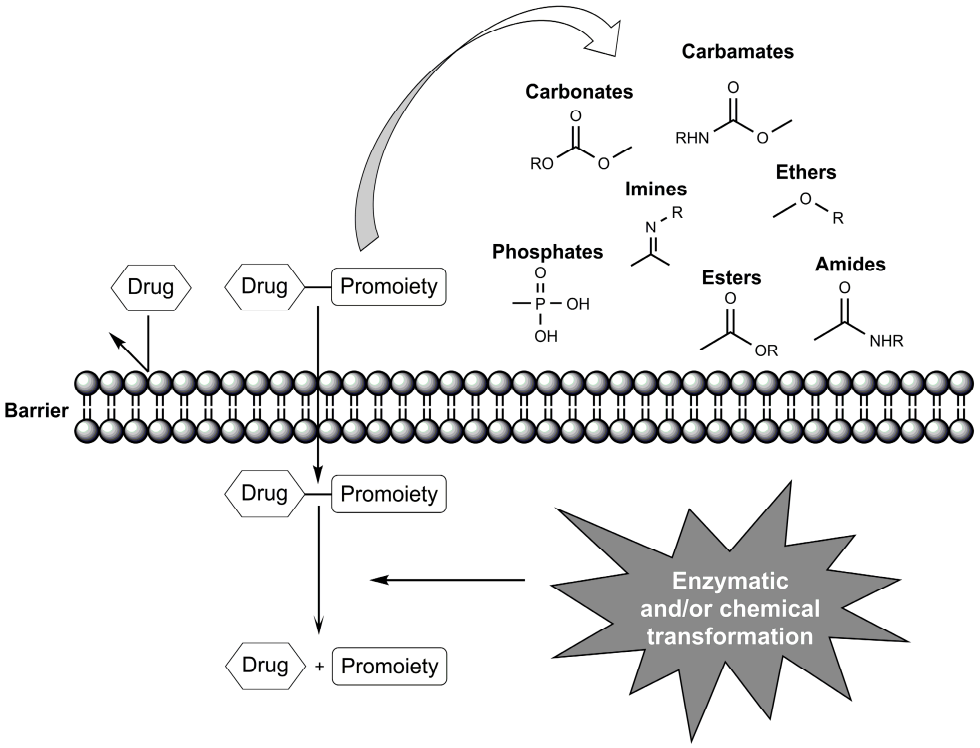

Figure 1.3 The bioactivation of prodrugs by enzymatic and/or chemical transformations in vivo (Jornada et al. 2016)

Dabigratan etexilate is a bifunctional prodrug using carbamic ester and carboxylic acid ester attached to the two polar groups of dabigratan, amidinium moiety and carboxylic in order to mask their polarity and increase the drug lipophilicity. This results in absorption enhancement by 7% (Eisert et al. 2010). For anti-cancer treatment, many prodrugs are designed to be responsive to the aberrant physiological conditions of the target tissue. Solid tumours mostly show selective enzyme expression, hypoxic cells and lower extracellular pH. The application of prodrugs for lung-targeting has been previously studied. Zhang et al.,

(2015) used a prodrug-based nano-drug delivery system to encapsulate chemotherapy agents, paclitaxel (PTX) and carboplatin (CBP) for lung cancer treatment. PLGA-PEG-CBP prodrug was formed by attaching the carboxylic group of PLGA-PEG-COOH with the amino group of CBP. Then, the self-assembled nanoparticles combining PTX and PLGA-PEG-CBP (PTX/CBP NPs) were synthesized using solvent displacement technique. PTX/CBP NPs displayed the highest anti-cancer activity when tested in human non-small lung carcinoma cell line (H460). In a different study by Webster et al., (2015) showed a significant antitumor activity of bisphosphonates prodrugs when tested in human lung carcinoma (A549) cells. The synthesized prodrugs exhibited >250-fold increase in cancer inhibitory activity compared to the free bisphosphonates. Chung et al., (2006) assessed the antitumor activity of 20 synthesized troxacitabine prodrugs in two non-small cell lung cancer cell line (A549 and SW1573). Their results suggested that prodrugs with long linear aliphatic chains (>8 CH_2) were more potent than the free drug with the IC_{50} values in the nanomolar range. However, the pro-drug metabolism shows patient-to-patient variability and this is a significant concern for this targeting approach.

1.1.3 Liposomes-mediated lung targeting

Liposomes were first discovered in 1960's. They are spherical in shape which are normally synthesized from cholesterol and natural non-toxic phospholipids. The advantageous of liposomes amongst others are biodegradable, non-immunogenic for both systemic and non-systemic administrations, low toxicity and flexible (Allen & Cullis 2013; Akbarzadeh et al. 2013; Sercombe et al. 2015). There are four main types of liposomes, conventional, PEGylated, ligand-targeted and theranostic liposomes (Figure 1.4).

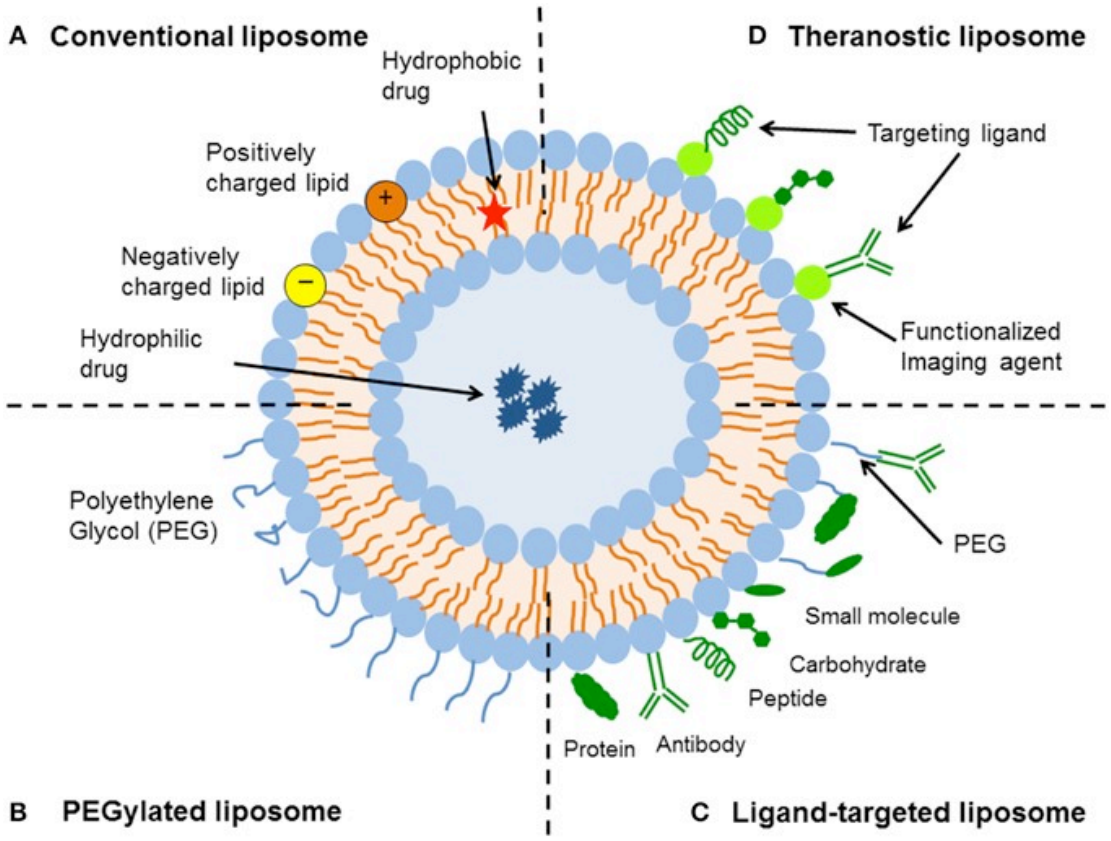

Figure 1.4 Types of liposomes in drug delivery (Sercombe et al., 2015)

Type one liposomes i.e., conventional liposomes were the first of its type to be developed. They are composed of a lipid bilayer that can be cationic, anionic or neutral phospholipid. The used of conventional liposomes has been shown to reduce toxicity through bioactivity of the drugs but however its therapeutic efficacy was limited by rapid elimination from the bloodstream (Gabizon et al. 2002). The second generation of liposomes, PEGylated liposomes were next introduced to combat the stability issue resulting in a more sterically-stabilized liposomes with longer circulation time in the blood. Through incorporating PEG to the liposomes did prolong their blood circulation time, it appeared that this could reduce the

affinity of active agents with the intended targets (Northfelt et al. 1996). Ligand-targeted liposomes offer a more site-specific drug delivery. However, this approach can only be applied to particular types of cells that selectively express of over-express specific ligands (Puri et al. 2009). The ligands incorporated in liposomes could be receptors or cell adhesion compounds. However due to poor pharmacokinetics and immunogenicity, the use of ligand-specific liposomes often results in poor enhancement or no therapy enhancement at all. Considering the problems above, the newer generation of liposomes are designed using a combination of the previous designs to improve their targeting delivery.

Meng and Xu (2015) assessed the organ distribution of pirfenidone-loaded liposomes for lung targeting after i.v administration in mice. Their results showed a sustained delivery and an improved lung uptake of the liposomes formulation compared to the free drug solution. However, the histopathological data showed possible alleviation of lung injury of the liposomal formulation due to the physical trapping of the liposomes in the vascular network of the lung. Another study by Zhang et al. (2009) investigated the injectable levofloxacin loaded liposomes to target the lung for the treatment of pulmonary inflammation. The liposomal formulation was prepared using ammonium sulfate gradients method. The size of the formulated liposomes was relatively uniform (7.424±0.689 μm) with a zeta potential (+13.11±1.08 mV). The entrapment efficiency of levofloxacin-loaded liposomes ranged from 82.19% to 86.23%. The in-vivo results showed a prolong elimination half-life of the liposomal formulation compared to the free levofloxacin solution after i.v injection in rabbits. A change in the bio-distribution profile of levofloxacin-loaded liposomes was also observed where a significant lung targeting of the molecule was achieved using the liposomal formulation compared to the organ distribution profile of free levoflaxcin solution. However,

liposomes are not very physically stable and this can be worsened upon the attachment of ligands and incorporation of drugs and this hinders this approach.

1.1.4 Ion-paired in drug delivery

Approximately half of the clinically used drugs are ionisable at physiological pH (Patel et al. 2016). This permits the ionized forms of the drugs to form links with the other charged species through a chemical process known as ion-pairing (Song et al. 2013). Ion-pairing can be described as the association of the oppositely charged molecules in solution (Figure 1.5) (Elshaer et al. 2014).

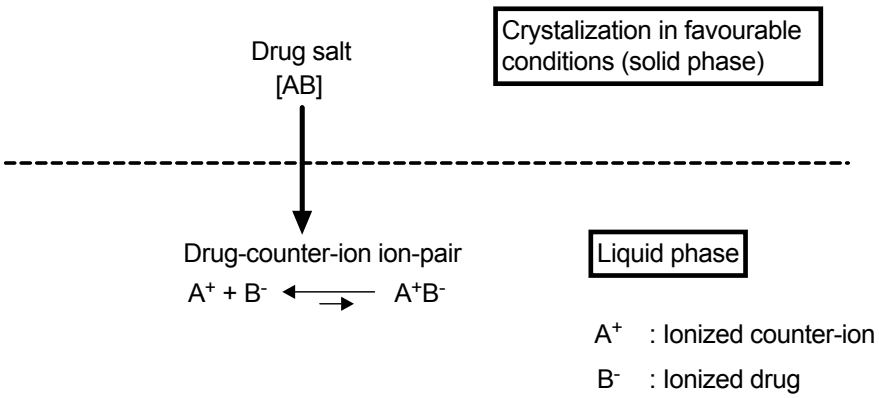

Figure 1.5 A diagrammatic representation of "salt form" and an "ion-pair"

In solution, three types of ion-pair could exist depending on the distance of the interaction which is limited by solvent permittivity (Figure 1.6). The production of a drug-counter ion ion-pair often results in the formation of relatively neutral species and hence improves the drug partitioning of polar drugs into the lipophilic membranes. Thus this approach can

improve absorption without the need to disrupt the membrane integrity (Nam et al. 2011; W. Wang et al. 2017). The pH partitioning theory suggested that only the unionized form of drug molecules can easily penetrate the biological membranes whilst the charged species do not pass the membranes (Shore et al., 1957). Once a drug is ion-paired with a counter-ion, they behave as a single unit (Marcus & Hefter 2006). This pair of oppositely charged ions is held together by long-range, non-directional electrostatic forces which making ion-pairing slightly different from covalent complexes. In case of complexes, they are formed through short-range, directional donor-acceptor (coordinative) covalent bonding (Haas & Franz 2010). In addition, the formation and dissociation constants of most ion-pairs are weaker compared to covalent complexes due to the nature of interactions (Marcus & Hefter 2006; Kumar & Nussinov 2002).

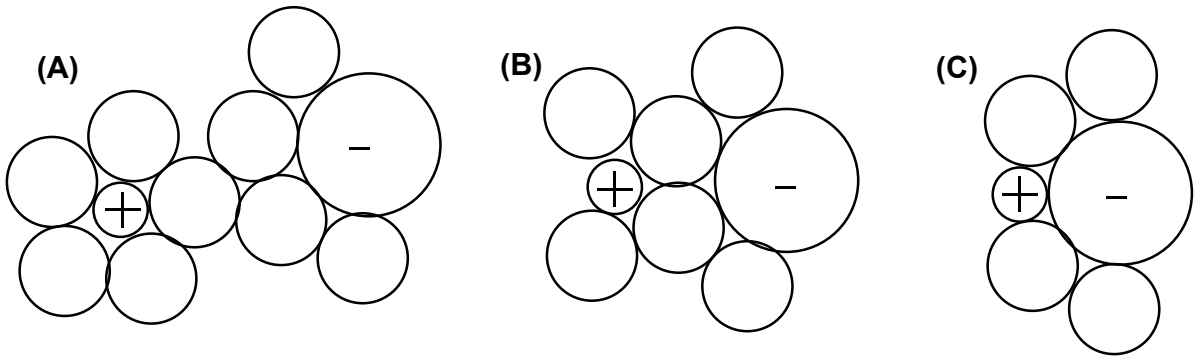

Figure 1.6 A schematic representation of ion-pair types: (A) solvent separated (2SIP), (B) solvent shared (SIP) and (C) contact ion-pair (CIP). 2SIP refers to double solvent-separated ion-pair, SIP occurs when only a single layer of solvent which is shared between the ions and CIP when no solvent exist between ions (Marcus & Hefter 2006).

The ion-pairing approach is simple in principle, but due to a low physical stability, quantification and tracking these complexes is difficult. When ion-pairs distribute in the

body, they will almost certainly dissociate to into their parent ions and eliminated individually (W. Wang et al. 2017; Zhao et al. 2017b). Therefore, this strategy represents a novel way to alter the physicochemical properties of a drug, such as solubility or partitioning behavior and receptor interactions without actually altering the molecular structure or the pharmacological activity of the API on a temporary basis. However, the major setback of this approach is that the non-covalent bonding might be too weak in solution to facilitate membrane permeation.

It is experimentally difficult to measure ion-pairs lifetimes. However, previous studies have shown using simple electrolytes that their lifetimes ~1 ns but drug ion-pairs have not undergone a similar analysis process (Buchner et al. 2003). It is hypothesized that a high stability constant of the ion-pair in aqueous (K_{11aq}) medium is required for the ion-pair formulation to remain intact when it enters the biological system due to binding competition from the endogenous ions (Marcus & Hefter 2006). The existence of an ion-pair can be questioned when the association constants is too low (< 2 M^{-1}) even though previous studies have shown association when constants are even lower, *e.g.,* $Me^{4+}Cl^{-}$ (0.29 M^{-1}) and $Me^{4+}Br^{-}$ (0.83 M^{-1}) (Geng & Romsted 2005). The proposed ideal log D of the ion-pair for a facilitated passive membrane permeation was between 2-5 (Miller et al., 2009). It appears that the physicochemical properties of both the drug and the counter-ion strongly influenced the ability of the formulated ion-pairs to alter the drug behavior (Samiei et al. 2014; Samiei et al. 2017; Elshaer et al. 2014). In general, drugs lipophilicty can be increased by pairing with lipophilic counter-ions. This approach has been studied as an alternative approach to alter the transport of ionisable drugs across biological barriers (Table 1.1).

For lung-targeting delivery, Zara et al. (1999) assessed the the pharmacokinetics of doxorubicin incorporated as ion-pair into solid lipid nanospheres (SLN) was compared with that of the commercial solution of the drug in rats. Animals injected with SLN carrying doxorubicin exhibited higher lung uptake of the drug compared to animals treated with commercial doxorubicin solution (Adriablastina). A lower doxorubicin concentration in liver, heart and kidney was also found in SLN-treated animals. This study suggested that SLN increased the area under the curve (0-180 min) of doxorubicin compared to conventional doxorubicin solution and led to a different body distribution profile. Patel et al., (2016) showed that the selection of the counter-ions was crucial in determining the biological behaviour of the parent drug molecule. The results from their study showed a superior bronchodilator effect ($p < 0.05$) of salbutamol when presented with excess 1-hydroxy-2-naphthoate (1H2NA) counter-ion compared to effect of salbutamol base. This affect was assigned to the effect of ion-pairing formation. Ion-pairing formoterol or salmeterol with the counter-ions aspartate, maleate, fumarate, and 1H2NA showed no effect on the drugs to reduce airway resistance in-vivo. For active lung-targeting, one interesting group of molecules that could form ion-pair for lung-targeting drug delivery are the polyamines.

1.2 Polyamines

Polyamines (PA) are organic compounds bearing two or more amino groups $–NH_2$. Endogenous polyamines e.g., putrescine ($NH_2(CH_2)_4NH_2$), spermidine ($NH_2(CH_2)_3NH(CH_2)_4NH_2$) and spermine ($NH_2(CH_2)_3NH(CH_2)_4NHCH_2)_3NH_2$) are derived from intracellular biosynthesis whilst exogenous polyamines could be obtained from diet and luminal bacteria (Jr. Casero & Woster 2010). PA are present in almost all cells where they are actively involved in gene expression, cell proliferation, cellular stress and human disease (Poulin et al. 2012; Miller-Fleming et al. 2015; Jr. Casero & Woster 2010). The polyamine

transport system (PTS) has been previously described in bacteria and single celled eukaryotes. However, in mammals, the system is still not been fully characterized. To date, no PA specific transporter has been identified. Poulin et al., (2012) proposed that an endocytic mechanism might be involved in PTS in animal cells. It has also been suggested the involvement of SLC7 (Lys/Arg/Orn permeases), CCC9 (an inorganic ion transporter) and OCT6 (cation/anion/zwitterion transporter) in PAs uptake in mammalian cells.

Table 1.1 Previous studies on the use of ion-pairing in drug delivery

Drug	Therapeutic function	Counter-ion	Biological barrier	Study output	Reference
Indomethacin (IND)	Anti-inflammatory	Arginine, lysine	• Human epithelial colorectal adenocarcinoma (Caco-2) cells	• Significant increase of IND cell permeability when paired with the respective counter-ions	(Elshaer et al. 2014)
Alendronate (ALD)	Treat and prevent osteoporosis	Arginine, hyoscine, pyridostigmine, phenazopyridine	• Human epithelial colorectal adenocarcinoma (Caco-2) cells • Parallel artificial membrane permeability assay (PAMPA) model	• Arginine and phenazopyridine enhanced the apparent permeability of alendronate by 14- and 26-fold in the PAMPA model and 6.5- and 4.4-fold across caco-2 cell monolayers, respectively.	(Samiei et al. 2017)
Amifostine (AMS)	Anti-cancer	Succinic acid, phtalic acid, benzoic acid	• Parallel artificial membrane permeability assay (PAMPA) model	• 1.6-fold increase of log P of the drug when paired with phtalic acid whilst for benzoic acid and succinic acid the values increased by 1.2 and 0.75-fold respectively. • Significant increase of AMS PAMPA permeability in the presence of phthalic acid (42-fold), benzoic acid (37-fold)	(Samiei et al. 2014)

				and succinic acid (10.5-fold).	
Methotrexate (MTX)	Anti-cancer	Arginine	• Rabbit nasal mucosa	• The partition coefficient of MTX was 24 times greater in the methotrexate-L-arginine ion paired systems than that of the methotrexate system without L-arginine.	(Ivaturi & Kim 2009)
Scutellarin (SC)	Anti-cancer	Organic amines	• Rat skin	• Increased of skin permeation through ion-pair formation.	(Wang et al. 2008)
Zanamivir heptyl ester (ZHE) Guanidino oseltamivir (GO)	Anti-viral	1-hydroxy-2-naphthoic acid (HNAP)	• Human epithelial colorectal adenocarcinoma (Caco-2) cells • Rat jejunal	• Enhanced in the apparent permeability (P_{app}) of both compounds across Caco-2 cell monolayers in a concentration-dependent manner in the presence of HNAP. • Significant enhancement in the rat jejunal permeability of ZHE by the addition of HNAP in a concentration-dependent manner (zero without HNAP to 4.0×10^{-5} cm/s with 10 mM HNAP).	(Miller et al. 2010)
Zaltoprofen (ZAL)	Anti-inflammatory	Organic amines	• Rabbit skin	• The permeation of ZAL was significantly improved with alkylamines and cycloalkanolamines but	(Cui et al. 2015)

				significantly retarded with alkanolamines.	
Insulin	Anti-diabetic	Amino acids	• Human buccal epithelium (TR146) cell layers	• Basic amino acids improved insulin solubility in water while 200 and 400 µg/mL lysine significantly increased insulin solubility in HBSS. • Significant improvement in the insulin permeation: 10 µg/mL of lysine ($p < 0.05$), 10 µg/mL of histidine ($p < 0.001$), 100 µg/mL of glutamic acid ($p < 0.05$), 200 µg/mL of glutamic acid and aspartic acid ($p < 0.001$) without affecting cell integrity.	(Iyire et al. 2016)

1.3 Aims and scope of thesis

In healthy cells, the pulmonary tissue has been reported to express a more active polyamine uptake system (PTS) compared to cells derived from other tissues (Hoet & Nemery 2000). Considering that at physiological pH, PAs primarily exist as protonated polycations, there is a great potential of using polyamine ion-pairing to target drug into the lung from the pulmonary circulation when administered intravenously. Different approaches have been studied using polyamine to target drug to specific cells before but polyamine ion-pairing mediated active lung targeting is yet to be tested (Figure 1.7).

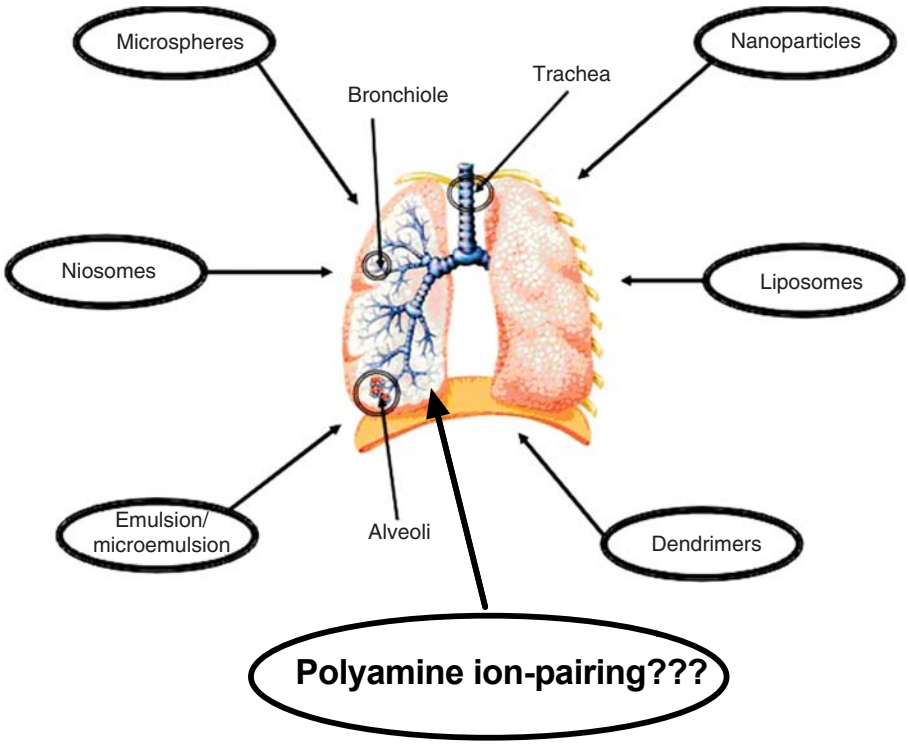

Figure 1.7 The existing startegies to target drug to the lung. Picture was taken from Serombe et al (2015) with some modifications made by the author.

The aim of this thesis was to evaluate the use of polyamine ion-pairing approach for the development of an intravenous active lung-targeting delivery of theophylline. To address this aim, the following objectives were set:

1. To assess the binding of theophylline with a selection of polyamine counter-ions. Since the ability of a molecule to permeate through biological barrier is highly dependent on its physicochemical properties, changes in the physicohemical properties of theophylline on aqueous solubility, lipophilicity and chemical stability upon forming ion-pair with polyamines was evaluated.
2. To characterize cyclodextrin-theophylline-polyamine complex. It is known that the issue with the ion-pairing approach is the weak non-covalent interaction between the ions could result in break downs prior to reaching the target site. Thus, cyclodextrin was used to try to stabilize the theophylline-polyamine ion-pair association. Characterization of cyclodextrin-theophylline-polyamine complex was performed using NMR and a 3D modelling technique was used to predict the interaction between cyclodextrin and the ion-pair.
3. To assess the effect of delivery co-solvent on the complex and to study pH-induced dissociation of the ion-pair. It is known that the solvent properties *e.g.,* polarity influenced complex formation. An ideal solvent could thus enhance the ion-pair stability hence slow down its break down in solution.
4. To assess the in-vitro cytotoxicity and cellular uptake of cyclodextrin-theophylline-polyamine complex in lung cell

CHAPTER 2

THEOPHYLLINE-POLYAMINE ION-PAIR: BINDING AND PHYSICOCHEMICAL CHARACTERIZATION

Chapter summary:

This chapter characterized the strength of association between theophylline and a selection of amine counter-ions. In addition, it evaluated how the theophylline-amine interactions influenced the lipophilicity and aqueous solubility of the drug. A series of polyamines, increasing in the number of amine functional groups were used as the ion-pairing agents: ethylenediamine, spermidine and spermine with a monoamine, ethylamine, as a control. The chemical stability of the drug when mixed with excess counter-ion and stored up to 4-week was also reported.

2.1 Introduction

The natural polyamines are ubiquitous in all prokaryotic and eukaryotic cells where higher accumulation of these polycations has been reported in animal lung cells (Hoshino et al. 2005; Hoet & Nemery 2000; Saunders et al. 1989; Smith et al. 1990; Minois et al. 2011). At physiological pH, these poly-cations are charged which allows them to associate non-covalently with other negatively charged molecules (Hoshino et al. 2005; Hoet & Nemery 2000). This interactive potential of polyamines makes it possible for them to form ion-pair with ionisable xenobiotics in a manner that could facilitate their uptake into the lung.

Using theophylline as a model drug, the present study assessed the impact of forming ion-pairing with polyamines on the biopharmaceutical properties of the drug. Theophylline is a well-established bronchodilator for the treatment of asthma and chronic obstructive pulmonary disease (COPD) (Malamatari et al. 2016). Delivering theophylline through inhalation to patients was found to be irritating and ineffective. In clinic, injectable theophylline (aminophylline) is used to treat acute severe asthma. Aminophylline is a 2:1 theophylline:diethylamine salt used to overcome theophylline poor solubility so that i.v administration of the drug is possible (Barnes 2010). Theophylline has a narrow therapeutic index (10 - 20 ug mL^{-1}) and unspecific distribution in the body after administration often leads to poor side-effect profile, which is normally manifested by nausea, dizziness, vomiting, tachycardia, arrhythmias and seizures (Powell et al. 1978; Jusko 1984; Nakura et al. 1998; Malamatari et al. 2016). Despite its poor side-effect profile, theophylline is still extensively prescribed worldwide, because it is inexpensive. When administered (both orally and intravenously) to rats, theophylline was found to be almost evenly distributed in liver, muscle, lung, spleen and heart where higher theophylline distribution was found in liver and kidney (Jusko 1984; Powell et al. 1978; Gabrielsson et al. 1984). It was also reported that

theophylline can cross the placenta and distributed in the organs of the fetus of the pregnant rats (Gabrielsson et al. 1984). With the aim to reduce these side effects, there is a need to reformulate this API for targeted lung delivery upon intravenous delivery. One interesting approach is by manipulating the PTS to target theophylline delivery to the lung. This can be achieved by forming theophylline ion-pairs with polyamines which are the PTS substrate. Previous studies have shown the success of using ion-pairing as a strategy to improve the transport of ionisable drugs across the skin (Wang et al. 2008), nasal (Ivaturi & Kim 2009) and intestinal (Ester et al. 2012) mucosa but has yet to be tested for the lung targeting system.

Ion-pair describes the formation of a temporary, spontaneous, non-covalently bound complex in solutions (Samiei et al. 2017). The intermolecular association between the molecules changed the physicochemical features of the parent drug which affected the molecules absorption (Zhao et al. 2017a; W. Wang et al. 2017). A study by Ivaturia and Kim (2009) demonstrated a 3-fold increase of methotrexate flux across rabbit nasal mucosa *in-vitro* when combined with a counter-ion, L-arginine when compared to the flux of the drug alone. Another study by Samiei et al., (2014) showed increased in the permeability of amifostine across a lipophilic membrane in the presence of the counter-ions: phthalic acid (46-fold), benzoic acid (37-fold) and succinic acid (10.5-fold) resulting from the ion-pair formation. The magnitude of change in the apparent permeability value (P_{app}) of the drug was found to be dependent on the concentration of the counter-ion applied. The permeability of indomethacin was also found to be counter-ion concentration dependent when studied in Caco-2 monolayers (Elshaer et al. 2014). In this study, L-arginine and L-lysine were used as the counter-ions.

Drugs can be absorbed through membranes via a considerable number of routes. Amongst those, passive transport is the most common one (Sugano et al. 2010). The ability of a molecule to passively permeate through the biological membranes normally depends on the non-polar fraction of the molecules as well as the physicochemical properties of the permeant such as molecular size, hydrogen bond capacity, lipophilicity, pK_a and solubility (Liu et al. 2011; Nam et al. 2011). In case of carrier-mediated transport, this usually occurs through site-specific interactions (Sugano et al. 2010). Lipophilicity can be measured by determining the distribution of a molecule between an organic layer (normally n-octanol) and an aqueous layer (Kah & Brown 2008). The partition coefficient (log P) obtained can be used to predict the lipid affinity of a molecule. In case of ionisable drugs, the apparent distribution coefficient (log D_{pH}, equation 2.01) is often used instead of log P which is only valid for a single species.

$$\log D_{pH} = \log (f_N \,.\, P^N + f_I \,.\, P^I) \qquad (2.01)$$

Where f_N and f_I are the molar fractions of the neutral and ionized forms, and P^N ad P^I are their respective partition coefficients. A molecule with log $D_{7.4}$ between 0 – 1 may demonstrate an ideal balance between solubility and permeability, < 0 – high solubility with susceptible to renal clearance, > 5 – poor solubility, bioavailability and can cause erratic absorption (Andres et al. 2015). The association between an ionized drug [A^-] with the oppositely charged counter-ion [B^+] normally results in neutralizing the charge of the parent drug that often improves the lipophilicity of the molecule. Nam et al., (2011) demonstrated an increase of risedronate (RS) (log P_{RS} = -3.6) lipophilicity in the presence of the counter-ions: L-arginine (ARG) (log P_{ARG} = -4.2), L-lysine (LYS) (log P_{LYS} = -3.2) and diethylenetriamine (DIE) (log P_{DIE} = -1.73) by 8.9%, 12.0% and 2.1%, respectively when compared to the lipophilicity of

the drug alone. Contrary to this, ElShaer et al., (2014) demonstrated a decreased of lipophilicity of indomethacin (IND) (log P_{IND} = 4.2) when the counter-ions L-arginine and L-lysine were presence in excess. They postulated that the drop of lipophilicity of the drug could be due to high hydrophilicity of the counter-ions. In another study, it was found that the change of the drug's lipophilicity when formed the ion-pairs was not solely influenced by the lipophilicity of the counter-ions, but also by the association strength and overall charge reduction over the drug molecule (Samiei et al. 2014).

In our case, we expect an increase in the solubility of theophylline which in return might diminish its lipophilicity when mixed with the amine counter-ions since all selected counter-ions are very hydrophilic (Table 2.1). Theophylline has a poor solubility but its solubility increased considerably when combined with diamine, ethylenediamine (Aslaksen et al. 1981). However, the magnitude of change in the physicochemical properties of theophylline when the drug forms ion-pairs with the amines might also be influenced on the affinity of the drug to bind to the counter-ions since the counter-ions are different in the hydrogen bonding capacity. Direct analytical techniques for binding measurements are normally reported for metal-ion complexes, metal-protein complexes and protein-protein complexes (Gromiha & Yugandhar 2017; Alberti et al. 2016; Kocyła et al. 2015) but rarely studied for ion-pair complexes.

The aims of this chapter were to assess the theophylline-amines binding in water and to investigate the consequences of the ion-pairing process on the lipophilicity, solubility and chemical stability of theophylline. The binding association between theophylline and a selection of different amine counter-ions in water was assayed by means of Fourier Transform Infrared spectroscopy (FT-IR) and High Performance Liquid Chromatography

(HPLC). The physicochemical properties of theophylline and the respective counter-ions used in this study were summarized in (Table 2.1). The pH of all mixtures was adjusted to 9.6 to mimic the normal formulation pH of aminophylline[1]. We specifically used 9.6 $\pm$ 0.1 as our working pH to maximize the percentage of ionized theophylline which then provides the optimum condition for the ion-pairing process to take place between the oppositely charged molecules. The IR spectroscopy was used for this purpose due to its high sensitivity that can detect the changes in the chemical composition of small molecules which provides the insights of different levels of structural features apart from short measuring time, cost-effective and low amount of sample required (Nafisi et al. 2012; Kim et al. 2010; Malathi 2012).

The reversed phase (RP)-HPLC approach is based on substance partition between a non-polar stationary phase and an aqueous. This method is cheap and cost-effective. The retention of theophylline is governed by the partition between the aqueous mobile and stationary phase. When the amines counter-ions were added to the mobile phase, there is an additional contribution to the drug retention due to the ion-pairing process. The changes in the retention of theophylline will then reflect the degree of intermolecular interactions formed between the drug and the level of amines counter-ions presence in the mobile phase.

[1] Aminophylline (a 2:1 complex of theophylline:ethylenediamine) is the commercial product of injectable theophylline. The USP solution of aminophylline has a pH between 8.5 – 9.7.

Table 2.1 Physicochemical properties of theophylline and the respective counter-ions used in the present study. pK_a - acid dissociation constant; Log P (o/w) – octanol/water partition coefficient; THE = theophylline; EA = ethylamine; EDA = ethylenediamine; SPD = spermidine; SP = spermine

Compound	Mol. weight ($g\ mol^{-1}$)	pK_a	Log P[§] (o/w)	Chemical structure
THE	180.16	8.6[a,c]	-0.02	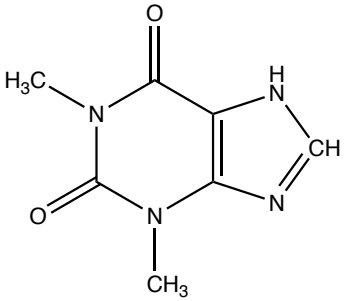
EA	45.08	10.60[b]	- 0.13	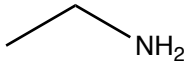
EDA	60.10	pK_1 = 10.21[e] pK_2 = 7.16[e]	- 2.04	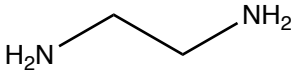
SPD	145.25	pK_1 = 10.89[d] pK_2 = 9.81[d] pK_3 = 8.34[d]	- 0.66	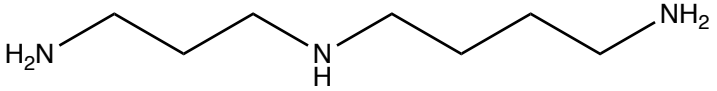
SP	202.34	pK_1 = 10.98[d] pK_2 = 10.09[d] pK_3 = 8.83[d] pK_4 = 7.94[d]	- 0.7	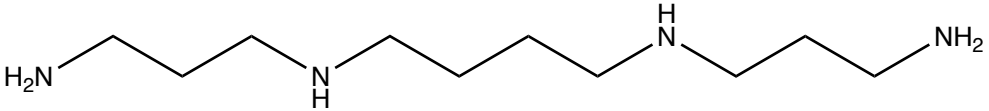

[a](Kustin et al. 1971); [b](Rajan & Muraleedharan 2017); [c](Turner 1948); [d](Frassineti et al. 2003); [e](Potter et al. 1994); [§]values obtained from ChemSpider

2.2 Materials

Theophylline (THE) (anhydrous, ≥ 99%), spermine (SP) (≥ 99%), spermidine (SPD) (> 99%), ethylamine (EA) 70 *wt*. % in H_2O, ethylenediamine (EDA) (> 99%), 1-octanol, deuterium oxide (D_2O) (D atom > 99%), sodium hydroxide (NaOH), hydrochloric acid (HCl), sodium chloride (NaCl) were purchased from Sigma Aldrich, UK. All reagents for HPLC analysis were HPLC grade.

2.3 Methods

2.3.1 Fourier Transform Infrared spectroscopy (FT-IR) binding studies

The Infrared (IR) conditional binding constant ($pK_{FT\text{-}IR}$) of theophylline-amines complexes were assessed using a universal liquid cell system (Omni-Cell, Specac Ltd, UK) fitted with CaF_2 windows and 0.025 mm mylar spacer (Specac Ltd, UK) was used for the absorbance measurements. D_2O was employed as the solvent for the measurements as it showed less interference with the IR absorption of theophylline compare to H_2O. The absorbance spectra of 0.015 M theophylline at 1:0 – 1:20 theophylline-amines molar ratios were recorded within the range of 1725 – 1500 cm^{-1} using D_2O pH adjusted to 9.6 ± 0.1 using NaOH/HCl. NaCl was added when necessary to keep a constant ionic strength (0.5 M) in all mixtures. All spectra were subtracted with the spectra of the blank solutions and baseline corrected. The blank solutions refer to the exact compositions of the test solutions in the absence of theophylline. Changes in the peak absorbance ratio at ca. 1530/1551 cm^{-1} were calculated where the peak at 1551 cm^{-1} was assigned as the uncomplexed theophylline and the peak at

1530 cm^{-1} as the complexed theophylline. The change in the IR ratio was used to determine the percentage of theophylline bound as a function of amine concentration (Figure 2.1). The percentage of theophylline bound *vs* $-\log[amine]_{free}$ were plotted and fitted with a regression model (GraphPad Prism7) to determine the FT-IR conditional binding constant ($pK_{FT\text{-}IR}$) of theophylline-amines complexes in water. The percentage of theophylline bound to amine counter-ion was calculated using Equation 2.02.

$$\%\ \text{theophylline bound} = \frac{(X_1 - B)}{A - B} \times 100 \qquad (2.02)$$

Where A represented the maximum abs ratio of theophylline peaks at ca. 1530/1551 cm^{-1} when mixed with the counter-ions. B indicated the abs ratio of theophylline peaks at ca. 1530/1551 cm^{-1} of free theophylline. X_1 indicated the abs ratio of theophylline peaks at ca. 1530/1551 cm^{-1} when mixed with a known concentration of counter-ion. The concentration of free amine was calculated using Equation 2.03.

$$[\text{amine}]_{\text{free}}(\text{M}) = [\text{amine}]_{\text{tot}}\ (\text{M}) - ([\text{theophylline}]_{\text{tot}}\ (\text{M}) \times (\frac{\%\ \text{theophylline bound}}{100})) \qquad (2.03)$$

Where $[amine]_{free}$ represented the free unbound amine to theophylline. $[amine]_{tot}$ referred to the initial concentration of amine in the mixture. $[theophylline]_{tot}$ referred to the initial concentration of theophylline (0.015 M). The value for $[amine]_{free}$ was calculated with an assumption that theophylline formed a 1:1 ionic complex with the amine counter-ion. All spectra were recorded using a Spectrum One spectrometer (Perkin Elmer Ltd, UK) and spectral analysis was performed with Spectrum version 10 software (Perkin Elmer Ltd, UK).

The resolution was set at 4 cm^{-1} and 12 scans were performed for each measurement. Experiments were repeated in triplicate and the results were presented as mean ± SD.

2.3.2 High Performance Liquid Chromatography (HPLC) binding studies

The HPLC conditional binding constant (pK_{HPLC}) of theophylline-amines complexes in water at pH 9.6 ± 0.1 was assessed using a HPLC system equipped with a pump (Waters 600-MS system controller) that was connected to an automated sample injector (Waters 717-plus auto sampler) and coupled with a UV detector (Waters 2487 Dual λ abs detector). The HPLC system was connected to a computer installed with a Millenium software that was used to record and analyse all chromatograms. A Phenomenax Kinetic 5 µ Biphenyl 100 A 250 x 4.6 mm HPLC column (Phenomenax, UK) was used as the stationary phase. The mobile phase used was 100 % water in which increasing concentrations of amines were added, pH adjusted to 9.6 ± 0.1 using HCl. All solutions were filtered through 0.45 µm pore size nylon membrane filter and sonicated for 1 hour. The flow rate was set at 1 mL min^{-1} and the UV detector was set at 273 nm. Briefly, 10 µL of 0.5 mM theophylline was injected into the system and the change of theophylline retention time when treated with increasing concentrations of amines was recorded. The change in theophylline retention in the column was used to determine the percentage of theophylline bound as a function of amine concentration. The percentage of theophylline bound vs $-\log[amine]_{free}$, was plotted and fitted with regression model (GraphPad Prism7) to determine the pK_{HPLC} of theophylline-amine complex. Experiments were repeated in triplicate and the results were presented as mean ± SD.

2.3.3 Water-octanol distribution coefficient (Log $D_{o/w}$) studies

The Log D protocol used in the study was similar to the protocol reported by Miller et al., (2010) and Samiei et al., (2014). Equal volumes of 500 mL of deionized water and 1-octanol were thoroughly mixed in a separating funnel to saturate the two phases. The mixture was subsequently allowed to stand for 24 h prior to use to enable complete phase separation. The organic upper-phase (UP) and aqueous lower-phase (LP) were separated shortly before use. The apparent octanol-water distribution coefficient ($D_{o/w}$) of theophylline was assessed in the excess amines solutions (theophylline-amine molar ratios: 1:0 – 1:100). Theophylline was mixed with the amines in the 5-mL total volume of LP, pH adjusted to 7.4 and 9.6 (± 0.1). Subsequently, an equal 5-mL of UP was added to each solution. The mixtures were left to mix in a water bath with gentle stirring for 48 h at 37 ^{o}C. The two layers were later separated and the aqueous layers were further analysed using UV spectrophotometer (Lambda 2S, Perkin Elmer, UK) to determine the concentration of theophylline in the aqueous phase, $[\text{theophylline}]_{aq}$. The concentration of 0.05 mM theophylline used throughout the experiments was sufficiently low so that it can be presumed that the solute was in 'infinite dilution' in each phase that solute-solute interactions were minimal (Kah & Brown 2008). The concentration of theophylline in the organic layer, $[\text{theophylline}]_{oct}$ was calculated using Equation 2.04.

$$[\text{theophylline}]_{\text{octanol}} = [\text{theophylline}]_{\text{initial}} - [\text{theophylline}]_{\text{aqueous}} \qquad (2.04)$$

Log $D_{o/w}$ of theophylline was calculated using Equation 2.05.

$$\text{Log } D_{o/w} = \text{Log } \frac{[\text{ionized+unionized theophylline}]_{\text{octanol}}}{[\text{ionized+unionized theophylline}]_{\text{aqueous}}} \qquad (2.05)$$

2.3.4 Solubility studies

Excess theophylline was added to a series of amines solutions ranging from 0.0 – 2.0 M. The mixtures were stirred in a water bath for at least 48 h at 37 ^{o}C to allow equilibrium to be reached, then filtered and assayed using UV (Lambda 2S, Perkin Elmer, UK) to determine the concentration of theophylline. The final pH of the mixtures was adjusted to 7.4 and 9.6 (±0.1) using HCl. Experiments were repeated in triplicate and data was presented as mean ± SD.

2.3.5 HPLC assay method verification

A Phenomenax Kinetic 5 µm Biphenyl 100 A 250 x 4.6 mm HPLC column (Phenomenax, UK) was used as a stationary phase. The mobile phase used was a mixture of 90:03:07 water:methanol:acetonitrile H_2O:MeOH:ACN (v/v), pH 4. All solutions were filtered through 0.45 µm pore size nylon membrane filter and sonicated for 1 hour. The injection volume was 10 µL and the flow rate was set at 1 mL min^{-1}. The UV detector was set at 273 nm. To verify the method was 'fit-for-purpose' standard solutions of 5, 25, 50, 75 and 100 µg mL^{-1} of theophylline were prepared using the mobile phase and assayed using HPLC. The mean peak area vs concentration (n = 5) was plotted for the five concentrations to generate the calibration curve that was fitted with a regression model (GraphPad Prism7). The peak symmetry (A_s) was calculated (n = 15) using equation 2.06.

$$A_s = \frac{W_{0.05}}{2\mathrm{d}} \qquad (2.06)$$

where $W_{0.05}$ is the width of the peak at one-twentieth peak height above peak baseline, d is the distance between the perpendicular dropped from the peak maximum and the leading edge of the peak at one-twentieth of the peak height. A peak symmetry of 1 was considered ideal as this represents a perfectly symmetrical peak. The theoretical plates which indicate column efficiency was calculated (n = 15) using equation 2.07 where, t is the retention time of peak and $W_{h/2}$ equals the width of the peak at half the peak height.

$$N = 16\left(\frac{\mathrm{t_r}}{\mathrm{W_{h/2}}}\right)^2 \qquad (2.07)$$

The LOD (the lowest concentration of an analyte in a sample that can be detected but not necessarily quantified) and the LOQ (the minimum injected amount of analyte that gives precise measurements) was calculated according to equations 2.08 and 2.09, respectively.

$$\mathrm{LOD} = Y_B + 3s_B \qquad (2.08)$$

$$\mathrm{LOQ} = Y_B + 10s_B \qquad (2.09)$$

s_B is the standard error of the y estimate and Y_B is the intercept from the regression equation. The precision of the HPLC method was determined by the repeatability (intra-day) and assessment of the intermediate precision (inter-day). Intra-day precision was obtained by

evaluating the variance between three standard curves assayed from the same standard solutions (five injections per standard). The intermediate precision of the test molecules was determined by comparing three calibration curves using independently prepared standard solutions (five injections per standard) on three separate days. The accuracy HPLC assay was determined by assaying freshly prepared solutions of known concentration. The ability of the assay to quantify the compound was calculated using the following equation 2.10.

$$\text{Accuracy (\%)} = \frac{A}{T} \text{ X } 100 \qquad (2.10)$$

A is the actual (known) concentration and T is equal to the theoretical analyte concentration.

2.3.6 Chemical stability studies

The chemical instability of theophylline in varying concentrations of spermine solutions was assessed at pH 7.4 and 9.6 (± 2) at room temperature (21 ± 2 ^{0}C). Spermine was used since the changes in the physicochemical properties of theophylline were the greatest when mixed with spermine. 1 mg mL^{-1} of theophylline was dissolved in 0, 50 and 100 mM of spermine solutions. pH adjustment was made by using HCl. The mixtures were stored in a dark environment away from light for 4-weeks. At 0, 1, 2, 3 and 4-week time points, 100 µL of each mixture was withdrawn, mixed with 900 µL of mobile phase and assayed with HPLC. The results were interpreted according to the percentage (%) of peak recovery and appearance of new peaks in chromatogram that can be associated with degradation products of theophylline.

2.4 Results and discussion

2.4.1 Theophylline-amine binding studies

The liquid cell FT-IR trace of 0.015 mol L^{-1} free theophylline in water (Figure 2.1) at pH 9.6 displayed characteristic peaks of the C=O stretching at 1600 – 1700 cm^{-1} (Mobaraki & Hemmateenejad 2011) and the C=N stretching at 1580 - 1520 cm^{-1} (Suydam 1963) of in great agreement to the previously reported FT-IR studies (Nafisi et al. 2012; Malathi 2012; Kustin et al. 1971). Structurally, theophylline has two carbonyl groups, C_2-O_{11} and C_6-O_{13} which are linked to the N_1 atom. The C=O assignments of theophylline are complexed by the tautomerization of this molecule caused by the ability of the C=N of theophylline to switch positions between the N_7 and N_9 (Figure 2.2) which have distinguishable IR frequencies from each other (Table 2.1). This generated four C=O peaks and two C=N peaks all of which could be assigned using the literature (Table 2.2).

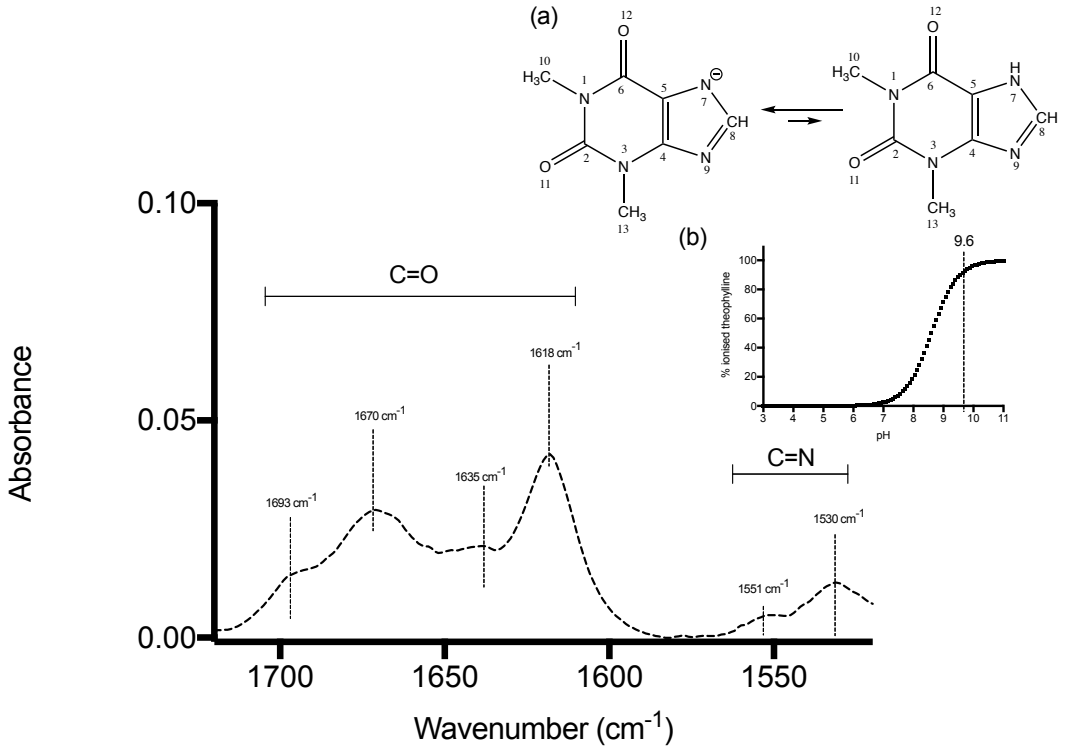

Figure 2.1 The liquid cell FT-IR spectrum of 0.015 mol L^{-1} theophylline in D_2O at pH 9.6 (± 0.1). The insert figures show (a) the chemical structure of neutral and deprotonated theophylline at pH 9.6 and (b) predicted microspeciation plot of theophylline against pH. Note that at pH 9.6, a significant percentage of theophylline is in the deprotonated form (Marvinsketch).

Table 2.2 IR stretching frequencies (cm^{-1}) of theophylline tautomers (Singh 2015)

Functional group	Experimental frequencies (cm^{-1})	
	Tautomer N_7-H	Tautomer N_9-H
$C_2=O_{11}$	1670	1693
$C_6=O_{12}$	1618	1635
C=N stretching	1530	1551

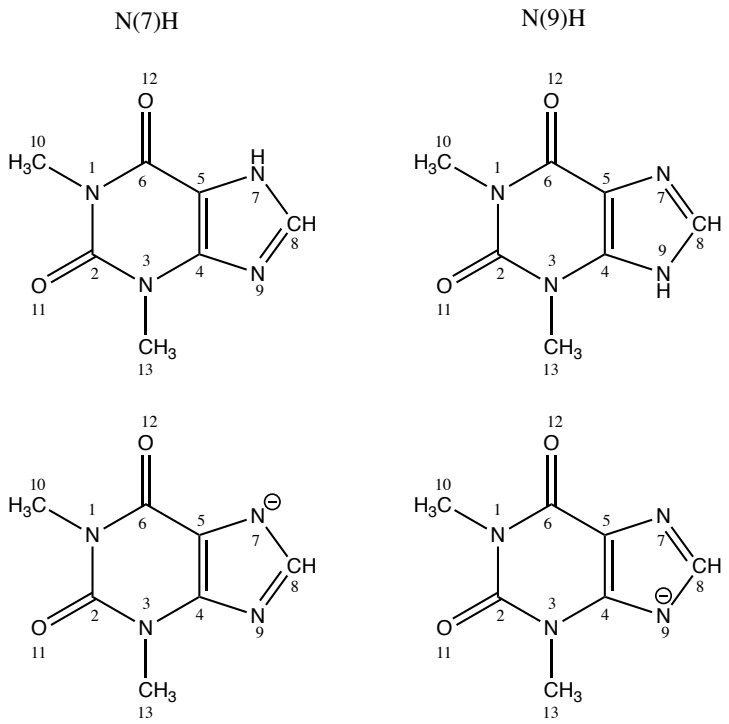

Figure 2.2 Chemical structures of the two most stable tautomers of neutral and deprotonated theophylline (Singh 2015).

Mixing theophylline with increasing level of amines while maintaining the pH at 9.6 led to a gradual increase in the absorbance of the two C=O peaks of theophylline at 1670 and 1618 cm^{-1} of the N_7 tautomer and a gradual decrease of the other two C=O peaks at 1693 and 1635 cm^{-1} of the N_9 tautomer. It is also interesting to note a gradual increase in the peak height ratio between the two C=N theophylline peaks (1530/1551 cm^{-1}) when the drug was mixed with excess counter-ions (Figures 2.3 – 2.4). Changes in the IR spectrum of the complex when compared to the spectrum of the free drug provide evidence for the direct associations of the two molecules (Nafisi et al. 2012; Kustin et al. 1971; Malathi 2012). The FT-IR peak shifts indicated that the C=O and C=N of theophylline were actively involved in the non-covalent bonding with amines. Similar observations were reported by Marta et al. (2009) when studied the ionic hydrogen bond interaction between protonated theophylline and

ammonia using infrared multiphoton dissociation (IRMPD). Nafisi et al. (2012) also reported changes in the C=N and C=O of theophylline when complexed with cadmium (Cd^{2+}), mercury (Hg^{2+}), strontium (Sr^{2+}) and barium (Ba^{2+}) in an aqueous solution at physiological pH using FT-IR.

The suppression of the N_9-H tautomer of theophylline signals at 1693, 1635 and 1550 cm^{-1} when excess amines were added to the mixtures evidenced that the formation of the non-covalent interactions between theophylline and amines may have also perturbed the equilibrium of the tautomeric conversion process between the N_7-H and N_9-H tautomers of theophylline. Reports on the structural complexation of theophylline indicate that C_6=O carbonyl site, which is in close proximity with the N_7-H position is involved in the formation of intermolecular hydrogen bonds, which could explain the conformational preference of the N_7-H tautomer over the N_9-H tautomer. Stasyuk & Krygowski (2014) and Huang et al., (2011) previously reported the same effect of drug complex formation between metals and adenine. A similar trend was observed for all amine counter-ions.

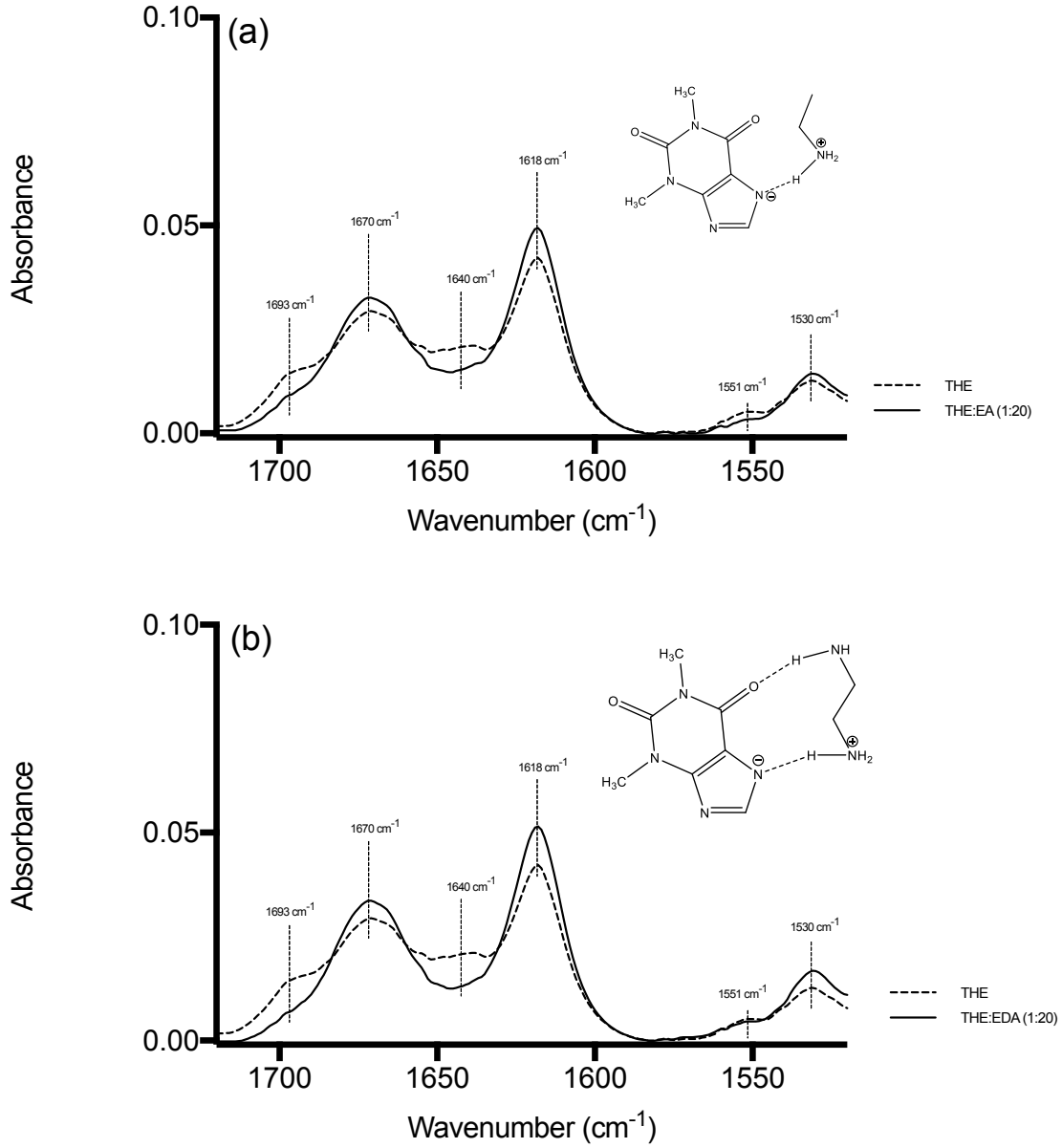

Figure 2.3 The liquid cell FT-IR of free theophylline (0.015 mol L^{-1}) (*dotted lines*) and theophylline (0.015 mol L^{-1}) mixed with 0.3 mol L^{-1} of (a) ethylamine and (b) ethylenediamine (*continuous lines*) from 1520-1750 cm^{-1} wavenumber in 0.5 M ionic solution pH 9.6 $\pm$ 0.1. Insert figures are the proposed structures of the complexes. The dotted line indicates possible hydrogen bonding between the two molecules. THE-theophylline, EA – ethylamine, EDA – ethylenediamine. The insert figures indicate the proposed structures of the ion-pair complexes. Dotted lines indicate possible hydrogen bonding.

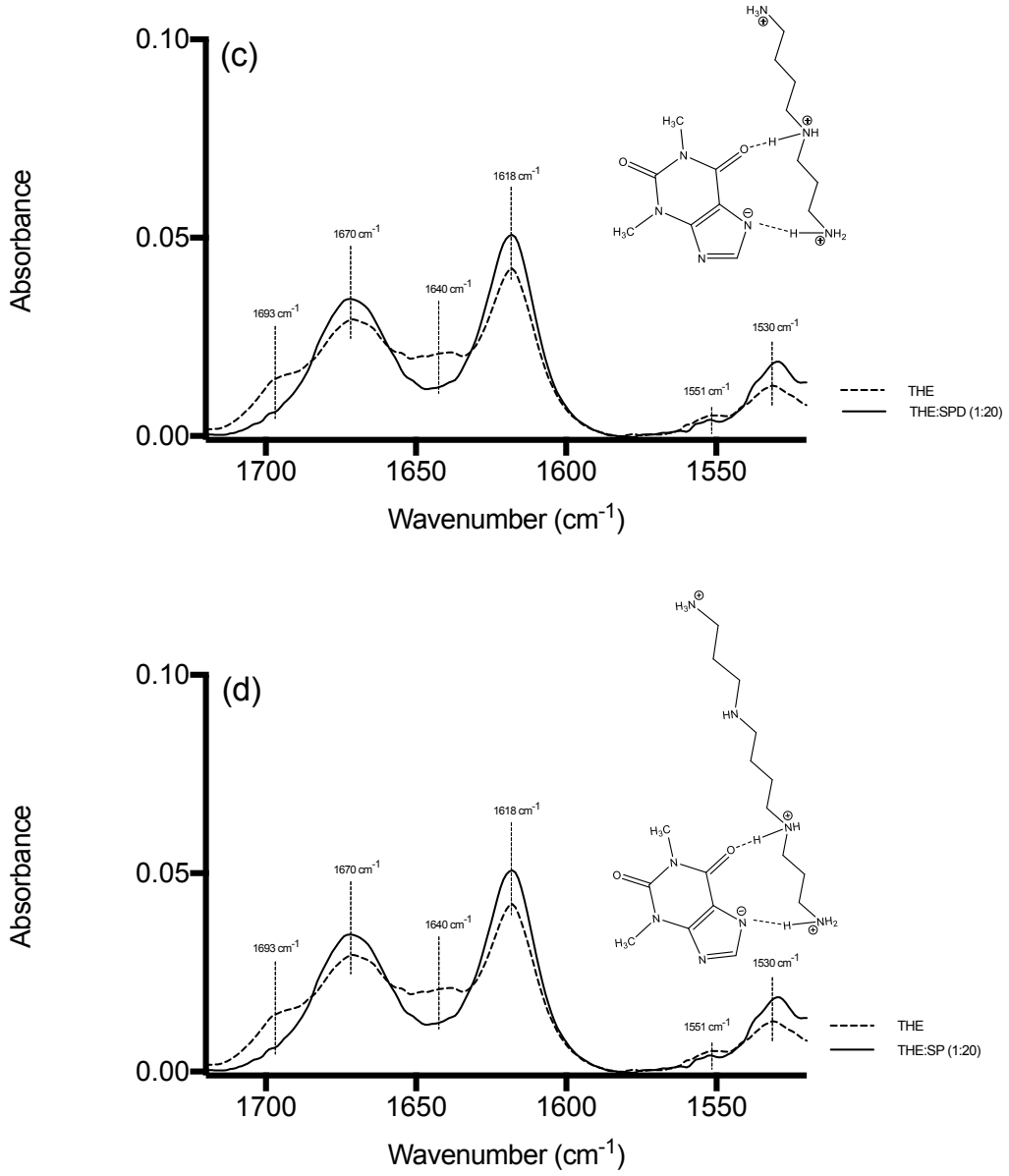

Figure 2.4 The liquid cell FT-IR of free theophylline (0.015 mol L^{-1}) (*dotted lines*) and theophylline (0.015 mol L^{-1}) mixed with 0.3 mol L^{-1} of (c) spermidine and (d) spermine (*continuous lines*) from 1520-1750 cm^{-1} wavenumber in 0.5 M ionic solution pH 9.6 $\pm$ 0.1. The dotted line indicates possible hydrogen bonding between the two molecules. THE – theophylline, SPD – spermidine, SP – spermine. The insert figures indicate the proposed structures of the ion-pair complexes. Dotted lines indicate possible hydrogen bonding.

The theophylline-amine association curves derived from the IR data were fitted with a Sigmoidal model ($R^2 > 0.97$) (Figure 2.5). It was found that theophylline bound stronger to spermine than spermidine followed by ethylenediamine and the least with ethylamine (Table 2.3).

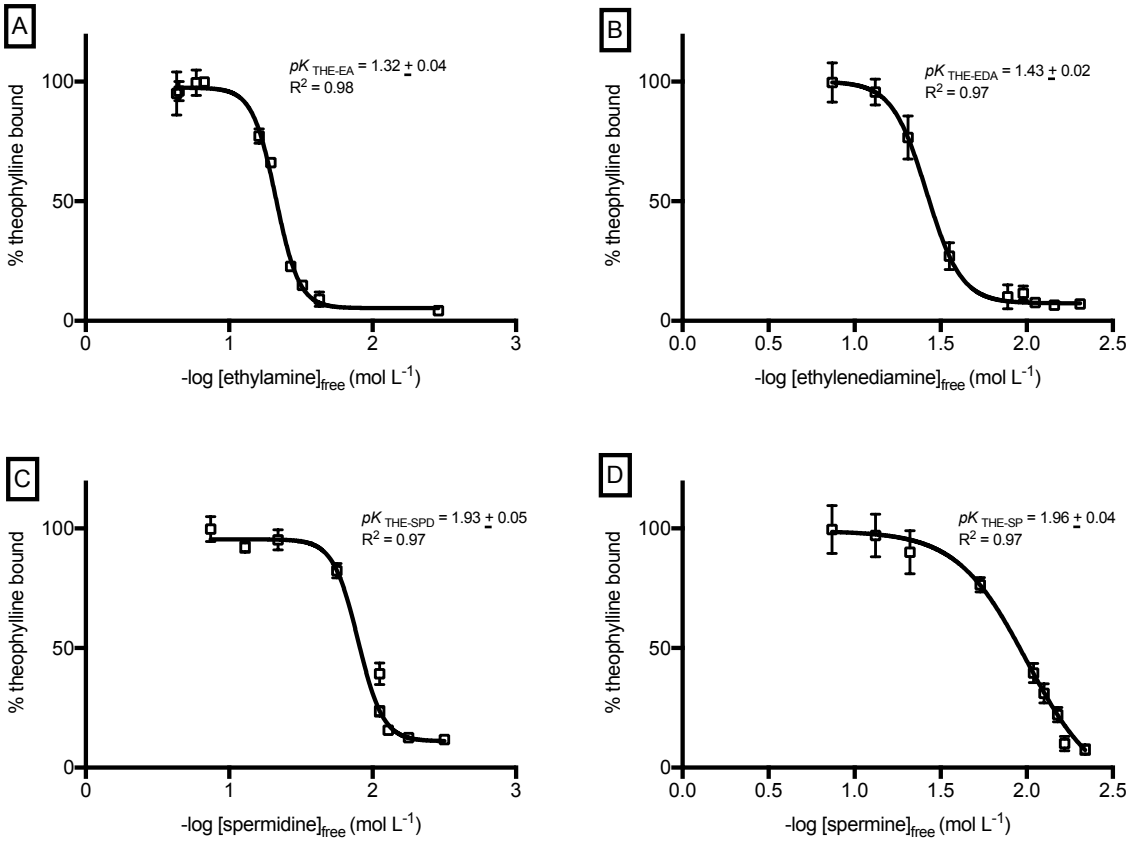

Figure 2.5 Theophylline-amine associations curves at pH 9.6 ± 0.1, 21 ± 2 ^{o}C. The values represent n=3 ± SD. The association curves were fitted with a sigmoidal regression model (GraphPad Prism 7) to determine the THE-amine FT-IR conditional binding constants (pK_{FT-IR}) which were determined at 50 % of bound theophylline. (A) Theophylline-ethylamine association, (B) theophylline-ethylenediamine association, (C) theophylline-spermidine association and (D) theophylline-spermine association.

The stronger intermolecular association between theophylline-polyamine counter-ions compared to theophylline-monoamine counter-ion could be due to higher hydrogen capacity of polyamines counter-ions (spermine = 4, spermidine = 3, ethylenediamine = 2) compared to monoamine (ethylamine = 1). A similar observation was reported for indomethacin (IND) complexed with arginine (ARG) and lysine (LYS). ARG which possessed higher hydrogen binding capacity (13) and was found to bind more strongly to indomethacin ($pK_{IND\text{-}ARG}$ = 3.04) when compared to lysine ($pK_{IND\text{-}LYS}$ = 2.72) which has lower hydrogen binding capacity (9) (Elshaer et al. 2014). Only one possible hydrogen bonding could be formed between the ionized nitrogen of theophylline at the N_7 position with the hydrogen atom of the protonated primary amine of ethylamine. For theophylline-polyamine ion-pair complexes, the first hydrogen bond could occur between the negatively charged nitrogen of theophylline with the hydrogen atom of the ionized primary amine of the polyamines. The second hydrogen between the oxygen atom at the C_6 position and the hydrogen atom of the charged secondary amine of polyamines (but second unionized primary amine for ethylenediamine) increased the total strength of the theophylline-polyamine ion-pair complexes (Figures 2.3-2.4). The interaction between two theophylline with one polyamine i.e., spermine is unlikely to happen due to low percentage of ionization of the N1 and N2 of spermine to initiate the non-covalent interaction between the molecules. Spermine has 4 NH groups with the pKa of 7.94 (N1), 8.83 (N2), 10.09 (N3) and 10.89 (N4). At pH 9.6, the percentage of ionization of these NH groups is as follows: 7.94% (N1), 8.83% (N2), 73% (N3) and 96 % (N4). During HPLC analysis, the retention time of theophylline in the biphenyl column was shortened when increasing concentrations of the counter-ions were mixed in the mobile phase indicating an increase in the interaction of ion-paired theophylline compared to the free form of the drug (Figure 2.6). HPLC analysis was in agreement with the binding affinity trend identified in the IR studies (THE-SP, pK_{HPLC} = 2.81 $\pm$ 0.06; THE-SPD, pK_{HPLC} = 2.79 $\pm$

0.0065; THE-EDA, pK_{HPLC} = 2.49 ± 0.05; THE-EA = pK_{HPLC} = 2.43 ± 0.042.) (Figure 2.7). Nafisi et al., (2012) previously reported a stronger association of theophylline-metals complexes: $pK_{Cd\text{-}theophylline}$ = 5.76, $pK_{Hg\text{-}theophylline}$ = 5.40, $pK_{Ba\text{-}theophylline}$ = 4.48 and $pK_{Sr\text{-}theophylline}$ = 4.66.

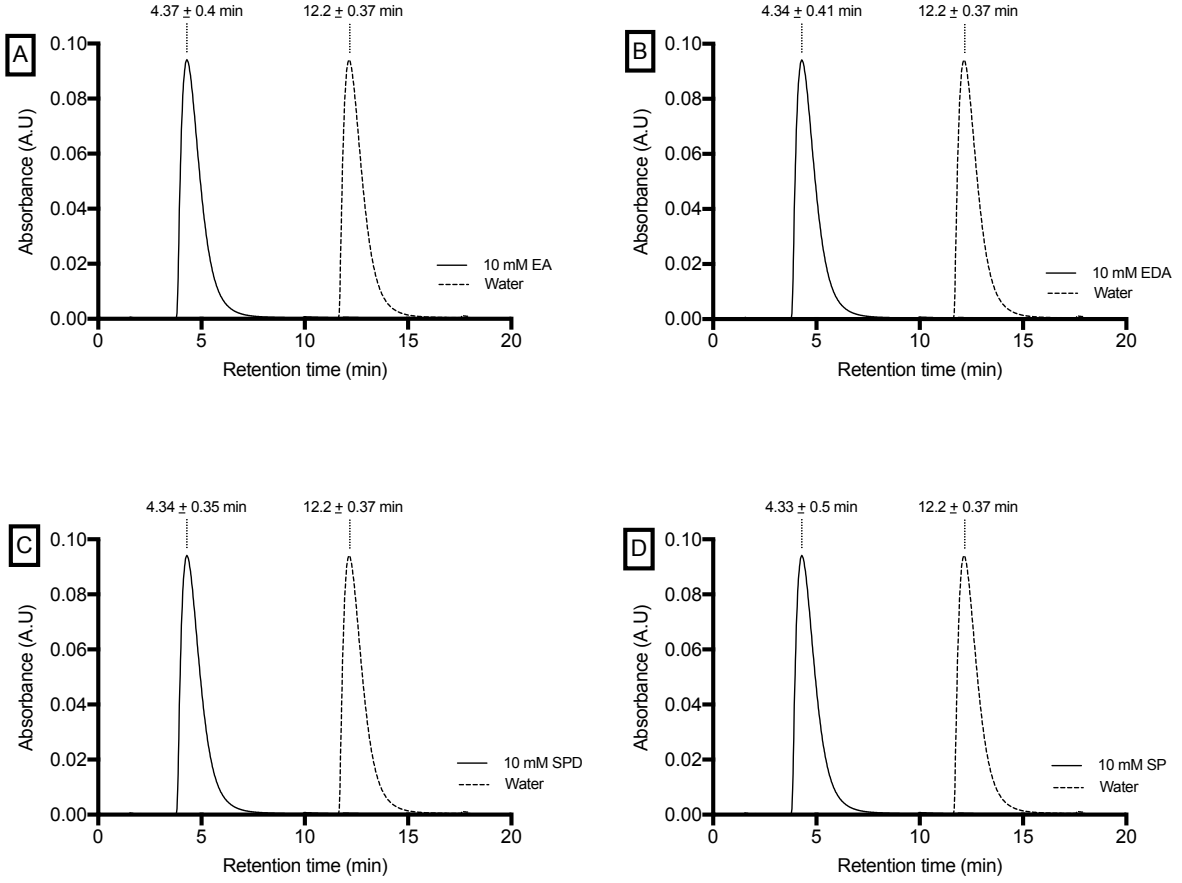

Figure 2.6 The HPLC chromatograms of theophylline. The stationary phase used was a 5 µm biphenyl 100 Å HPLC column 250 X 4.6 mm. The continuous line indicates the HPLC chromatogram of theophylline in a 100% water mobile phase while the dotted lines indicate the HPLC chromatograms of theophylline in 10 mM amine spiked water mobile phase. The pH of all mobile phases used was adjusted to 9.6 ± 0.2 using HCl.

Note that this study was performed at physiological pH where only a small percentage of theophylline was deprotonated: ± 7% deprotonated of theophylline at pH 7.4 vs 100% at pH

9.6. The reported pK values obtained from strong complexes such as divalent transition metal ions-EDTA complexes: $pK_{Zn\text{-}EDTA}$ = 15.7 ± 0.3, $pK_{Ni\text{-}EDTA}$ = 17.1 ± 0.5, $pK_{Cu\text{-}EDTA}$ = 15.0 ± 0.1 (Boija et al. 2014) suggested that theophylline formed a relatively weak ion-pair complexes with amines in solution at pH 9.6.

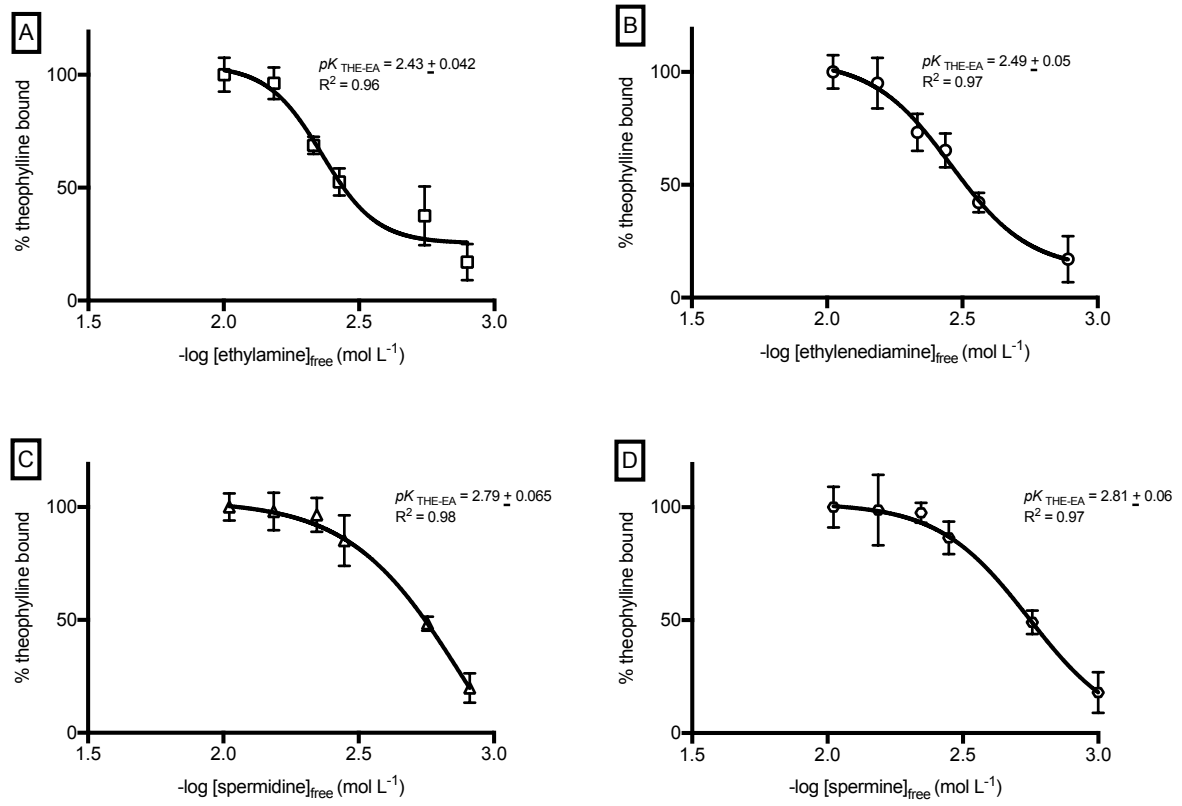

Figure 2.7 Theophylline-amine associations at pH 9.6 ± 0.1, 21 ± 2 ^{o}C determined by HPLC. The values represent n=3 ± SD. The association curves were fitted with a sigmoidal regression model (GraphPad Prism 7) to determine the THE-amines HPLC conditional binding constants (pK_{HPLC}) which were determined at 50 % of bound theophylline from the curves. (A) theophylline-ethylamine association, (B) theophylline-ethylenediamine association, (C) theophylline-spermidine association and (D) theophylline-spermine association.

The ionisation of theophylline (pK_a =8.6) is pH driven which means that a drop of pH from the formulation pH which is 9.6 to the physiological pH 7.4 upon administration would

weaken the theophylline-polyamine ion-pairs and if the strength of the initial association was not strong enough, it would not be sufficient to influence the drug uptake when applied to the biological system due to rapid break down. Using theophylline pK_a value and the $pK_{FT\text{-}IR}$ the strongest ion-pair complex, theophylline-spermine (1.96), the HySS calculations predicted at pH 7.4, ~60 % of theophylline can still ion-paired with spermine using the FT-IR analysis (total concentration of theophylline for IR analysis was 15 mM). However, in the clinic, the administration concentration of theophylline used is far lower. If we then applied the therapeutic concentration of theophylline (0.056 mM), the HySS calculation predicted only ~1% of theophylline of the total theophylline could remain ion-paired to spermine in-vivo (Figure 2.8b).

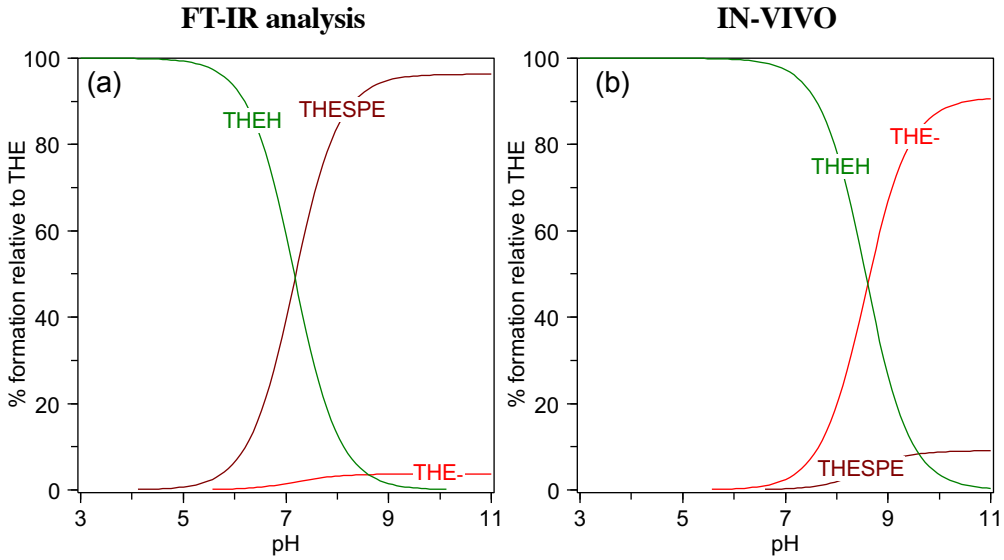

Figure 2.8 An example of HySS microspeciation plots using 1:20 ratio of theophylline-spermine (THE-SPE) as a function of pH. Graph (a) refers to 0.015:0.3 M of theophylline-spermine (this concentration was used in the FT-IR analysis) and graph (b) refers to 5.6×10^{-5}:1.11×10^{-3} M of theophylline-spermine mixture (this is the therapeutic concentration of theophylline in the plasma). The predominant species were ionised theophylline (THE^-), theophylline-H (THE-H; Log Beta = 8.6) and theophylline-spermine (THE-SPE; log $Beta_{FTIR}$ = 1.96).

We used the pK_{FT-IR} value instead of the pK_{HPLC} for this calculations since in the HPLC assay, the intermolecular interactions of the ion-pairs might be influenced by the presence of the stationary phase. Based on this prediction, there is a need to control the breaks down of this ion-pair complex when facing a rapid physiological change upon administration. To combat this issue, a biodegradable, non-toxic excipient (*i.e.,* cyclodextrins) could be used to engineer physically stable ion-pair complex. In addition, a careful manipulation of formulation vehicle properties could also be employed to promote ion-pair stability.

Table 2.3 Theophylline-amine conditional binding constants assayed by FT-IR (pK_{FT-IR}) and HPLC (pK_{HPLC}). Values represent n=3 $\pm$ SD.*statistically significant ($p<0.05$) when compared to the pK_{FT-IR} of THE-EA (Student's t-test).

Theophylline-amine	pK_{FT-IR}	R^2	pK_{HPLC}	R^2
Theophylline-ethylamine	1.32 $\pm$ 0.04	0.98	2.43 $\pm$ 0.042	0.96
Theophylline-ethylenediamie	1.43 $\pm$ 0.02	0.97	2.49 $\pm$ 0.05	0.97
Theophylline-spermidine	1.93 $\pm$ 0.05*	0.97	2.79 $\pm$ 0.065	0.98
Theophylline-spermine	1.96 $\pm$ 0.04*	0.97	2.81 $\pm$ 0.06	0.97

2.4.2 Log D and solubility studies

Increasing the levels of amine counter-ions add to the theophylline solution significantly decreased the drug lipophilicity with a greater effect at pH 9.6 compared to pH 7.4 (Figure 2.9 a,b). The decrease in the lipophilicity of the drug when mixed with excess amines suggested that the charges on the amines were not being totally shielded by complexation with theophylline. The high inherent hydrophilicity of all counter-ions (Log P ethylamine = - 0.13; Log P ethylenediamine = - 2.04; Log P spermidine = - 0.66; Log P spermine = - 0.7) could have been also the reason behind the significant drop of the log D values for

theophylline when formed an ion-pair with the amines. When comparing between all theophylline-amines mixtures studied, the magnitude of change was the greatest for theophylline-spermine pair followed by theophylline-spermidine then theophylline-ethylenediamine and the least for theophylline-ethylamine.

The reversed effect was seen in the solubility studies where increasing the levels of amine counter-ions in the theophylline solutions led to a significant increase in the aqueous solubility of theophylline (Figure 2.9 c,d). Mixing theophylline with increasing levels of the amine counter-ions significantly increased its aqueous solubility. The magnitude of change was the greatest for theophylline mixed with spermine $\geq$ spermidine > ethylenediamine > ethylamine. The results demonstrated that ion-pair properties are a function of both the drug and counter-ion properties and when these two elements are held together in a complex it can be more hydrophilic compared to the parent compound. The effects of ion-pair formation on solubility were more apparent at pH 9.6 compared to pH 7.4 presumable due to the greater proportion of ion-pairs formed at the more alkaline pH due to the theophylline's pKa. From the binding studies, theophylline showed the greatest affinity towards spermine > spermidine > ethylenediamine > ethylamine. These results suggested that the magnitude of change in the physiochemical properties of theophylline was not only influenced by the lipophilicity of the amines but also the extent of the intermolecular theophylline-amine ion-pairs associations in the solution state. We expected that the change of the theophylline log D was the greatest when mixed with ethylenediamine due to higher lipophilicity (Log P = -2.04) of this counter-ion compared to the other counter-ions but interestingly, our results showed that the greatest change of theophylline was instead when paired with spermine (Log P = -0.7). Thus, this

suggested that the strength of the ion-pair ($pK_{FT\text{-}IR}$ THE-SP (1.96 ± 0.04 > pK_{FTIR} THE-EDA 1.43 ± 0.02) is key to influence the change in the physiochemical of the drug

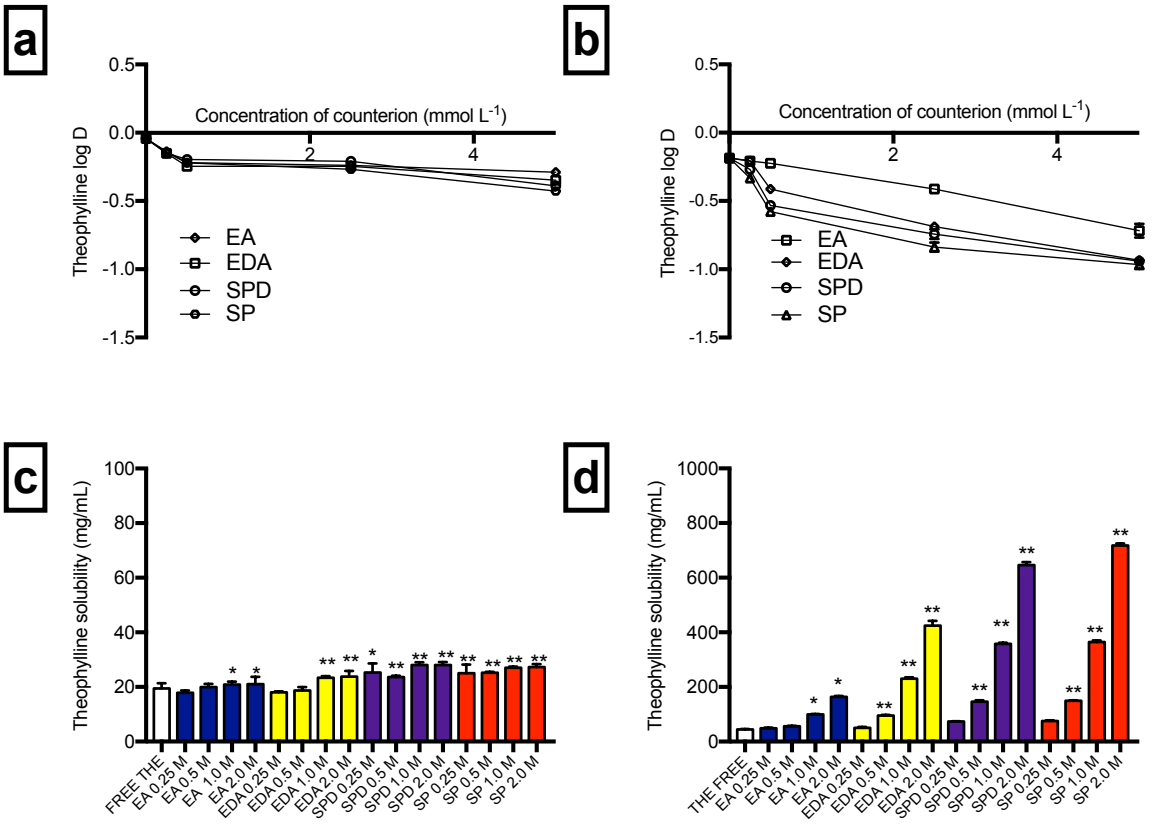

Figure 2.9 The log D profiles at (a) pH 7.4 ± 0.2, (b) pH 9.6 ± 0.2 and the aqueous solubility at (c) pH 7.4 ± 0.2, (d) pH 9.6 ± 0.2 and of theophylline in increasing concentrations of a selection of amine counter-ions. Both studies were performed at 37 ± 1 ^{o}C. THE – theophylline, EA – ethylamine, EDA – ethylenediamine, SPD – spermidine, SP – spermine. Values represent means from n = 3 ± SD. Statistically significant ($p < 0.05$)**($p< 0.001$)(One-way ANOVA) when compared to the solubility of free theophylline.

Similarly, this was previously reported by Samiei et al., (2014) when evaluating the influence of forming amifostine ion-pairs with different counter-ions that have different lipophilicity, shape and flexibility on the lipophilicity of the drug. They found that the magnitude of

change in the drug's lipophilicity was not only dependent on the lipophilicity of the counter-ions and but also the ion-pair association strength.

2.4.3 Stability studies

Theophylline displayed a well-resolved peak with retention time of 7.4 ± 0.03 min (Figure 2.10). The standard calibration curves of theophylline (Figure 2.11) were linear ($R^2 \geq 0.99$) which demonstrated the capacity of the developed technique to generate good results that can be directly associated to the concentration of the drug present in the sample.

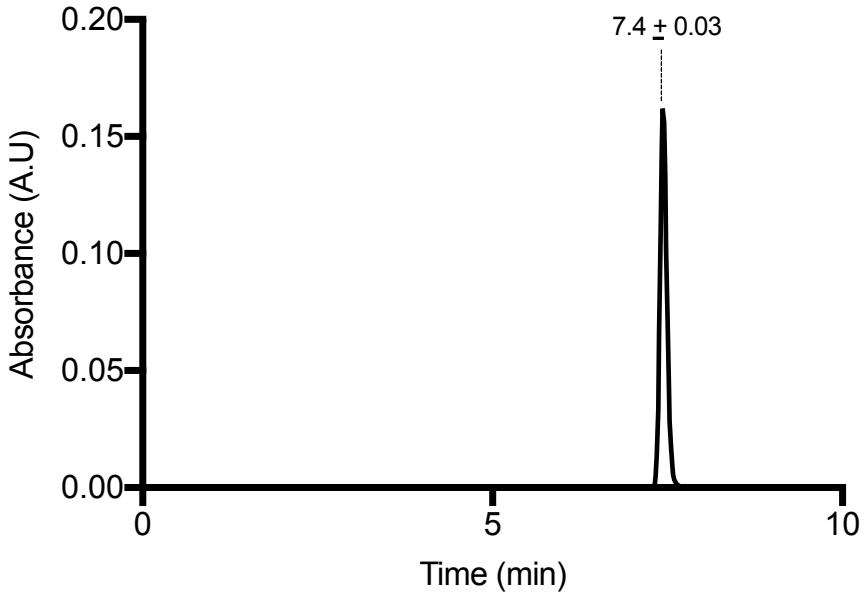

Figure 2.10 Chromatogram of 100 ug mL^{-1} of theophylline in 90:03:07 water:methanol:acetonitrile H_2O:MeOH:ACN (v/v), pH 4.

All validation parameters tested were within the recommended limits by the International Conference of Harmonisation (ICH, 1995) (Table 2.4). Thus, the present developed method was considered to be 'fit-for-purpose'.

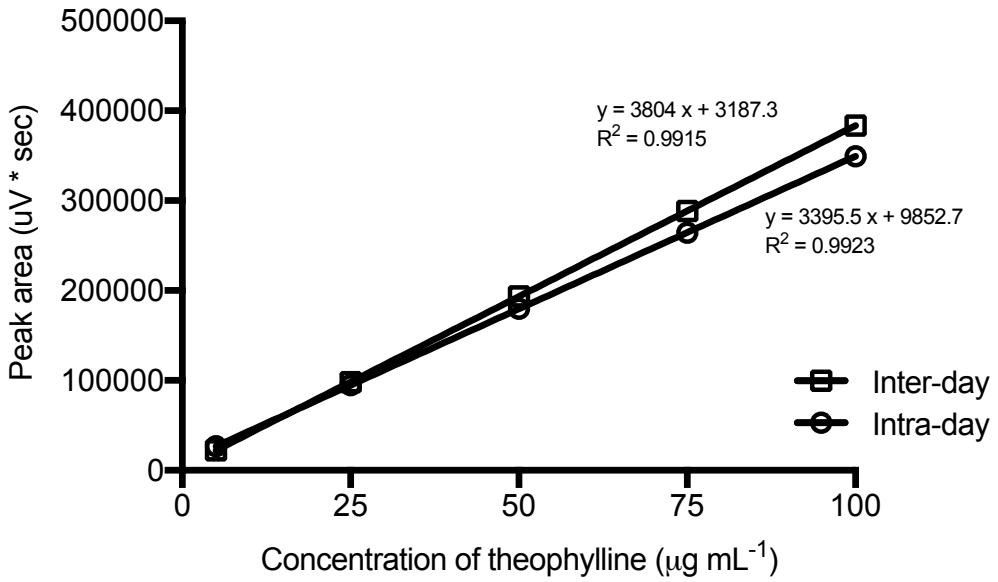

Figure 2.11 Intra-day and inter-day calibration curves of theophylline showing peak area as a function of concentration. Data represents mean ± SD (n=15). Error bars are too small to be seen.

It is crucial to assess the chemical stability of theophylline when mixed with the counter-ions to ensure any subsequent results are not influenced by degradation products. Spermine was used in this study because: (i) the magnitude of change in the physicochemical properties of theophylline was the greatest when theophylline was mixed with spermine compared to other counter-ions and (ii) theophylline-spermine complex will be used in a large number of excess in the subsequent chapters of this thesis.

Table 2.4 A summary of the assay validation data for theophylline and comparisons to the ICH guidelines for analytical method validation (ICH, 1995).

Validation parameter	Compound *Theophylline*	Recommend level/limit by ICH
System suitability		
Linearity (R^2, *n* = 15 calibrations, $\pm$ SD)	0.996 $\pm$ 0.004	> 0.99
Peak symmetry, A_s, (n = 15 $\pm$ SD)	1.14 $\pm$ 0.2	< 2, Ideal A_s = 1
Theoritical plate number, N (n = 15 $\pm$ SD)	17798 $\pm$ 1032	N > 2000
Limit of Detection (μg mL^{-1})	1.24	---
Limit of Quantification (μg mL^{-1})	4.12	---
Precision		
Intra-day variability (repeatability, % CV)	0.39%	< 1%
Inter-day variability (intermediate precision)	< 2%	< 5%
Accuracy (% $\pm$ SD, n = 6)	97.8 $\pm$ 2.1	95 – 105%

The retention of theophylline was consistent at week 1, 2, 3 and 4 when compared to its retention at week 0 (Tables 2.5-2.6). A small change in the retention time of theophylline mixed with spermine compared to the retention of free theophylline could be attributed to the ion-pairing effect. The presence of new peaks in the HPLC chromatograms, which could indicate degradation products of the drug (Blessy et al. 2014) was not detected in any of the samples tested. No significant reduction of theophylline concentration in all samples (calculated from the peak area) was found. Based on these result as summarized in Tables

2.6, it can be concluded that theophylline was found to be chemically stable when mixed with excess spermine at room temperature (21 ^{o}C $\pm$ 0.1), pH 7.4 and 9.6 ($\pm$ 0.2) for up to 4 weeks. It can be noted in the literature that theophylline was also found to be stable in biological fluids (serum, saliva and plasma) up to 1 week at -20, 6 and 25 ^{o}C (Young 1981). The commercial product of injectable theophylline, aminophylline (1 mg mL^{-1}) (a 2:1 complex of theophylline:ethylenediamine) was reported to be stable in 20 % mannitol and 0.9 % NaCl after 20 h at two pH ranges, 6.5 – 7.5 and 10 – 11 where it showed the highest stability at the alkaline pH when assayed using HPLC (Alves et al. 2011).

Table 2.5 Retention time (min), peak area (μV*sec) and percentage recovery of theophylline (1 mg mL^{-1}/ 5.56 mmol L^{-1}) when mixed with 50 and 100 mmol L^{-1} of spermine pH adjusted to 9.6 (± 0.2) stored in the dark at room temperature (21 ± 2 ^{o}C) at week 0, 1, 2, 3 and 4 when assayed using RP-HPLC.

Treatment, concentration of spermine (mmol L^{-1})	**Retention time of theophylline (min) (*n*=3 ± SD)**	**Time (week)**	**Peak area (μV*sec) (*n*=3 ± SD)**	**% recovery = (peak area (w1/2/3/4) /peak area (week 0) *100 (*n*=3 ± SD)**
0	7.40 ± 0.03	0	336449 ± 5070	100
	7.43 ± 0.05	1	335635 ± 4115	99.75 ± 0.11
	7.44 ± 0.09	2	337111 ± 3090	100.20 ± 0.09
	7.45 ± 0.07	3	336449 ± 4115	100.19 ± 0.10
	7.44 ± 0.05	4	336449 ± 5070	100.73 ± 0.11
50	7.39 ± 0.11	0	350045 ± 5361	100
	7.38 ± 0.09	1	354541 ± 5091	100.28 ± 0.11
	7.39 ± 0.11	2	351187 ± 4361	100.33 ± 0.09
	7.37 ± 0.06	3	349089 ± 4441	99.73 ± 0.09
	7.38 ± 0.09	4	351172 ± 5361	100.32 ± 0.12
100	7.34 ± 0.10	0	361172 + 4524	100
	7.35 ± 0.07	1	362387 ± 3019	100.34 ± 0.06
	7.31 ± 0.10	2	362291 ± 2981	100.31 ± 0.05
	7.32 ± 0.09	3	364019 ± 4531	100.79 ± 0.08
	7.33 ± 0.11	4	361198 ± 4401	100.01 ± 0.07

Table 2.6 Retention time (min), peak area (μV*sec) and percentage recovery of theophylline (1 mg mL^{-1}/ 5.56 mmol L^{-1}) when mixed with 50 and 100 mmol L^{-1} of spermine pH adjusted to 7.4 (± 0.2) stored in the dark at room temperature (21 ± 2 ^{o}C) at week 0, 1, 2, 3 and 4 when assayed using RP-HPLC.

Treatment, concentration of spermine (mmol L^{-1})	**Retention time of theophylline (min) (*n*=3 ± SD)**	**Time (week)**	**Peak area (μV*sec) (*n*=3 ± SD)**	**% recovery = (peak area (w1/2/3/4) /peak area (week 0) *100 (*n*=3 ± SD)**
0	7.40 ± 0.03	0	336449 ± 5070	100
	7.43 ± 0.05	1	335635 ± 4115	99.75 ± 0.11
	7.44 ± 0.09	2	337111 ± 3090	100.20 ± 0.09
	7.45 ± 0.11	3	336449 ± 4115	100.19 ± 0.10
	7.44 ± 0.04	4	336449 ± 5070	100.73 ± 0.11
50	7.41 ± 0.05	0	350045 ± 5361	100
	7.41 ± 0.10	1	354541 ± 5091	100.28 ± 0.11
	7.35 ± 0.09	2	351187 ± 4361	100.33 ± 0.09
	7.37 ± 0.06	3	349089 ± 4441	99.73 ± 0.09
	7.39 ± 0.06	4	351172 ± 5361	100.32 ± 0.12
100	7.38 ± 0.09	0	361172 + 4524	100
	7.39 ± 0.06	1	362387 ± 3019	100.34 ± 0.06
	7.38 ± 0.10	2	362291 ± 2981	100.31 ± 0.05
	7.35 ± 0.11	3	364019 ± 4531	100.79 ± 0.08
	7.38 ± 0.09	4	361198 ± 4401	100.01 ± 0.07

2.5 Conclusion

Theophylline was found to form ion-pair complexes with all the amine counter-ions tested when dissolved in water at pH 9.6. Spermine showed the strongest binding to theophylline followed by spermidine then ethylenediamine and ethylamine when assayed using FT-IR and HPLC. Forming polyamine ion-pairs with theophylline was shown to significantly decrease the drug's lipophilicity and increase its aqueous solubility. The change in the physicochemical properties of the drug was found to be dependent on how strong the drug binds the counter-ions. However, the theophylline-polyamine ion-pairs complexes formed were found to be relatively weak. Upon administration, due to rapid dilution, a significant drop of pH as well as binding competition from other charged species to the drug, it was thought that the theophylline-polyamine ion-pair was likely to dissociate. It was thought that through complexation with cyclodextrins and manipulation of formulation vehicle, a more physically stable ion-pair could be formed. These sections will be discussed in the subsequent chapters of this thesis.

CHAPTER 3

CHARACTERIZATION OF CYCLODEXTRIN-THEOPHYLLINE-POLYAMINE COMPLEXES

Chapter summary:

Chapter 3 characterized the formation of cyclodextrin complexes with theophylline-spermine ion-pair in water using NMR. Three types of cyclodextrins namely beta-cyclodextrin, 2-hydroxypropyl-beta-cyclodextrin and gamma-cyclodextrin which have different physicochemical characteristics were used. A continuous variation method (Job's plot) was employed to establish the stoichiometry of the complexes formed. Using the 3D molecular docking technique, the proposed structure of the complex was presented.

3.1 Introduction

In Chapter 2, the association of theophylline-polyamine ion-pair was found weak and prone to dissociation. The instability of this interaction was thought could be enhanced by formulating with cyclodextrins. Cyclodextrins (CDs) have been found to have the ability to alter the physicochemical properties of the entrapped guest molecules through the formation of inclusion complexes (Wouessidjewe et al. 1999). CDs are cyclic (α-1,4)-linked-oligosaccharides that display a cone-shape with a hollow tapered cavity (Horiuchi et al. 1990). The size of the top and bottom diameters is dependent on the number of glucopyranose units (Figure 3.1).

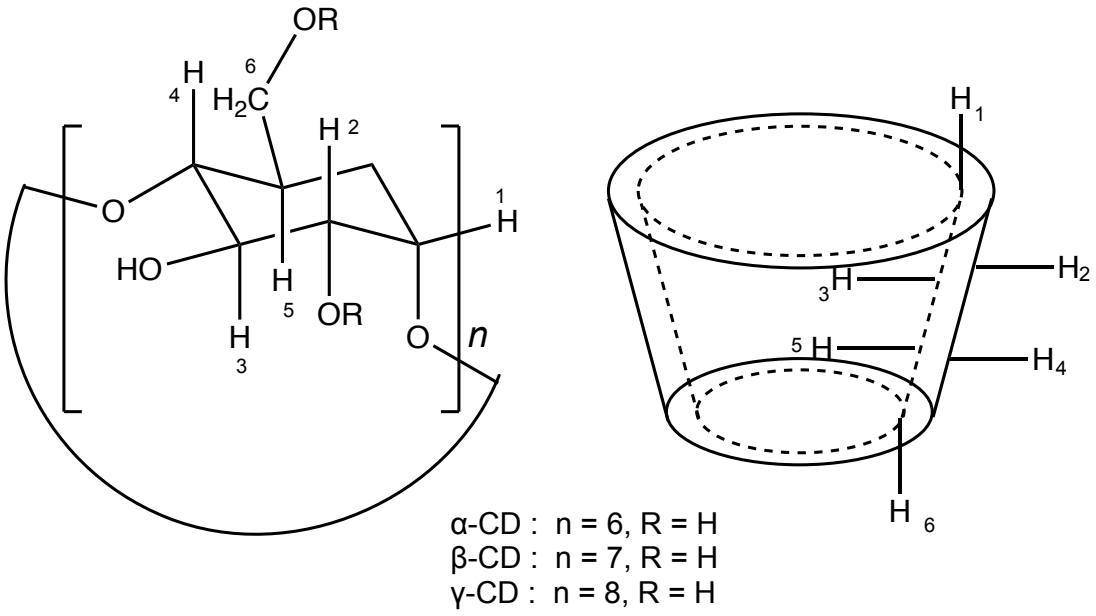

Figure 3.1 The chemical structure and the truncated cone-shape of the three most common parent cyclodextrins. n = 6, 7 and 8 for α-, β-, and γ-cyclodextrin, respectively (Roy et al. 2016).

The three most common types of parent CDs are α-, β-, and γ-CDs (Table 3.1). They are composed of 6, 7 and 8 glycopyranose units, respectively. The exterior surface is hydrophilic while the central cavity is relatively hydrophobic (Horiuchi et al. 1990). CDs with ten or more ring member units can be theoretically synthesized, but due to their expected high solubility and poor complex ability, it seems unlikely that they will be used in the pharmaceutical industry. Whilst for CDs with fewer than six ring members, they cannot be formed due to steric reasons (Szejtli 1998). CDs derivatives can be formed through disruption of hydrogen bonding via molecular manipulation including substitution of any of the hydrogen bonding forming hydroxyl groups by hydrophobic moieties including methoxy and ethoxy which often results in modification of the CD physicochemical properties (Wouessidjewe et al. 1999).

Table 3.1 Some characteristics of α-, β-, and γ-cyclodextrin (Szejtli 1998)

	α	β	γ
No of glucose units	6	7	8
Molecular weight	972	1135	1297
Central cavity diameter (Å)	4.7 – 5.3	6.0 – 6.5	7.5 – 8.3
Water solubility at 25 ^{0}C (g/100 mL)	14.5	1.85	23.2

Hydroxypropyl-beta-cyclodextrin (HPβ-CD) is an example of a modified form of natural β-CD that has an aqueous solubility of > 600 mg mL^{-1} while the parent β-CD only possesses an aqueous solubility of 1.85 mg mL^{-1}. Through a host-guest interaction (Figure 3.2), complexation with CD can result in solubility enhancement of water-insoluble guests, stabilization of labile guests against degradative attack, control of physical state, taste

masking, suppressed of unpleasant odours and controlled release (Szejtli 1998; Juluri & Narasimha Murthy 2014; Wouessidjewe et al. 1999). The type of guest that can be accepted by cyclodextrins varies from straight or branched aliphatics, aldehydes, ketones, alcohols, organic acids, fatty acids, aromatics, gaseous, and polar compounds such as halogens, oxyacids and amines (Szejtli 1998). Approximately 30 pharmaceutical formulations containing CDs are now available in the market worldwide of which three of them were marketed as intravenous, i.v. pharmaceutical products. The natural CDs are listed in the list of FDA as generally regarded as safe (GRAS) for use in food additive while both modified forms of β-CD which are HP-β-CD and SBE-β-CD are listed as inactive pharmaceutical ingredients in the FDA list (Stella & He 2008). This highlights the high possibility to formulate a safe, non-toxic i.v. formulation containing CDs.

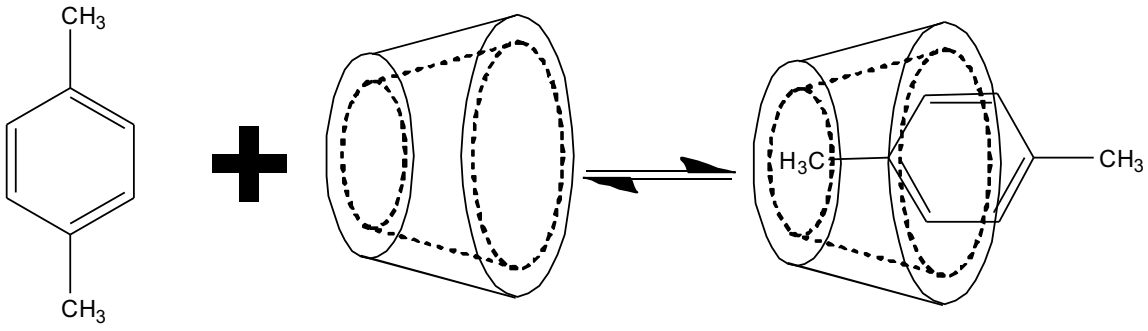

Figure 3.2 A typical representation of a binary 1:1 host-guest cyclodextrin complex structure

The interactions between host (H) and guest (G) are normally recognized as combinations of several non-covalent interactions which include ionic, dipolar, π and van der Waals interactions, hydrogen bonding and hydrophobic association. Even though most of the CD complexations studies were reported for the binary 1:1 host-guest complexes, there have been

studies using ternary CD complexes which refer to the systems composed of three different molecular entities: drug/CD/metal ion (He et al. 2011), drug/CD/organic ion (Granero et al. 2008; Hamai 2009), drug/CD/polymer (Loftsson et al. 2003), $drug_1$/CD/$drug_2$ (Higashi et al. 2010), drug/CD_1/CD_2 (Jansook & Loftsson 2008) and drug/CD/liposomes (Cabeça et al. 2011; Cirri et al. 2009). Often, the third together with CDs optimized the efficacy of a drug and this suggests that it could be possible to use a CD complex to stabilize the theophylline-polyamine ion-pairs.

In the case of the ternary complexes, the aqueous solubility of doxycycline was 4-fold increased when a metal ion, 0.5% (w/v) Mg^{2+} which acted as the third component was added to the doxycycline/HPβ-CD (1:1) mixture solution (He et al. 2011). In another study by Jansook & Loftsson 2008, they showed the aqueous solubility of indomethacin increased by 30-50% when a mixture of HPβ-CD and γ-CD was added to the drug solution compared when just using one type of CD to complex with the drug. Organic ions were mostly used to improve the affinity of an ionized drug to the CD cavity. The electrostatic interaction between the oppositely charged drug and a counter-ion neutralized the charge of the drug molecule resulting in a more stable complex formation. This was previously also seen in a binary pyrene sulfonate (PS): γCD complex where the presence of the cationic organic additives neutralized the sulfonate moiety of PS which was negatively charged forming a 2-fold stronger complex compared to the charged PS-CD complex (Hamai 2009).

It was thought that CD could be employed in this present study to promote a stable theophylline-polyamine ion-pair complex in the solution state. This inclusion process could offer to shield the labile theophylline-polyamine guest complex from the degradative aqueous environment hence controls the breaking down of this ion-pair complex. If this can be

achieved, the release rate of theophylline could be controlled which could result in an improved uptake of the drug into the lung tissue. At pH <12, CDs do not deprotonate hence they will show a greater affinity towards the neutral part of the ion-pair complex than the ionized regions of the ion-pair (Gaidamauskas et al. 2009). The aim of this chapter was to characterize the supramolecular assemblies of the theophylline-spermine ion-pair complex with three different types of cyclodextrins: β-CD, HPβ-CD and γ-CD in aqueous at pH 9.6 using NMR. This technique has been extensively used to characterize CD complexes in the literature due to its high sensitivity and ability to ascertain information about the inclusion complex on the atomic level (Kundu et al. 2017; Aksamija et al. 2016; Roy et al. 2016).

3.2 Materials

Theophylline (THE) (anhydrous, ≥ 99%), spermine (SP) (≥ 99%), deuterium oxide (D_2O) (D atom > 99%), sodium hydroxide (NaOH), hydrochloric acid (HCl), beta-cyclodextrin (β-CD), gamma-cyclodextrin (γ-CD) and 2-hydroxypropyl-beta-cyclodextrin (HPβ-CD) were purchased from Sigma-Aldrich, UK.

3.3 Methods

3.3.1 NMR measurements

The FT-IR method was not used in this chapter due to the overlapping IR peaks of cyclodextrins with theophylline IR peaks. Therefore, NMR method was used instead. All ^{1}H-NMR spectra were acquired at 300 ± 0.1 K using a Bruker Advance 400 MHz spectrometer

with a broad band inverse probe equipped with *x, y* and *z* gradients. The chemical shifts were referenced to the D_2O signal at 4.700 ppm that was consistent in all spectra measured. For each ^1H NMR experiment, 16 transients were collected into 65536 points over a 4010 Hz spectral window using 1 s relaxation delay. Prior to Fourier transformation the free induction decays (FIDs) were zero filled with 63 536 points and apodized by multiplication with an exponential decay to 1 Hz line broadening. A rotational overhauser enhancement experiment (ROESY) for detection of intermolecular nuclear overhauser effects (NOEs) between β-CD and the theophylline-spermine ion-pair (assuming a 1:1 THE-SP complex was formed when theophylline and spermine were mixed at 1:20 drug-spermine molar ratio) was conducted for the inclusion complex (1:1 molar ratio of β-CD:[THE-SP]) at 298 K. The 2D ROESY spectrum was collected with mixing time of 300 ms under the spin lock condition.

3.3.2 Theophylline-spermine binding

The NMR conditional binding constant (pK_{NMR}) of theophylline-spermine was assessed by titrating increasing concentration of spermine into the theophylline solutions prepared in D_2O. The concentration of theophylline was fixed at 5 mM whilst the concentration of spermine varied from 0 – 100 mM. The pH of all mixtures was adjusted to 9.6 using HCl. Changes in the proton signals of theophylline upon mixing with excess spermine were used to establish the theophylline-spermine association curve. The percentage of theophylline bound *vs* $-\log[\text{spermine}]_{free}$ were plotted and fitted with a regression model (GraphPad Prism7) to determine the pK_{NMR} of theophylline-amines complexes in D_2O. Results were presented as mean of n=3 ± SD.

3.3.3 Job's plot

The continuous variation method employed was in accordance with the previous studies (Roy et al. 2016; Korytkowska-Wałach et al. 2017). A series of solutions containing mixtures of β-CD/HPβCD/γ-CD with THE-spermine ion-pair at different CD-ion-pair molar ratios were measured. The total concentration of the interacting species [CD + (THE-SP)] in the solutions was kept constant at 5 mM. The molar fraction (*r*) of [CD]/[CD mixture] varied in the range of 0.1 – 0.9. The pH of all mixtures was kept at 9.6 ± 0.1. Any pH adjustment was made using HCl. Results were presented as mean n=3 ± SD.

3.3.4 Molecular docking studies

The atomic coordinates for theophylline and spermine were from the PubChem database (Bolton et al, 2011). For beta-cyclodextrin, the atomic coordinates were accessed through the Crystallography Open Database and taken from the dataset provided by Pop et al. (2002). Modelling of the ternary inclusion complex was carried out using Hyperchem™ and the structure was optimised using Polak-Ribiere conjugate gradient minimisation of the potential energy to an rms gradient of 0.001 kcal/(mol.Å). Images were generated using Discovery Studio Visualizer (Accelrys Inc, CA, USA).

3.4 Results and discussion

The ^{1}H-NMR spectrum of theophylline in D_2O, pH 9.6 revealed three singlet proton peaks (Figure 3.3). The peak at 7.579 ppm was assigned to the C_8-H of theophylline whilst the peaks at 3.303 and 3.489 ppm were assigned to the C_{10}- and C_{12}-H of theophylline which was in line with the literature (Terekhova et al. 2007). The hydrogen at N_7-H of theophylline was not visible in the spectrum due to deprotonation at pH 9.6. For spermine molecule, a singlet at 1.821 ppm was assigned to the C-H2 of spermine whilst the peaks at 1.569 ppm and at 2.882 ppm were assigned to the C-H1 and C-H3 of spermine, respectively. The N-H hydrogens of spermine were not detectable due to the proton exchange with the D_2O molecule. Addition of increasing level of spermine to the theophylline solution while maintaining the pH at 9.6 caused upfield shifts of theophylline protons which could be attributed to the ion-pairing effect (Figure 3.3). Of the three proton signals of theophylline, the proton at C_8-H was mostly affected upon forming ion-pair with spermine (Table 3.2). This might be due to its position. It was in close proximity to the N_7 of theophylline which was thought to be actively in contact with the spermine molecule through hydrogen bonding (Figure 3.3). Change in the chemical shift of the C_8-H of theophylline when mixed with increasing level of spermine was used to establish the theophylline-spermine association curve fitted with a Sigmoidal model ($R^2 > 0.99$) (Figure 3.4). From this model, the pK_{NMR} of theophylline-spermine was 1.51 ± 0.015.

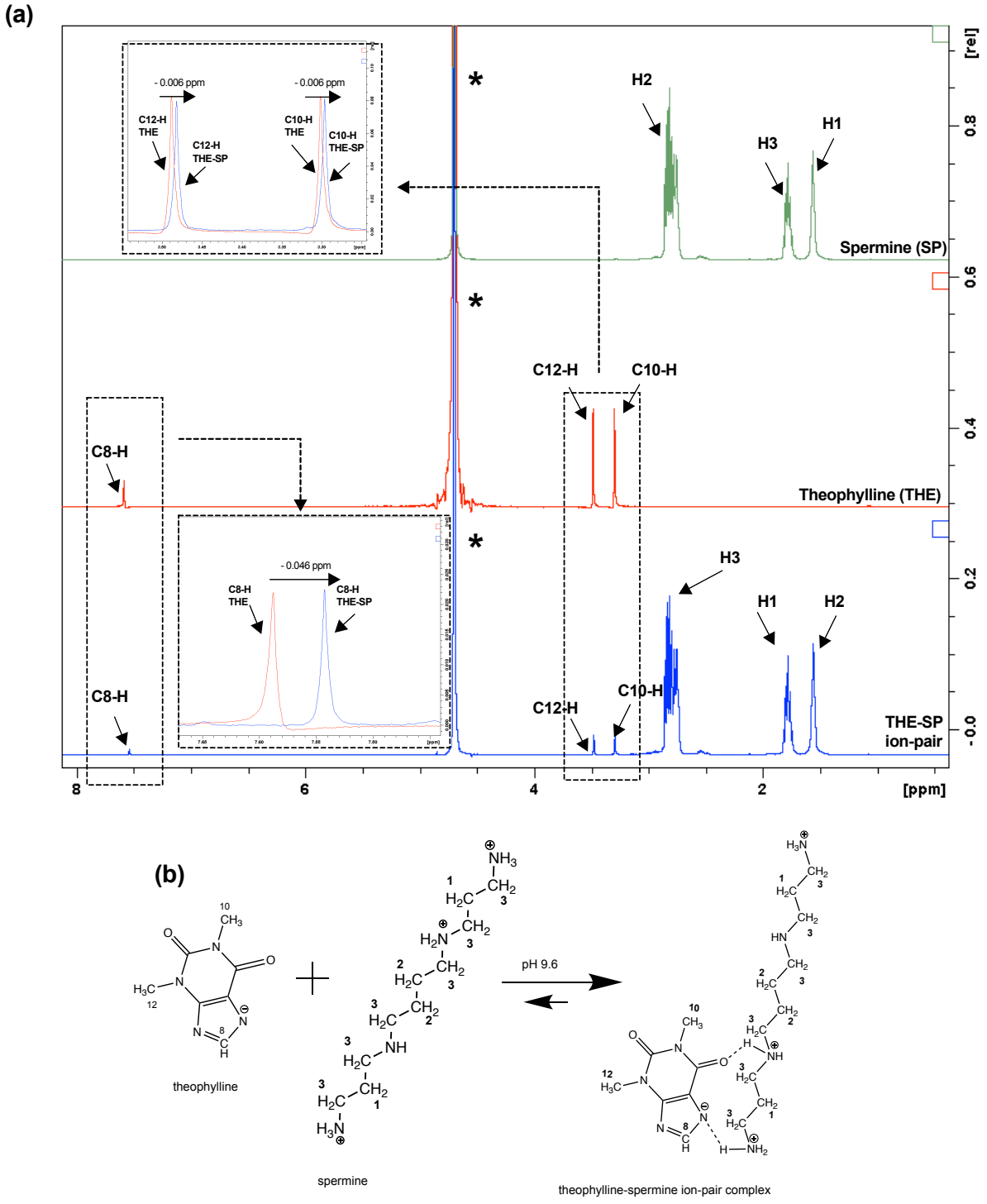

Figure 3.3 (a) The ^{1}H-NMR spectra of 0.005 M theophylline (*bottom graph*), 0.1 M spermine (*middle graph*) and theophylline-spermine 0.005:0.1 M mixture (*top graph*) in D_2O pH 9.6 $\pm$ 0.1 and (b) the proposed chemical structure of the ion-pair complex. Dotted lines indicate possible hydrogen bonding. * asterisk highlights the D_2O signal.

The shifts of the hydrogen signals of spermine when mixed with theophylline at 20:1 spermine:theophylline molar ratio were also affected but this change was small, which could be due to the broad multiple signals of the spermine and the free unbound spermine in the system. Of three proton signals of spermine, H-3 of spermine showed the greatest change compared to the H-1 and H-2 of spermine, this proton was adjacent to the hydrogens of the ionized primary and secondary amines of spermine which were postulated to form a link with theophylline through hydrogen bonding.

Table 3.2 Chemical shifts of free theophylline (5 mM), spermine (100 mM) and theophylline-spermine mixture (5:100 mM)

Compound	C-H protons	Chemical shift (ppm)		
		Free	Complex (1:20)	Complex-Free
Theophylline	C_8-H	7.589	7.543	- 0.046
	C_{10}-H	3.303	3.297	- 0.006
	C_{12}-H	3.489	3.483	- 0.006
Spermine	H-1	1.821	1.822	- 0.001
	H-2	1.569	1.563	- 0.003
	H-3	2.882	2.879	- 0.004

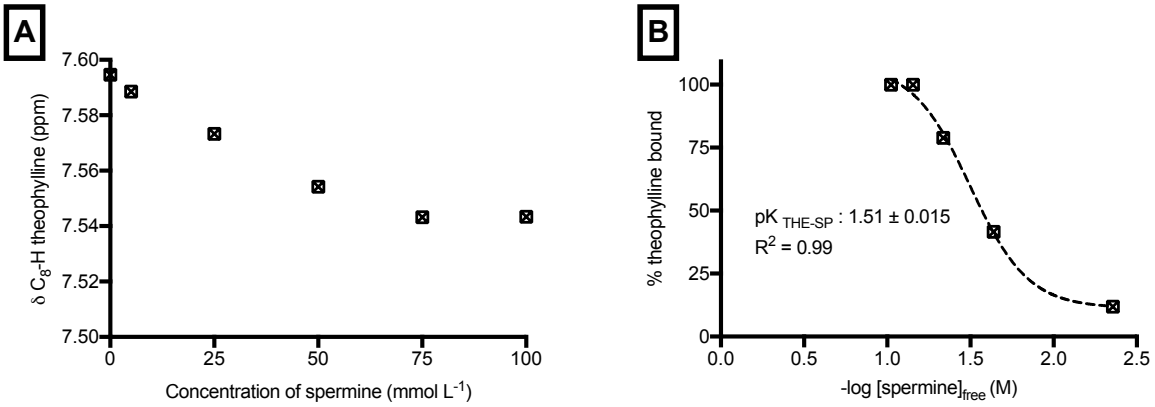

Figure 3.4 (A) The change of C_8-H of theophylline when mixed with increasing concentration of spermine in D_2O pH 9.6 ± 0.1 and (b) theophylline-spermine association curve. The values represent n=3 $\pm$ SD. Error bars are too small to be seen. The association curve was fitted with a Sigmoidal regression model (GraphPad Prism 7) to determine the THE-spermine NMR conditional binding constants (pK_{NMR}) which were determined at 50 % of bound theophylline.

Figure 3.5 showed the ^{1}H-NMR spectra of 5 mM β-CD, HP-β-CD and γ-cyclodextrin in D_2O pH 9.6. The peak assignments (Table 3.3) were in line with the previous studies (Wei et al. 2017; Weiss-Errico & O'Shea 2017). A continuous variation method known as Job's plot was used to establish the stoichiometry of the host-guest complexes using NMR. Job's plots were generated by plotting the change in the chemical shift of H-3 of cyclodextrins (Δppm*[CD](mM)) against varying molar fractions (r) of [CD/CD:(THE:SP) complex] which was set between 0.1 – 0.9 at a constant total concentration of 5 mM. The stoichiometry of the complexes was found to be 1:1 as the maximum plots were obtained at r = 0.5 (Figure 3.6) (Roy et al. 2016; Korytkowska-Wałach et al. 2017). Note that *r* = 0.5 means that CD-[THE-SP] = 1:1.

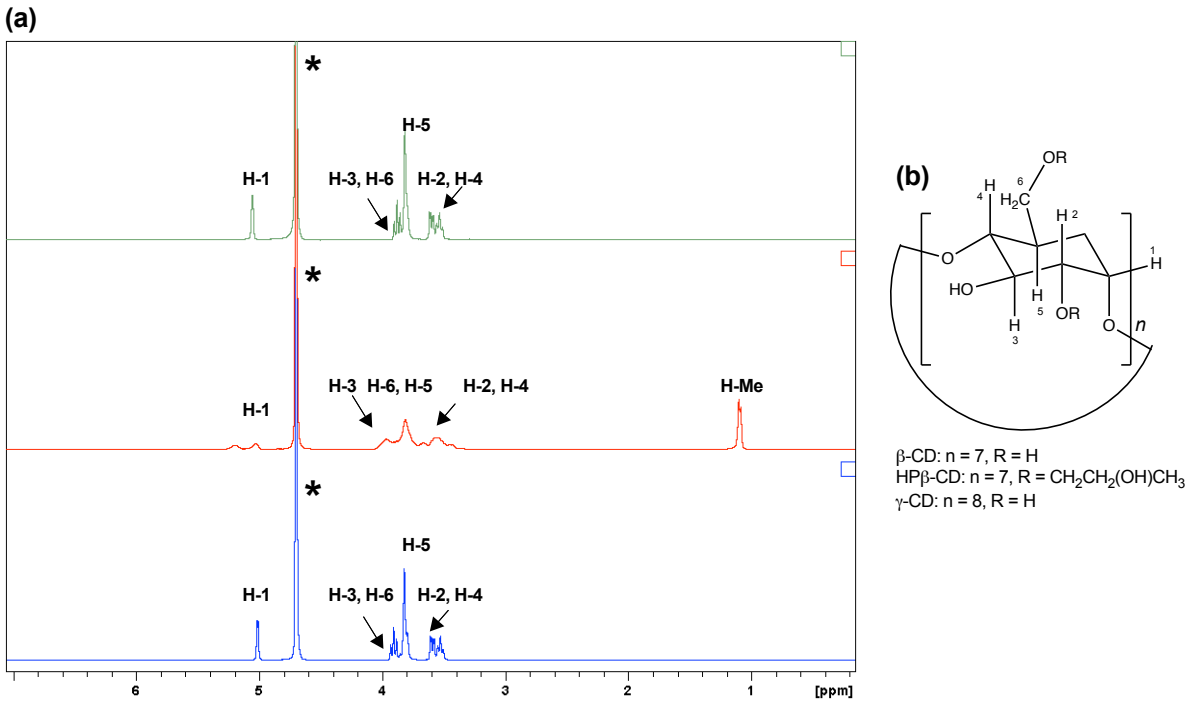

Figure 3.5 (a) The ^{1}H NMR spectum of 0.005M beta-cyclodextrin (*bottom graph*), 0.005 M hydroxypropyl-beta-cyclodextrin (*middle graph*) and 0.005 M gamma-cyclodextrin (*top graph*) in D_2O pH 9.6 $\pm$ 0.1 and (b) the chemical structure of the respective CDs. * asterisk highlights the D_2O signal.

The addition of theophylline-spermine ion-pair complex to the CD solutions induced upfield shifts in all of the hydrogens signals of all three CDs used (Table 3.3) which suggested that a host-guest complex was formed (Kundu et al. 2017). Upon complexation, the hydrogens of β-CD showed the greatest signal shifts followed by the hydrogens of γ-CD then HP-β-CD. This suggested stronger intermolecular interactions between theophylline-spermine ion-pair with β-CD > γ-CD > HP-β-CD (Table 3.4). In order to form a well fitted host-guest complex, the size of CD cavity must be compatible enough (Szejtli 1998). In addition, it is well established that the hydrophobic interaction plays a major role in stabilizing the cyclodextrin complexes (Taulier & Chalikian 2006; Ross & Rekharsky 1996). This means that the guest molecule

must possess an ideal hydrophobicity for a stable CD complex to be formed. The effects of size and polarity the guest molecules on the stability of the CD complexes have been observed previously. In per our case, as described in Chapter 2, that mixing theophylline with an excess spermine significantly increased its hydrophilicity. This could explain the relatively small shifts all CD protons regardless of the type used when mixed with the ion-pair which suggested the formation of relatively weak CD:[THE:SP] complexes. As for HP-β-CD, the bulky hydroxypropyl groups surrounding the CD cavity might provide an additional hindrance for the formation of a stable inclusion complex due to steric hindrance. In addition, the presence of bound spermine to theophylline increased the overall size of the guest molecule which could influence the complex formation. Overall, the magnitude of change of the hydrogens of β-CD molecule which are located in the inner cavity was the greatest for H-3 (-0.052 ppm) followed H-5 (-0.046 ppm) compared to the very small changes observed with H-6 (-0.03 ppm) which is located on the cavity rim at the narrow end of the molecule, upon mixing with the theophylline-spermine ion-pair. Signal changes were also observed for the hydrogens positioned on the outer cavity of β-CD: H-1= -0.036 ppm, H-2 = -0.035 ppm, H-4 = -0.038 ppm, but the changes were less than those in the inner cavity. The proton signals of theophylline and spermine were also affected where the hydrogen on the imidazole ring of the theophylline molecule at the C_8 position demonstrated the largest shift (- 0.038 ppm) followed by the hydrogens at C_{12} (- 0.030 ppm) and at C_{10} (- 0.028 ppm) (Table 3.4), indicating the penetration of the theophylline molecule into the β-CD cavity (Korytkowska-Wałach et al. 2017). This also suggested that theophylline entered the β-CD cavity through the imidazole ring from the wider end of the β-CD molecule. Spermine could exist in a mixture form of bound and free unbound to the drug molecule in the complex solutions which made the interpretation on the shifts of its signals complexed (Table 3.5). Identical observation was also found for THE-SP complexed with γ-CD and HPβ-CD.

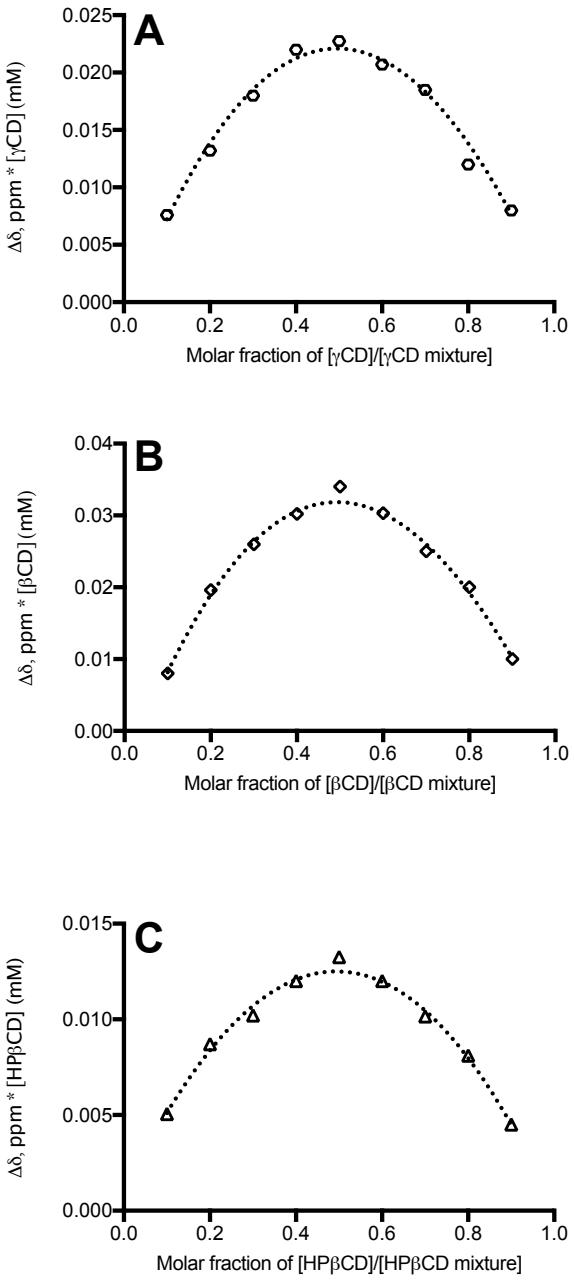

Figure 3.6 Job's plots of (A) γ-cyclodextrin, (B) β-cyclodextrin and (C) HP-β-cyclodextrin complexed with theophylline-spermine (1:20 molar ratio) at pH 9.6 ± 0.1 using the chemical shift of the H-3 signal of the cyclodextrins.

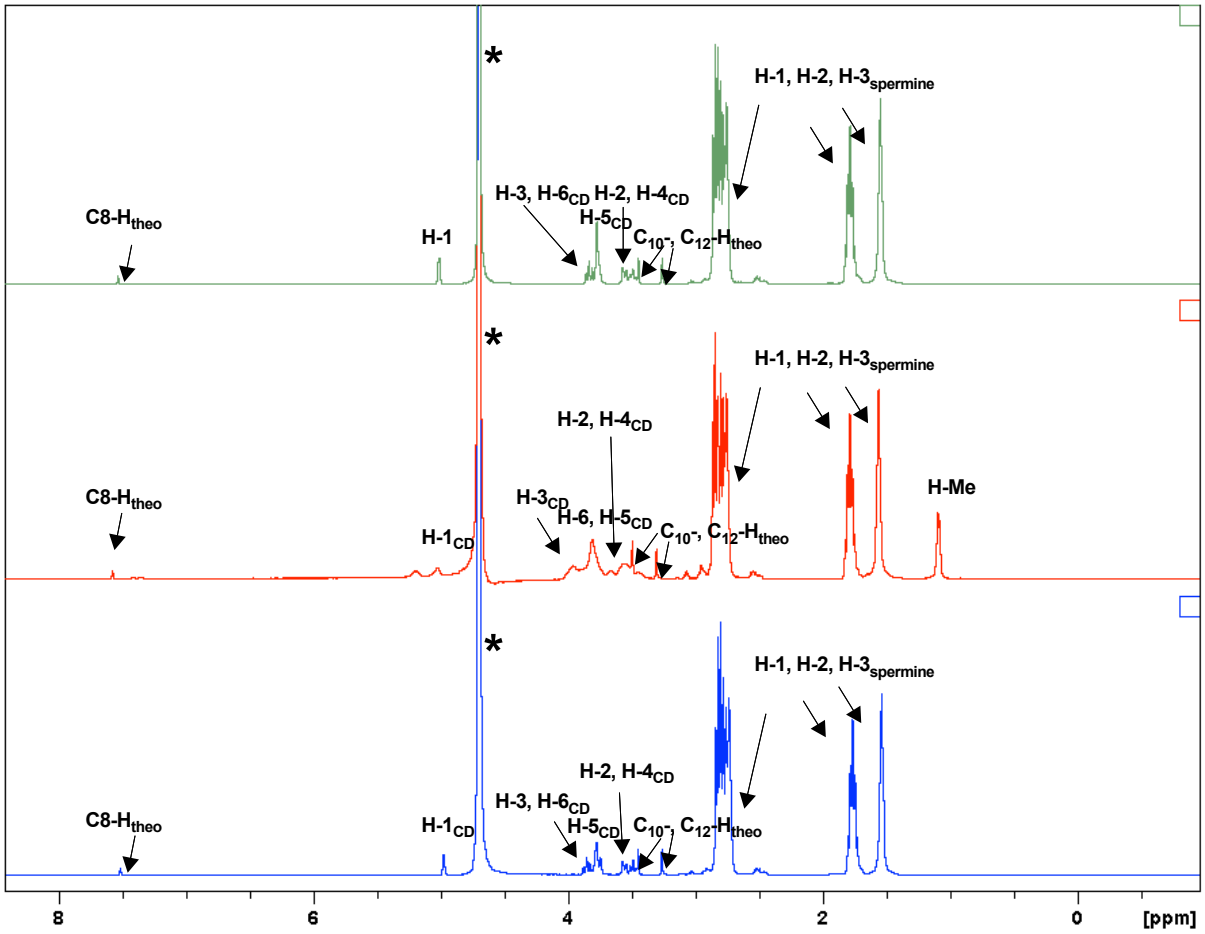

Figure 3.7 The ^{1}H-NMR spectra of β-CD-THE-SP (*bottom graph*), HP-β-CD-THE-SP (*middle graph*) and γ-CD-THE-SP (*top graph*) (CD-THE-SP molar ratio; 0.005:0.005:0.1 M) in D_2O pH 9.6 ± 0.1. * asterisk highlights the D_2O signal. CD-cyclodextrin, THE-theophylline, SP-spermine.

Table 3.3 The chemical shifts, ∂ (ppm) of the free cyclodextrins and when formed the complex i.e., cyclodextrin-theophylline-spermine complex (1:1:20 molar ratio) in D_2O pH 9.6 $\pm$ 0.1.

CD	C-H protons	Chemical shift (ppm)		
		Free CD	Complex	Complex-Free CD
HP- β-CD	H-1	5.198	5.177	- 0.021
	H-2	3.666	3.646	- 0.020
	H-3	3.971	3.949	- 0.022
	H-4	3.576	3.557	- 0.019
	H-5	3.816	3.795	- 0.021
	H-6	3.816	3.799	- 0.017
	H-Me	1.103	1.084	- 0.019
β -CD	H-1	5.014	4.978	- 0.036
	H-2	3.612	3.577	- 0.035
	H-3	3.933	3.881	- 0.052
	H-4	3.553	3.515	- 0.038
	H-5	3.824	3.778	- 0.046
	H-6	3.857	3.817	- 0.030
γ -CD	H-1	5.056	5.015	- 0.041
	H-2	3.619	3.577	- 0.042
	H-3	3.906	3.862	- 0.044
	H-4	3.560	3.519	- 0.041
	H-5	3.820	3.777	- 0.043
	H-6	3.855	3.815	- 0.038

Table 3.4 The chemical shifts, ∂ (ppm) of the ion-paired theophylline and when formed the complex i.e., cyclodextrin-theophylline-spermine complex (1:1:20 molar ratio) in D_2O pH 9.6 ± 0.1.

Complex	C-H protons	Chemical shift (ppm)		
		[THE-SP]	CD Complex	Complex – [THE-SP]
HP-B-CD-THE-SP	C_8-H	7.543	7.534	- 0.009
	C_{10}-H	3.297	3.287	- 0.010
	C_{12}-H	3.483	3.472	- 0.011
B-CD-THE-SP	C_8-H	7.543	7.505	- 0.038
	C_{10}-H	3.297	3.267	- 0.030
	C_{12}-H	3.483	3.451	- 0.032
G-CD-THE-SP	C_8-H	7.543	7.533	- 0.010
	C_{10}-H	3.297	3.285	- 0.012
	C_{12}-H	3.483	3.468	- 0.015

Table 3.5 The chemical shifts, ∂ (ppm) of the ion-paired spermine and when formed the complex *i.e.,* cyclodextrin-theophylline-spermine complex (1:1:20 molar ratio) in D_2O pH 9.6 ± 0.1.

Complex	C-H protons	Chemical shift (ppm)		
		[THE-SP]	CD Complex	Complex –[THE-SP]
HP-B-CD-THE-SP	H-1	1.821	1.816	- 0.005
	H-2	1.569	1.553	- 0.016
	H-3	2.882	2.867	- 0.015
B-CD-THE-SP	H-1	1.821	1.806	- 0.015
	H-2	1.569	1.541	- 0.028

	H-3	2.882	2.842	- 0.040
G-CD-THE-SP	H-1	1.821	1.827	- 0.006
	H-2	1.569	1.551	- 0.018
	H-3	2.882	2.864	- 0.018

Using the 3D molecular modelling technique, it was calculated that ~10% of the volume of the spermine, and ~10% of the volume of the theophylline were inserted into the β-CD cavity (Figure 3.8). In this (energy minimised) model, the theophylline-spermine N_7....H distance was 2.2 Å. The theophylline and spermine cannot penetrated the β-CD cavity to any greater depth, because the sum of their cross-sectional areas (~28 $Å^2$ and 25 $Å^2$, respectively) exceeded the cross-sectional area of the cavity (42 $Å^2$). The result from the 2D ROESY did not show any signals corresponding to the formation of the intermolecular association between CD and the ion-pair which could be due to its limited sensitivity to detect the association of a relatively weak complex as presented in this study (Figure 3.9).

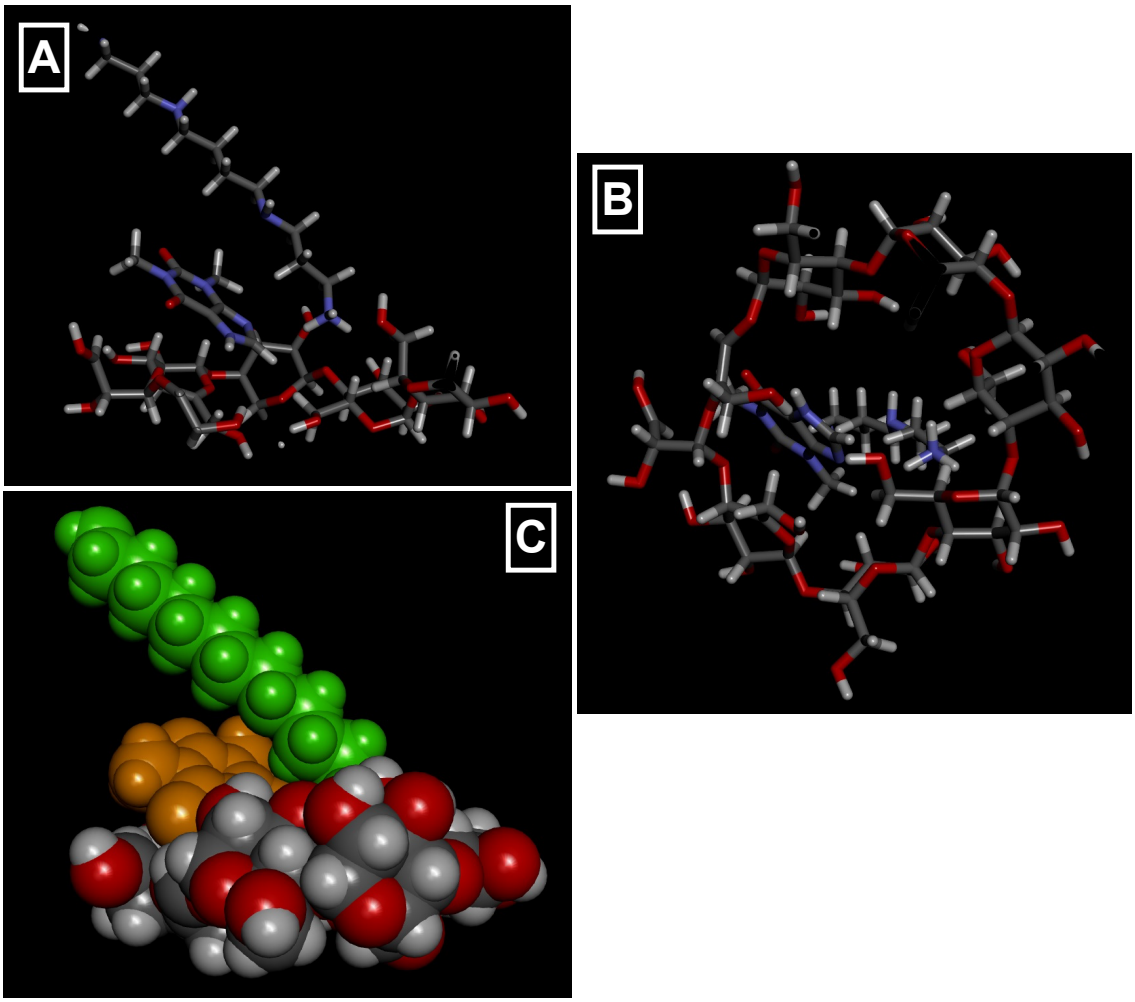

Figure 3.8 The proposed structure of a 1:1 βCD-[THE-SP] complex in water at pH 9.6. In pictures A and B, blue=nitrogen, red=oxygen, white=hydrogen, grey=carbon. In picture C, green was spermine, orange was theophylline and cyclodextrin was indicated by red and grey.

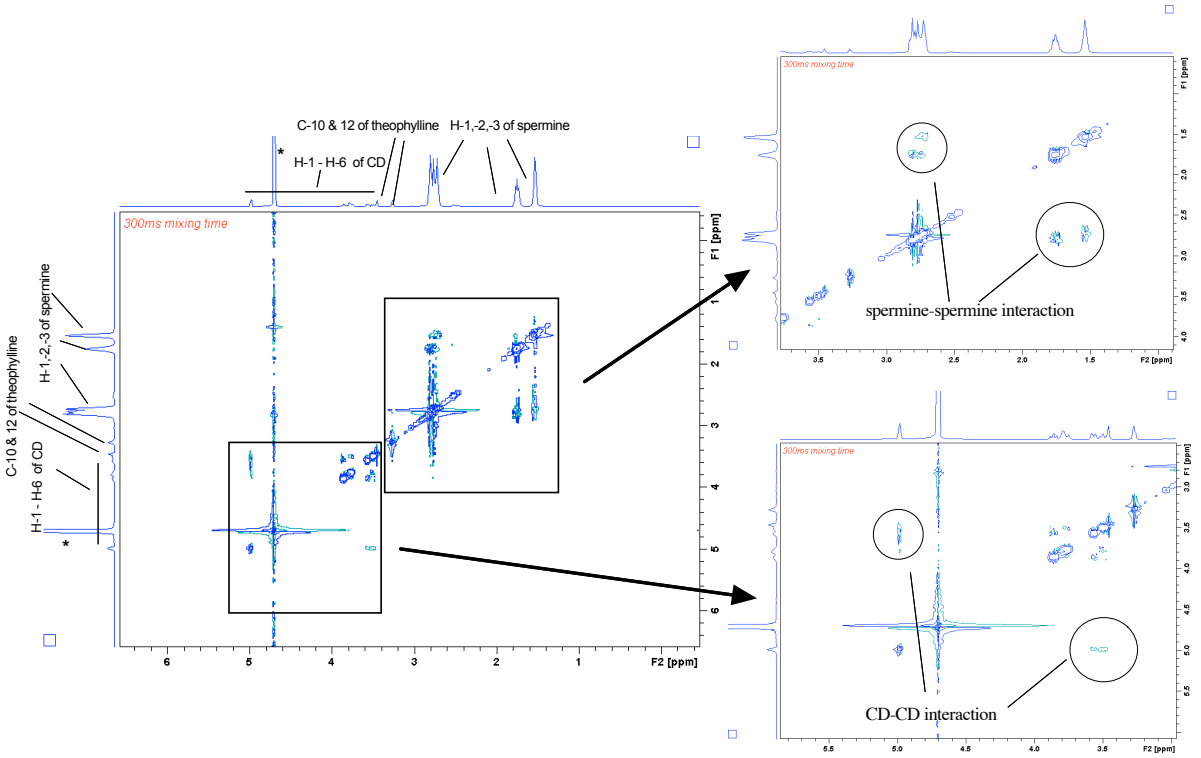

Figure 3.9 2D ROESY spectrum of 1:1 β-CD/[THE-SP] complex in D_2O pH 9.6. Insert figures show the ROESY signals assigned to the spermine-spermine and CD-CD intramolecular interactions. * asterisk highlights the D_2O signal.

3.5 Conclusion

The formation of CD-THE-SP complexes in aqueous was confirmed when assessed using NMR where β-CD was found to have the strongest affinity towards the ion-pair followed by γ-CD then HPβ-CD. The stoichiometry of the complexes was 1:1 as evidenced from the Job's plot studies. It was hypothesized that through encapsulation with CDs, an improved physical stability of the ion-pair can be achieved hence the uptake of the drug into the lung tissue could be optimized. This section will be covered in the subsequent chapter of this thesis.

CHAPTER 4

EFFECT OF CO-SOLVENT ON THE COMPLEX STABILITY AND pH-INDUCED DISSOCIATION OF THEOPHYLLINE-POLYAMINE ION-PAIR

Chapter summary:

This chapter assessed the effect of co-solvent on the theophylline-spermine association.The conditional binding constant of theophylline-spermine (pK_{THE-SP}) was measured in different mixed solvents: 5%, 10 % ethanol-D_2O and 30%, 70% propylene glycol-D_2O using FT-IR at pH 9.6 ± 0.1 and compared to the pK_{THE-SP} in D_2O. The pH-induced dissociation of the ion-pair with and without the presence of cyclodextrin was studied using FT-IR spectrophotometer to trace the break down of the ion-pair. The dissociation study was designed to simulate the ion-pair dissociation induced by the immediate drop of pH to 7.4 upon administration intravenously.

4.1 Introduction

Docking the theophylline-spermine ion-pair in a CD complex could enhance its stability, but as docking was not optimal as shown in Chapter 3, it was felt that an alternative stability strategy should be sought. It is known that the properties of a solvent greatly influenced the extent of the solute-solvent and solute-solute interactions exist in the pharmaceutical systems (Takjoo & Mague 2017; Yang et al. 2017; Chakraborty et al. 2017; Bartyzel 2017). The change in these interactions if ideal, can promote ion-pair stability. The effect of solvent properties on the metal-ligand complexes stability has been studied previously. Mui and McBryde (1974) reported an increased in the stability constant of metal complexes (nickel (II), zinc (II) and manganese (II)) with ethylenediamine and glycine in mixed aqueous solution with increasing composition of the co-solvent. Higher stability of the complexes were found in a less polar mixing co-solvent: dioxane > acetonitrile > methanol > water. This previous work postulated that the increased complex stability was due to the displacement of water molecules, which resulted in smaller solvating capacity, hence a more stable complex was formed. In an organic-rich mixed solvent, the solvent 'charge-shielding' effect is reduced due to the decrease of the dielectric constant (ε) which increases the long-range electrostatic interactions (Wang & Cole 1996). A similar observation was reported by Felmy et al., (2017) who studied the effect of mixed solvents on the complexation thermodynamics of Eu (III) with 2-hydroxyisobutyric acid (HIBA) and 2-aminoisobutyric acid (AIBA) in mixed methanol (MeOH)-water and N,N-dimethylformamide (DMF)-water solvents. A greater complex stability was obtained with increasing percentage of organic solvent in the mixing solvent. In another study conducted by Adam et al., (2016) it was shown that the complex formation constant (K) of the charge transfer complex between anticholinergic drug clidinium bromide with picric acid was more than 6-fold larger in EtOH (ε=24.5; K = 260 x

10^4 M^{-1}) compared when the complex was prepared in MeCN (ε= 37.5; K = 42 x 10^4 M^{-1}). A similar effect was reported by Asim et al., (2014) when the group studied exciplexes of 1-cyanonaphthalene with hexamethylbenzene in solvents with different polarity. These studies suggested that an organic solvent can modify the autoprotolysis constant of the solvent (pK_s) and the pK_a of the ligand, which can influence the complex stability constants. The changes in the solvent equilibria were governed by several properties of the solvent those include the dielectric constant of the solvent, the extent of hydrogen bonding, solvent size, and the preferential solvation of ions in solution. This strategy could also be useful to enhance the physical stability of the theophylline-spermine ion-pair. The dissociation of therapeutic ion-pairs is inevitable when enter the biological systems due to the effect of dilution, which exposes the liable complex to binding competition with the charge-bearing groups. Encapsulating the theophylline-spermine in the cyclodextrin cavity and using excess spermine to force the drug to bind to the counter-ion, it was thought that through careful manipulation of formulation vehicle properties, a more stable theophylline-polyamine ionic complex could be engineered. If this could be achieved, the dissociation rate of the ion-pair could be slowed down. The aims of this chapter were to (i) investigate the impact of co-solvents *i.e.,* propylene glycol (PG) and ethanol (EtOH) on the association of theophylline-spermine ion-pair and (ii) to assess the pH-induced dissociation of the ion-pair in different mixed solvents formulation vehicles by using FT-IR. The dissociation profile of the complexed ion-pair with cyclodextrin will be compared with the non-complexed ion-pair to assess the ability of cyclodextrin to control the break down of the ion-pair in response to the change of pH. The theophylline-spermine association was determined in different EtOH-D_2O and PG-D_2O mixtures at a constant pH 9.6 ± 0.1 using FT-IR. PG and EtOH are commonly used oral and intravenous formulation to improve the solubility of poorly soluble drugs (Thackaberry et al. 2014). The Food and Drug Administration (FDA) considers these

excipients safe for use in medication and cosmetics. The European Medicines Agency placed ethanol in class 3 solvents i.e., solvents with low toxic potential, whilst propylene glycol, following repeated administration in animals, it considered to show low systemic toxicity.

4.2 Materials

Theophylline (THE) (anhydrous, ≥99%), spermine (SP) (≥ 99%), beta-cyclodexetrin (ß-CD), deuterium oxide (D_2O) (>99% D), propylene glycol (USP standard), deuturated ethanol (EtOH-OD) (≥99.5% D), sodium hydroxide (NaOH), hydrochloric acid (HCl), sodium chloride (NaCl) were purchased from Sigma Aldrich, UK.

4.3 Methods

4.3.1 Theophylline-spermine binding studies

The infrared (IR) conditional binding constant ($pK_{FT\text{-}IR}$) of theophylline-spermine (0.015:0.3 mol L^{-1}) were assessed using a universal liquid cell system (Omni-Cell, Specac Ltd, UK) fitted with CaF_2 windows and a 0.025 mm Mylar spacer (Specac Ltd, UK) was used for the absorbance measurements. The $pK_{FT\text{-}IR}$ of theophylline-spermine was determined in EtOH-D_2O (5% and 10% v/v) and PG-D_2O (30% and 70% v/v) mixed solvents to assess the effect of co-solvents on the ion-pair association. The ethanol and PG concentrations tested were within the accepted limit by EMA. The absorbance spectra were recorded within the range of 1725 – 1500 cm^{-1}, pH adjusted to 9.6 ± 0.1 using NaOH/HCl. NaCl was added when

necessary to keep a constant ionic strength (0.5 M) in all mixtures. All spectra were subtracted with the spectra of the blank solutions and baseline corrected. The blank solutions refer to the exact compositions of the test solutions in the absence of theophylline. Changes in the peak absorbance ratio at ca. 1530/1551 cm^{-1} were calculated where the peak at ca. 1551 cm^{-1} was assigned to the uncomplexed theophylline and the peak at ca. 1530 cm^{-1} as the complexed theophylline. The change in the ratio of these peaks was used to determine the percentage of theophylline bound as a function of spermine concentration. The percentage of theophylline bound *vs* $-\log[\text{spermine}]_{free}$ were plotted and fitted with a regression model (GraphPad Prism7) to determine the FT-IR conditional binding constant ($pK_{FT\text{-}IR}$) of theophylline-spermine ion-pair. All spectra were recorded using a Spectrum One spectrometer (Perkin Elmer Ltd, UK) and spectral analysis was performed with Spectrum version 10 software (Perkin Elmer Ltd, UK). The resolution was set at 4 cm^{-1} and 12 scans were performed for each measurement. Experiments were repeated in triplicate and the results were presented as mean $\pm$ SD.

4.3.2 pH-induced dissociation studies

The test solutions consisted of 0.015 mol L^{-1} theophylline, 0.015 mol L^{-1} cyclodextrin and 0.3 mol L^{-1} spermine were made up in D_2O, EtOH-D_2O and PG-D_2O, pH adjusted to 9.6 ± 0.2 using HCl. To simulate the immediate change in the pH upon administration, the pH of the test solutions was adjusted to pH 7.4 ± 0.2 just prior to the spectral measurement using a pre-determined volume of HCl (5 M). The samples were then mounted in a universal transmission cell system (Omni-Cell, Specac Ltd., UK) fitted with CaF_2 windows and a 0.025 mm Mylar spacer (Specac Ltd., UK) then analyzed using Spectrum One FT-IR spectrometer

(Perkin Elmer Ltd., UK). A total of 25 ± 5 s elapsed before the first scan was taken (time needed to mount the cell onto the spectrometer). The monitoring of the C=N and C=O peaks of theophylline was carried out for a continuous 20 min using TimeBase™ software (Perkin Elmer Ltd., UK). The pH was monitored throughout the process. The FT-IR method was used because it is sensitive to detect ion-pair dissociation unlike UV or fluorescence analysis. NMR analysis was less sensitive that FTIR.

4.4 Results and discussion

4.4.1 Binding studies

Figure 4.1 demonstrated the IR spectra of free theophylline (0.015 mol L^{-1}) in different aqueous organic mixed solvents at pH 9.6. It appeared that the four carbonyl signals within the range of 1700 – 1500 cm^{-1} of theophylline were sensitive to the change in the polarity of the medium used whilst the C=N peaks at ca. 1551 and 1530 cm^{-1} of theophylline remained unaltered (Table 4.1). It should be noted that, as described in Chapter 2, theophylline forms dimer in solution. The self-association of theophylline could occur between the H on the C_8 position with the O at the C_6 position in aqueous at pH 9.6. A larger theophylline C=O peaks shift was seen when theophylline was dissolved in the PG-D_2O mixtures compared to the EtOH-D_2O mixtures. The shift of the peaks to higher wavenumbers suggested a weaker drug-solvent interaction resulted from a stronger drug-drug interaction. This suggested, that decreasing the overall medium polarity of the mixed solvent system increased the degree of the intramolecular association of theophylline. The total dielectric constant (ε) was used to

rank the formulation vehicles in terms of polarity: D_2O = 78; 5% (v/v) EtOH-D_2O = 75.35; 10% (v/v) EtOH-D_2O = 72.7; 30% (v/v) PG-D_2O = 64.23; 70% (v/v) PG-D_2O = 45.87.

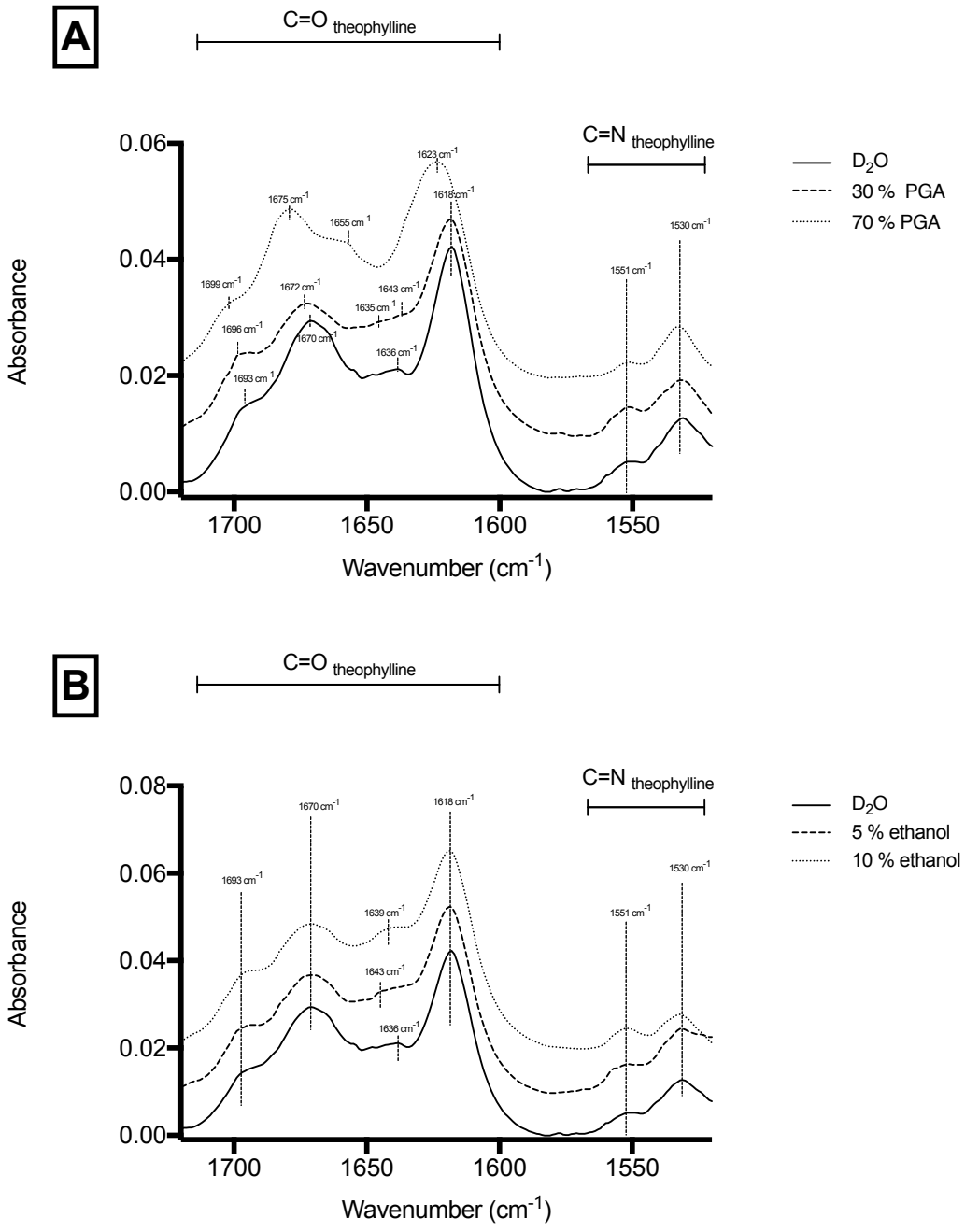

Figure 4.1 The liquid cell FT-IR spectra of 0.015 mol L^{-1} theophylline in different formulation vehicles at pH 9.6 $\pm$ 0.1, 21 $\pm$ 2 ^{o}C. (A) in 30 and 70 % (v/v) of propylene glycol (PGA)-D_2O and (B) in 5 and 10 % (v/v) of ethanol-D_2O.

Table 4.1 Experimental wavenumbers (cm^{-1}) of 0.015 mol L^{-1} theophylline in different solvent systems at pH 9.6 ± 0.1

Functional group	D_2O	5% Et-OH-D_2O (v/v)	10% Et-OH-D_2O (v/v)	30% PGA-D_2O (v/v)	70% PGA-D_2O (v/v)
$C_2=O_{11}$	1670	1670	1670	1672	1675
	1693	1694	1694	1696	1699
$C_6=O_{12}$	1618	1618	1618	1618	1623
	1636	1643	1639	1635	1655
				1643	
C=N	1530	1530	1530	1530	1530
	1551	1551	1551	1551	1551

The addition of increasing concentrations of spermine to the theophylline solutions caused a gradual increase in the absorbance of the two C=O peaks of theophylline at ca. 1670 cm^{-1} and 1618 cm^{-1} and a gradual decrease of the other two C=O peaks at ca. 1696 and 1637 cm^{-1}. This was in agreement with the results in Chapter 2. In addition, the intensity of the C=N peak of the drug at ca. 1530 cm^{-1} which was assigned to the complexed theophylline increased gradually whilst the other C=N peak at ca. 1551 cm^{-1} that was assigned as the uncomplexed theophylline gradually decreased with an increase in the spermine concentrations. The FTIR peak shifts of the theophylline C=O and C=N were attributed to the ion-pairing effect. These trends of changes were seen in all of the mixed solvent systems studied (Figures 4.2-4.3). The theophylline-spermine association curves derived from the FT-IR data were fitted with a Sigmodial model ($R^2 \geq 0.95$) (Figure 4.4). The $pK_{FT\text{-}IR}$ of theophylline-spermine obtained in the ethanol and PG solvent systems were as follows (Table 4.2): theophylline-spermine pK_{FTIR}: 70% PG-D_2O = 2.11 ± 0.045; 30% PG-D_2O = 2.05 ± 0.057; 10% EtOH-D_2O = 2.05 ±

0.053; 5% EtOH-D_2O = 2.04 ± 0.05.; D_2O = 1.96 ± 0.04. However, there was not statistically significant change of the theophylline-spermine $pK_{FT\text{-}IR}$ value with solvent composition.

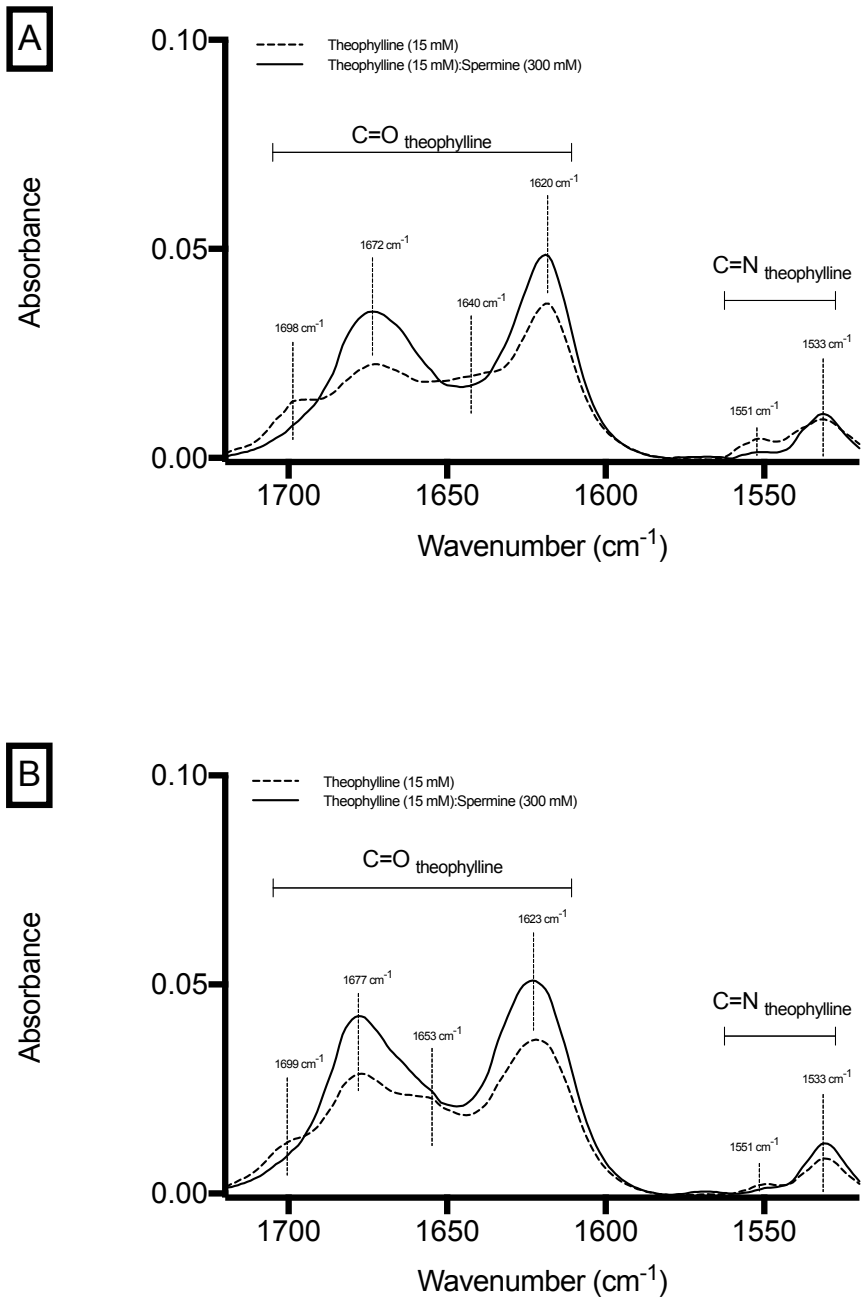

Figure 4.2 The liquid cell FT-IR of 0.015 M theophylline and 0.015 mol L^{-1} theophylline mixed with 0.3 mol L^{-1} spermine at pH 9.6 $\pm$ 0.1 in (A) 30/70 (v/v) propylene glycol/D_2O and (B) 70/30 (v/v) propylene glycol/D_2O.

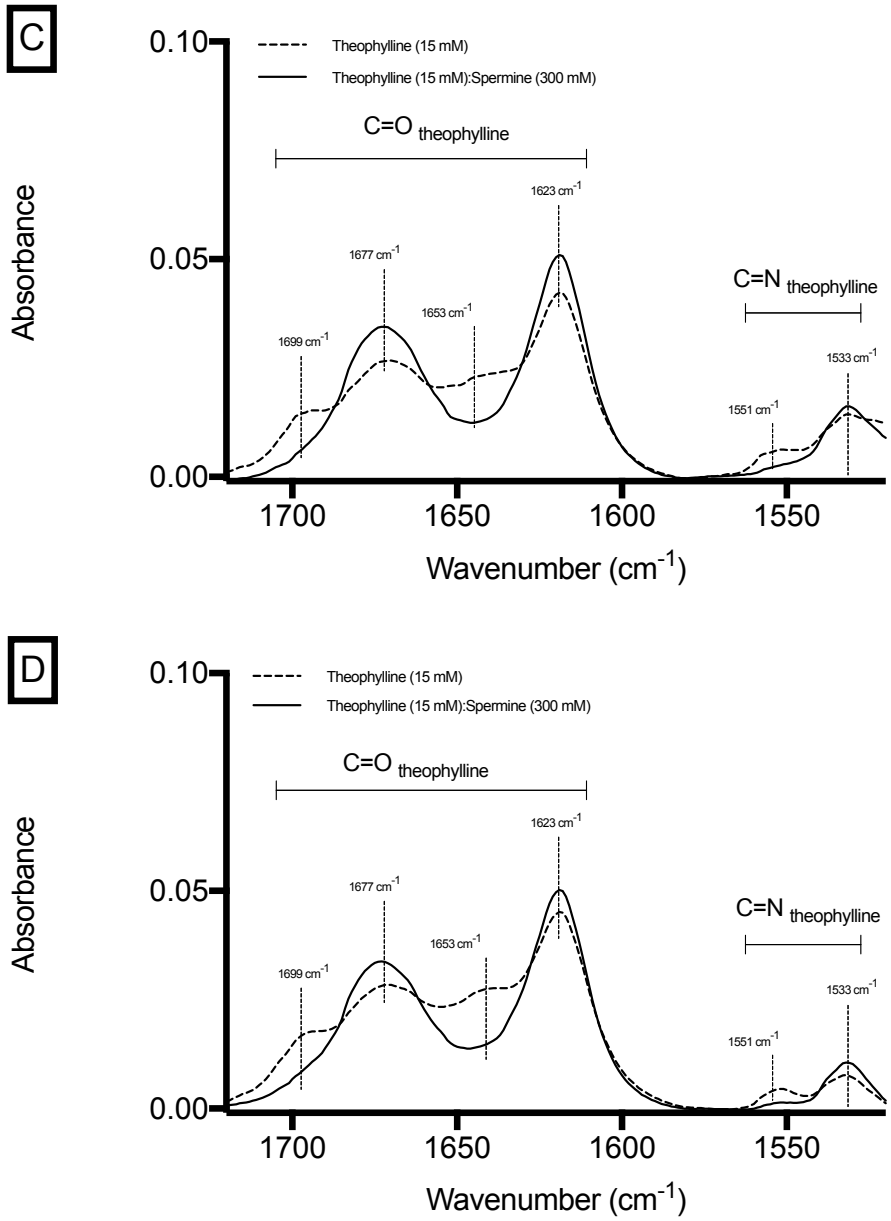

Figure 4.3 The liquid cell FT-IR of 0.015 mol L^{-1} theophylline and 0.015 M theophylline mixed with 0.3 mol L^{-1} spermine at pH 9.6 $\pm$ 0.1 in different solvent systems (A) 5/95 (v/v) ethanol/ D_2O and (B) 10/90 (v/v) ethanol/ D_2O.

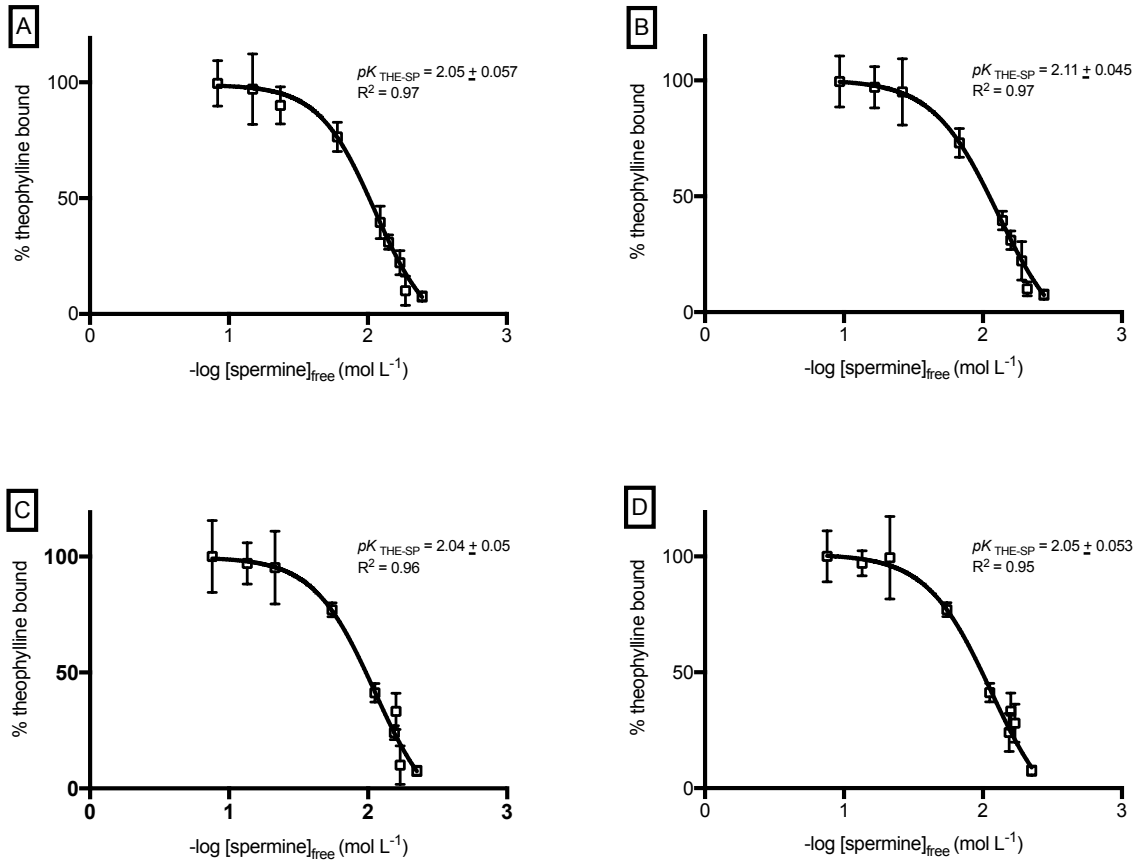

Figure 4.4 Theophylline-spermine binding association assayed by FT-IR at pH 9.6 ± 0.1, 21 ± 2 °C in different co-solvents systems: (A) 30/70 (v/v) propylene glycol/D_2O, (B) 70/30 (v/v) propylene glycol/D_2O, (C) 5/95 (v/v) ethanol/D_2O and (D) 10/90 (v/v) ethanol/D_2O. Values represent means from n=3 ± SD. The association curves were fitted with a sigmoidal regression model (GraphPad Prism 7) to determine the THE-spermine association constant (pK) which was determined at 50 % of bound theophylline from the curves.

Table 4.2 The conditional FT-IR theophylline-spermine binding constants (pK_{FT-IR}) in different solvent systems at pH 9.6 ± 0.2. Values represent means from n=3 ± SD.

Solvent system	pK_{FT-IR}	R^2
D_2O	1.96 ± 0.04	0.97
30/70 (v/v) propylene glycol/D_2O	2.05 ± 0.057	0.97
70/30 (v/v) propylene glycol/D_2O	2.11 ± 0.045	0.97
5/95 (v/v) ethanol/ D_2O	2.04 ± 0.05	0.96
10/90 (v/v) ethanol/ D_2O	2.05 ± 0.053	0.95

4.4.2 Dissociation studies

Dissociation studies were carried out to assess the pH-induced dissociation of the ion-pair. An immediate change of pH from pH 9.6 to pH 7.4 was achieved by adding a known amount of concentrated HCl. The mixture was then mixed and analyzed using FT-IR. The change of pH over time was monitored closely by inserting a pH checker into the test solutions. In order to understand the FT-IR dissociation, the IR spectra of the theophylline-spermine ion-pair (1:20) was prepared at different pHs (6, 8, 8.5, 9 and 10) (Figure 4.5). Using the spectra of the theophylline-spermine ion-pair at different pHs, the peaks (in D_2O) of at ca. 1550 cm^{-1}, 1673 cm^{-1} and 1617 cm^{-1} were assigned to the dissociated ion-pair whilst peaks at ca. 1530 cm^{-1}, 1619 cm^{-1} and 1673 cm^{-1} were assigned to the associated ion-pair. The FT-IR spectra at pH 9.6 were the associated ion-pair at t=0. Changing the pH to 7.4 upon addition of the HCl resulted in the significant suppression of all the ion-paired theophylline peaks regardless of the formulations tested (Figures 4.6-4.7) which suggested the ion-pair broke down almost immediately after the pH was dropped to pH 7.4. This indicated that the addition of

cyclodextrin in a co-solvent had a minimal impact on controlling the dissociation of the theophylline-spermine ion-pair when facing an abrupt pH change.

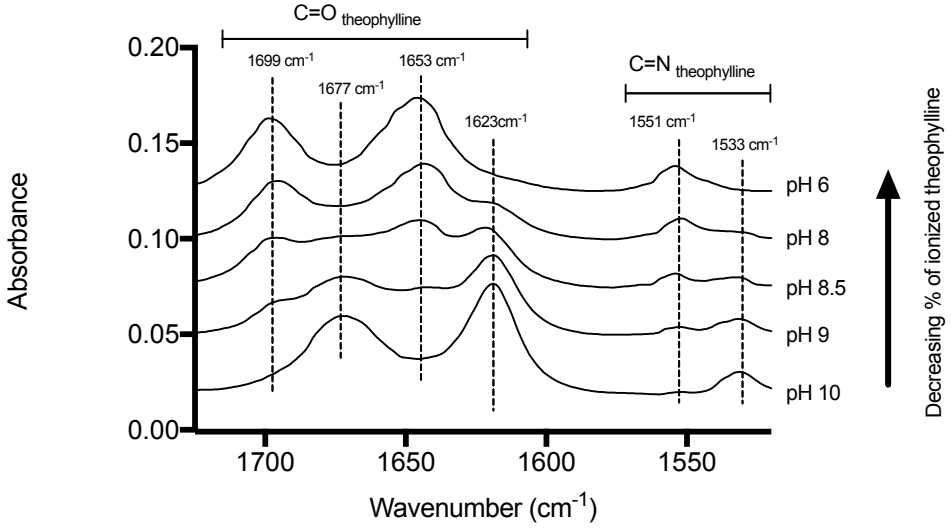

Figure 4.5 The liquid FT-IR spectra of theophylline-spermine (15:300 mM) in water at different pH. Note that a higher percentage of ionized theophylline reflects a greater possibility of theophylline to form ion-pair with spermine.

The sudden drop in the pH of the mixture caused solvent rearrangements. This could significantly perturb the thermodynamic stability of the ion-pair complex which resulted in a rapid break down of the complex. Identical observations have been reported previously (Pey 2014; Ballard & Dellago 2012). Unfortunately, the process between adjusting the pH until the test solutions could be assured in the static FT-IR cell to start the measurement took ca. 25 sec which was thought to be longer than the time for the ion-pair to reach the lung tissue from the site of infusion. However, the ion-paired peaks at ca. 1618 cm^{-1} and 1530 cm^{-1} were still able to be detected up to 20 mins, which suggested the existence of some ion-paired

theophylline even at pH 7.4 (as predicted in Chapter 2). The appearance of multiple peaks within the C=N region at 1520 – 1550 cm^{-1} suggested that after ion-pair dissociation a small proportion of theophylline dimers were formed.

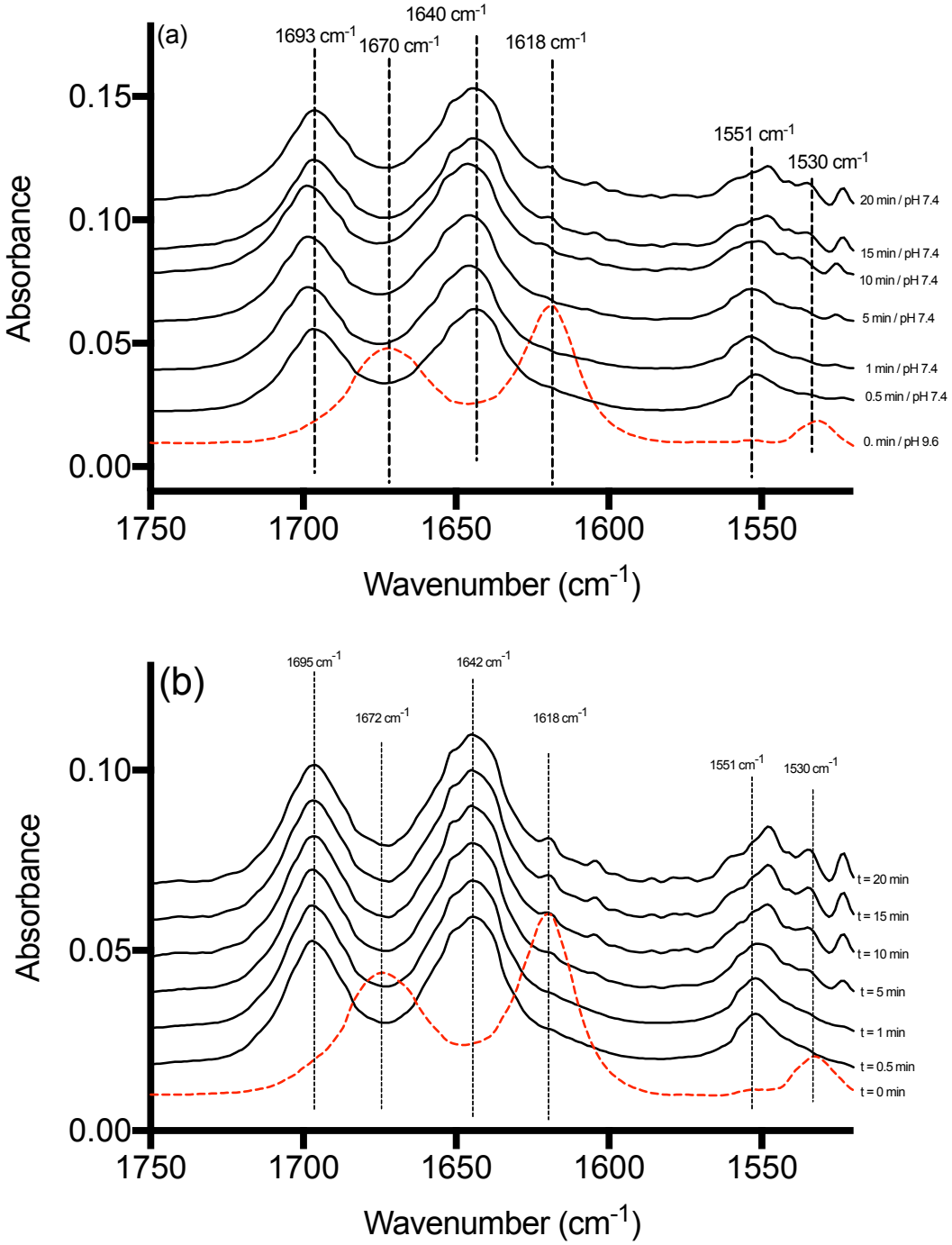

Figure 4.6 The liquid FTIR of theophylline-spermine (15:300 mM) in (A) D_2O and (B) 10 % ethanol at pH 7.4 $\pm$ 0.05 measured continuously over time from 0.5-20 mins.

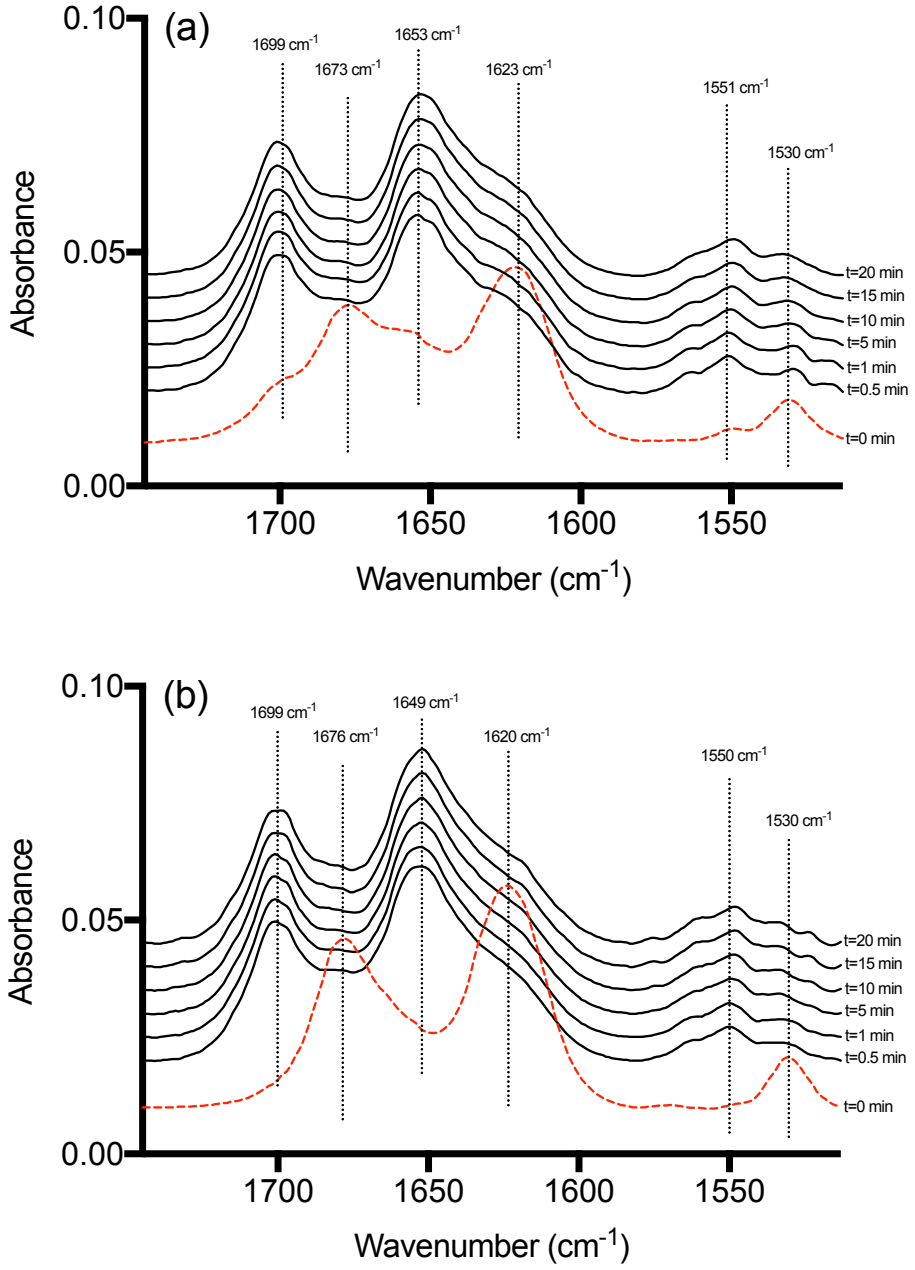

Figure 4.7 The liquid FTIR of (A) theophylline-spermine (15:300 mM) and (B) beta-cyclodextrin-theophylline-spermine (15:15:300 mM) in 70% PG-D_2O measured continuously over time from 0.5-20 mins.

4.5 Conclusion

Theophylline was found to bind more strongly to spermine in the mixed solvent with the presence of increasing concentrations of the organic solvent. Regardless of the formulation vehicles tested, theophylline-spermine ion-pair dissociated almost immediately when the pH of the test solutions was dropped to 7.4. However, a small portion of the theophylline peaks at ca. 1530 and 1618 cm^{-1} was still able to be detected even at pH 7.4 suggested that the small percentage of theophylline was still able to remain intact with spermine.

CHAPTER 5

IN-VITRO CELL BIOCOMPATIBILITY AND CELLULAR UPTAKE OF THEOPHYLLINE-POLYAMINE COMPLEXES FORMULATED USING CYCLODEXTRINS

Chapter summary:

The data reported in this Chapter demonstrated that free theophylline, spermine, cyclodextrin and the theophylline-spermine ion-pair complex formulated with cyclodextrin, were all biocompatible with human lung epithelial (A549) cells. The formation of a theophylline-spermine ion-pair enhanced theophylline uptake into the A549 cells, time-dependent accumulation of the drug was not observed due to the theophylline efflux by P-gp. Formulating the ion-pair with cyclodextrins increased the total accumulation of theophylline over time and provided a sustained transport enhancement, which suggested that association with the cyclodextrin enhanced the theophylline-spermine physical stability

.

5.1 Introduction

In Chapter 4 the theophylline-spermine ion-pair, formulated at pH 9.6, showed rapid dissociation when the pH of the solution was dropped to 7.4 (i.e., physiological conditions). A similar outcome was observed even when the ion-pair was mixed with cyclodextrins in a co-solvent, which suggested if an ion-pair complex was formed the pH change would drive dissociation. It was not possible to measure the speed of complex dissociation hence in this chapter, we further investigated if the remaining theophylline paired to the spermine could have an impact on the drug uptake in lung epithelial using a functional assay in order to assess if formulating ion-pairs with cyclodextrins can alter the drug transport into the cells.

The ability of a molecule to permeate into cells depends on many factors, but one of the most important factors is the molecule's physicochemical properties e.g., size, lipophilicity and hydrogen bond capacity (Kell & Oliver 2014). A small molecule with moderate hydrophilicity can passively diffuse through the cell membrane whilst polar molecules often utilize the membrane transporters, which facilitate their membrane penetration (Muth et al. 2013). Cell transport facilitated by transporters is dependent on the specific substrate-transporter binding. Since the expression of the transporters varies according to the cell type, this can enable drug targeting (Scott et al. 2017). The most important transporter for the theophylline spermine ion-pair studied in this thesis is the active polyamine transport system (PTS). The PTS regulates the intracellular level of polyamines, which are essential for cell growth, division and differentiation (Guminski et al. 2009; Palmer & Wallace 2010). In healthy cells, the pulmonary tissue appears to express high levels of polyamine transporters, observed as a consequence of their ability to accumulate higher polyamine compared to cells derived from other tissues (Hoet & Nemery 2000). Given their pulmonary activity, the PTS

might offer a means to target drug delivery to the lung. The PTS has been identified and functionally characterized in lung alveolar type 1 and type 2 cells, Clara cells (Nemery 1987; Wyatt 1988; Dinsdale 1991; Kameji 1984) and the pulmonary arterial endothelial cells (Sokol et al. 1992). From the published studies, it appears that the PTS is a saturable, carrier-mediated, time, temperature, pH, energy and concentration-dependent transporter system (Seiler and Dezeure, 1990; Cullis et al. 1999; Dot et al. 2000; Raksajit et al. 2009; Kruczynski et al. 2009; Kuramoto et al. 2003).

The ability of PTS to target the delivery of molecules to cancer cells, which overexpressed the PTS has been previously investigated (Palmer & Wallace 2010), but the use of this transporter to target lung cells has only been tested using nanomaterials. Li et al., (2017) investigated the active delivery of doxorubicin (DOX), a chemotherapeutic agent loaded in spermidine-modified nanoparticles (SPD-DOX-NPs) in human lung carcinoma (A549) cells. Spermidine is an endogenous polyamine with a moderate chain length that is protonated at physiological pH. In Li et al's study, cells treated with a spermine coat (SPD-DOX-NPs) showed the brightest fluorescence, which indicated a higher cell uptake of DOX-loaded NPs compared to free DOX and DOX-NPs, without the polyamine. Results from flow cytometry showed a significant increase of SPD-DOX-NPs cell uptake compared to free DOX ($p<0.01$) and DOX-NPs ($p<0.05$) and this data suggested that the drug was actively taken up into the cell via specific SPD-PTS binding after 1 h of incubation. The SPD-DOX-NPs exhibited spermidine concentration-induced toxicity where the cytotoxicity was 1.6-fold and 2.0-fold greater compared to SPD-free and free DOX, respectively when the spermidine concentration was at the highest. Barret et al., (2008) assessed the targeted delivery of polyamine-containing drug in cancer cells using F14512, which is a toposimomerase II inhibitor. In the presence of spermine, the drug was found to be 73-fold more cytotoxic to Chinese hamster

ovary (CHO) cells compared when tested in a mutant cell line (CHO-MG) with a reduced PTS activity. The IC_{50} values for F14512 were 0.12 and 8.7 umol L^{-1} in CHO and CHO-MG cells suggested that PTS facilitated the internalization of the drug in the cells in the presence of spermine moiety.

Most of the studies in the literature generally reported an enhanced permeability of drugs when forming ion-pairs due to an increase in drug's lipophilicity, which allow a higher passive diffusion of the molecule across the biological barriers (Samiei et al. 2014; Tantishaiyakul et al. 2004; Liu et al. 2011). However, a study by Paugam and Smith (1993) proved that this strategy could also be used to improve the molecule uptake through an active transport. Their results demonstrated an active transport of uridine paired with phenylboronic acid across an organic liquid membrane through a F^- ion channel. The major concern when using the ion-pairing approach in drug delivery is the instability of the ion-pair association, which can result in a rapid dissociation, if a labile ion-pair is formed. This has been previously studied by Zhao et al., (2017) when assessing the skin permeation of bisoprolol ion-paired with a series of fatty acids. They concluded that the strength of the ion-pair stability is the key factor in controlling the dissociation of the ion-pair when applied to the biological system.

In addition to using excess spermine counter-ion to force to the drug to remain bound to the counter-ion, CDs could be used to stabilize this weak interaction. Many published studies have suggested that CDs can improve the stability of encapsulated guest molecules through host-guest complexation. The complexation provides insulation to the labile drug molecules against various degradation processes (Stella & He 2008; Wouessidjewe et al. 1999; Szejtli 1998).

The presence of active efflux mechanism is relevant to PTS activity as substrates for the PTS may be effluxed from the cells by P-gp transporters. It is known the activity of efflux pumps often limits the accumulation of a drug in cells (Gottesman & Pastan 2015; Hamilton et al. 2001; Borges-Walmsley et al. 2003). The P-gp substrates can be varied in their chemical structures, from a small molecule such cimetidine (MW = 250 g mol^{-1}) to a big molecule such as cyclosporin (MW = 1202 g mol^{-1}). Drugs with poor membrane permeability may also undergo a substantial extrusion (Amin 2013). The protein responsible for these pumps actively extruding absorbed drugs out of the apical membrane resulting in a very limited amount of drug ultimately available to be absorbed in target organs. Of all, the P-gp protein encoded by MDR1 gene which belongs to the ATP-binding cassette (ABC) superfamily of proteins has been considered as one of the most significant transporters in humans (Aszalos 2004; Kim 2002). Overexpression of P-gp transporters in cancer cells was found to form a strong link in resistance to many drugs used in chemotherapy (Peng et al. 2012).

The aim of this chapter was to understand how forming a theophylline-spermine ion-pair influenced its absorption into the lung. The objectives of the chapter were (i) to assess the accumulation theophylline in A549 cells when dosing the drug as an ion-pair with spermine, (ii) to study the cell uptake of theophylline when cyclodextrin was added to the ion-pair formulation and (iii) to investigate whether the accumulation of theophylline was affected by the presence of P-glycoprotein (P-gp) specific inhibitors.

5.2 Materials

Theophylline (THE) (anhydrous, ≥ 99%), spermine (SP) (≥ 99%), beta-cyclodextrin (B-CD) (≥ 97%), 2-hydroxypropyl-beta-cyclodextrin (HP-B-CD), gamma-cyclodextrin (G-CD), valspodar (≥ 98%), elacridar (≥ 98%), propylene glycol (PG, USP grade) and all reagents for cell culture (RPMI-1640 cell culture medium, fetal bovine serum (FBS), L-glutamine, penicillin-streptomycin, trypsin-EDTA 0.25%, phosphate buffered solution (PBS), Hank's Balanced Salt Solution (HBSS), trypan blue and Triton ^{TM}X-100) were purchased from Sigma Aldrich, UK. 8-^{14}C theophylline (0.1 mCi/mL, > 98%) was purchased from American Radiochemicals, USA. Human lung epithelial A549 cells were obtained from American Type Culture Collection (ATCC), USA and Optiphase "Safe" scintillation cocktail was purchased from Fisher Scientific International, UK.

5.3 Methods

5.3.1 Cell culture

In the present study, the human lung epithelial (A549) cells were not used as a target site of theophylline but rather it was used as a robust model to assess the effects of PTS and P-gp transporters on the cellular accumulation of the drug ion-pair. These transporters have been well characterized in these cells. The cells were used between passages 46-64. The cells were maintained in a 95 % humidified/ 5 % CO_2 atmosphere at 37 ^{o}C. They were grown in 75-cm^2 flasks and cultured using RPMI-1640 cell culture medium supplemented with 10 % FBS, 0.3 g/L L-glutamine, 100 ug/mL penicillin/streptomycin. The medium was changed

every 2/3 days. When the cells reached 90 % confluency (checked visually using a light microscope), they were sub-cultured at 1:3 split ratio using 0.25%trypsin/0.1% EDTA.

5.3.2 In-vitro cell biocompatibility

The cell biocompatibility of the individual compounds (THE, SP, B-CD, HP-B-CD, G-CD) and the mixtures with and without cyclodextrin (CD) (i.e., with CD: CD-THE-SP, without CD: THE-SP) was assessed by exposing the cells to the test solutions prepared at the desired concentrations. These concentrations once proven safe to the cells were later used in the accumulation studies of theophylline. The test solutions were prepared in two different vehicles, water and 70/30 (v/v) PG:water. The pH of all test solutions was adjusted to 9.6 ± 0.1 using 0.01 M NaOH/HCl. The toxicity of the test solutions was assayed using the standard MTT (3-(4,5-Dimethylthiazol-2-yl)-2,5-diphenyl-tetrazoliumbromide) test (Matilainen et al. 2008). Briefly, the cells were seeded into a 96-well plate at a density of 1.0 x 10^4 cells/cm^2. They were allowed to grow for 24 h at 37 ^oC in a 5 % CO_2 atmospheric air incubator. After 24 h, the old medium was removed and each well was rinsed three times with pre-warmed PBS. Subsequently, 100 µL of pre-warmed HBSS was added to each well. An aliquot (100 uL) of test solutions was added to initiate the experiment and the cells were incubated for 1 h. Untreated cells, i.e, cells incubated with cell culture medium only were used as a negative control whilst cells treated with 1% Triton X solution were used as a positive control. After treatment, the cell media was discarded and replaced with 10% of 5 mg/mL MTT in 100 µL of cell culture medium solution. This solution was incubated with the cells for 4 h. The cells were then lysed with 100 µL of lysis solution (10 % SDS in DMF:water 50:50, pH 4.7). The quantification of formazan crystal, which reflected the

number of viable cells, was carried out using a multiwell plate reader (Spectramax 190) at 570 nm (reference wavelength 690 nm). Relative cell viability was determined by dividing the optical density (OD) of treated wells over the OD of control. Experiments were repeated in triplicates (n=3 plates for each treated group) and the data were presented as mean $\pm$ SD.

5.3.3 Theophylline accumulation studies

Cells were seeded onto a 12-well plate at a density of 2 x 10^5 cells/cm^2. The culture medium was changed every other day until a confluent monolayer was established (approximately by 4 days post seeding), as determined visually using a light microscope. To investigate theophylline uptake, the cell culture medium was removed and the cells were washed three times with pre-warmed PBS. The cells were then submerged in 0.5 mL pre-warmed HBSS for 30-min. The uptake studies of theophylline were initiated by the application of 0.5 mL test solutions, containing [^{14}C]-theophylline. At 2, 5, 10 and 20-mins, the cell media was carefully aspirated and the cell layers were washed three times with ice-cold PBS. The cell layers were lysed by adding 1 mL of 1% Triton X solution for 45-mins at 37 ^{0}C. The activity associated with the cell layers was determined by scintillation counting following the addition of scintillation cocktail. The protein content of each monolayer was determined using the BCA assay reagent kit. The results were expressed as total accumulation of theophylline per microgram of protein. The experiments were performed at 37 and 4 ^{0}C. Each condition was studied in triplicate and the data were presented as mean $\pm$ SD.

5.3.4 P-glycoprotein (P-gp) inhibition studies

A similar protocol as the one described in 5.3.3 was employed for the P-gp inhibition studies except for before cells were exposed to the test solutions, they were pre-incubated with the appropriate inhibitors (5 μM of elacridar and 4 μM of valspodar) for 30-min. Both inhibitors were first dissolved in DMSO due to their low solubility in HBSS and further diluted to the desired concentrations using HBSS (the final vehicle composition contained <0.1% (v/v) of DMSO). The subsequent steps were identical as to the procedure as described in 5.3.3.

5.3.5 Statistical analysis

Data were presented as mean ± standard deviation (SD). Statistical significance was performed using paired student's t-test (SigmaPlot13). A $p < 0.05$ was considered as statistical significant.

5.4 Results and discussion

5.4.1 MTT assay

The MTT assay was performed to assess the A549 biocompatibility of the theophylline test solutions in two different vehicles, water and 70% PG-water. The application systems were pH adjusted to 9.6 to mimic the formulation pH, however it was appreciated that the cells of the lung would never be exposed to this kind of pH in-vivo. As a result, a system was used that mixed the pH 9.6 with the cell media. The optimum water (pH 9.6)-HBSS (pH 7.4) ratio was initially assessed. Above a ratio of 1:1, the percentage of cell viability started to decline

significantly (Figure 5.1). This reduction was thought to be induced by the change in the overall pH of the accumulation medium as reported by Cutaia et al., (2005), who noted the effect of alkaline stress-induced apoptosis in human pulmonary artery endothelial cells. As a consequence, a 1:1 mixing ratio was chosen for the subsequent cell culture studies. The ratio 1:1 refers to the application of 500 µL of test solution to the 500 µL submerged cells.

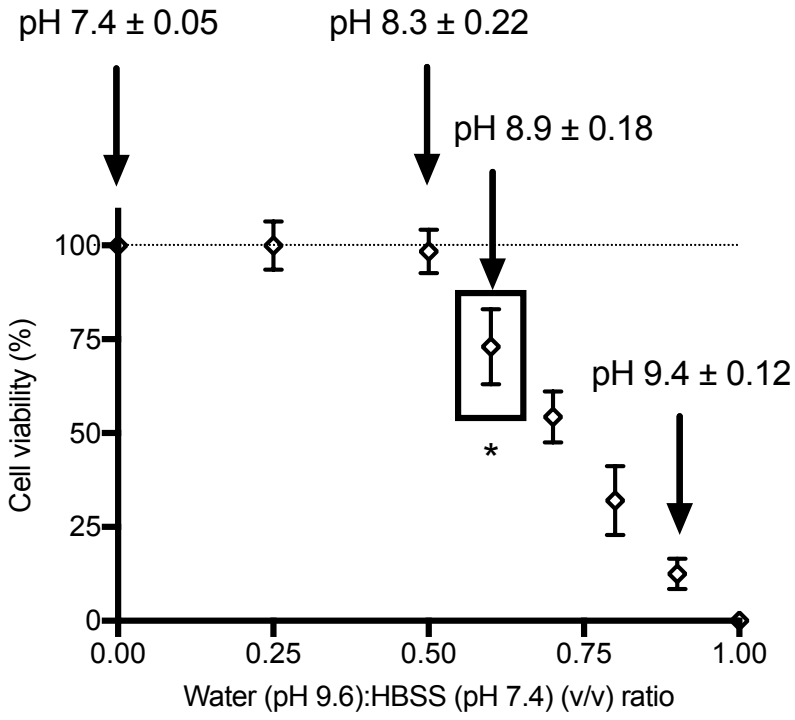

Figure 5.1 Percentage of A549 cell viability after 1h incubation at 37 ^{o}C with different ratios (v/v) water (pH 9.6):Hank's Balanced Salt Solution (HBSS), pH 7.4) assayed by MTT assay (n=3 $\pm$ SEM). All pH values indicated the final pH of the water:HBSS mixture. *statistically significant ($p<0.05$) when compared to 100% cell viability (Student's t-test). The data for pH 8.9 ± 0.18 was highlighted to justify the application of 500 µL of test solution to the 500 µL submerged cells (1:1 test solution:HBSS ratio) in the subsequent experiments as above this ratio, the cells viability will be compromised.

The free theophylline (THE), spermine (SP), cyclodextrins (CD) as well as the complexes, i.e., THE-SP and CD-THE-SP in water and 70% PG-water pH adjusted to 9.6 and added to the HBSS submerged cells at the respective concentrations did not show any adverse effect up to a 1 h time-point (Figure 5.2). Note in the subsequent accumulation studies, it was the intention that the cells would only be incubated with the test solutions for 20 min. The biocompatibility data recorded in this study aligned with previous work. For example, Matilainen et al., (2009) demonstrated that low concentrations of the parent (α-, β- and γ-CD) and modified CDs (hydroxypropyl-α and –β-CDs and randomly methylated-β-CD) ($\leq$ 1 mM) was safe for local pulmonary application when tested in Calu-3 cells. However, at higher concentrations ($\geq$ 2 mM), different cytotoxic effects were seen depending on the CD used. Of these three parent CDs, γ-CD was found to be the safest. This was thought due to its high solubility that limits its interaction with the cell membranes. Whilst between the modified types of CDs, they found that the methylated CD was more toxic compared to the hydroxypropyl- α and –β-CDs. This was most likely due to the ability of the methylated CD to interact and permeate through the cell membrane. The toxicity of CDs in cells was normally associated with the hemolytic activity and cholesterol-solubilizing ability of CDs (Boulmedarat et al. 2005; Ulloth et al. 2007; Kiss et al. 2010). In case of spermine, it can be toxic to cells when presented at 30 mM (Sharmin et al. 2001). This toxic effect was associated with the presence of amine oxidase enzyme in the culture medium. This enzyme degraded spermine into amino aldehydes, H_2O_2 and ammonia. These toxic products are able to induce stress-activated signal transduction pathways, leading to cell death, necrosis or apoptosis, in several cultured tumour cell lines (Averill-Bates et al. 2008). However, it should be noted that the presence of serum amine oxidase is species-specific, and the potential importance of this enzyme in humans, which are not good sources of the enzyme, is not fully

established (Averill-Bates et al. 2008). The toxicity of theophylline in-vitro has not been well documented.

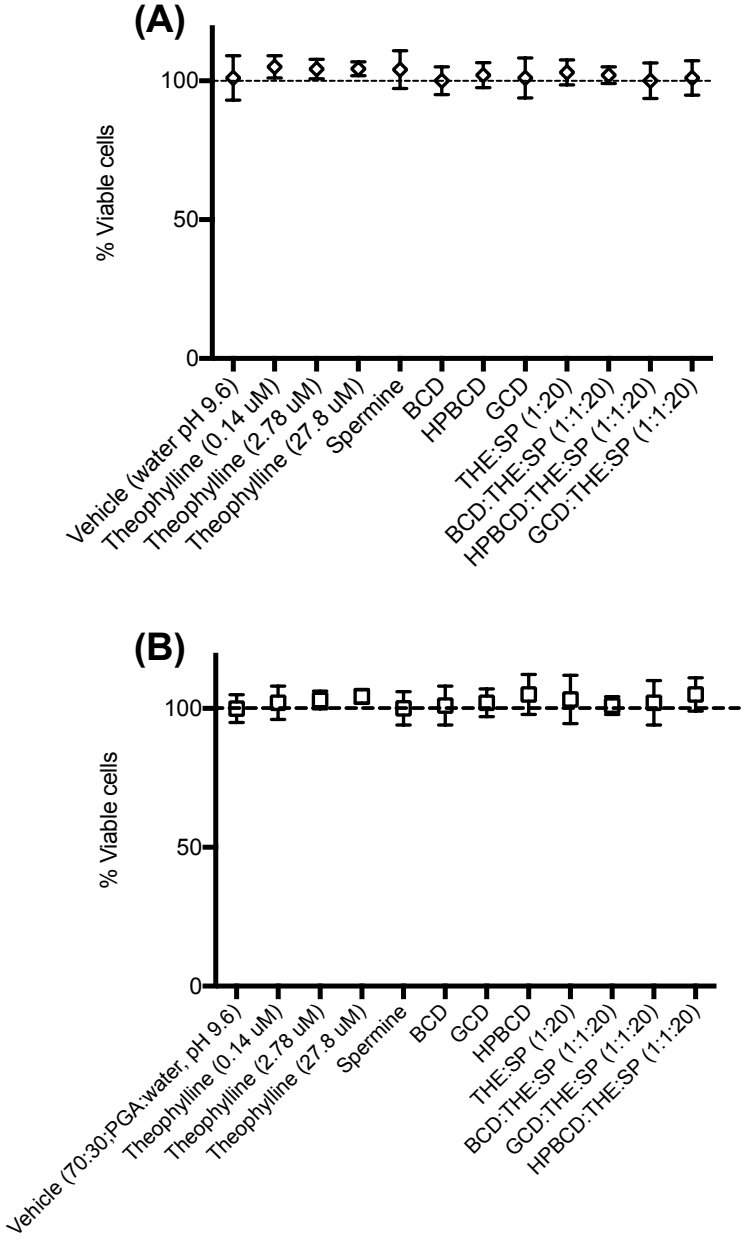

Figure 5.2 The percentage of viable A549 cells after 1h incubation at 37 ^{o}C with (i) (0.14, 2.78, 27.8 µM) free theophylline, (ii) free spermine (55.6 µM), (iii) free cyclodextrins (2.78 µM), (iv) theophylline-spermine ion-pair (2.78:55.6 µM; 1:20 molar ratio) and (v) theophylline-spermine ion-pair complexed with cyclodextrins (2.78:2.78:55.6 µM; 1:1:20 molar ratio) to the HBSS-submerged cells assayed by MTT test. All solutions were prepared in water (*graph A*) and 70/30 (v/v) propylene glycol (PG)/water (*graph B*) pH adjusted to 9.6. Values represent n=3 $\pm$ SD.

However, a study by Dolby et al., (1981) showed that the addition of 5 mM of theophylline to Hela-S3-cells caused a negative effect on the DNA synthesis. Murnane et al., (1981) showed that the lethal effect of caffeine which belongs the same family of methylxanthines as theophylline at high concentrations (7.5 and 10 mM) was due to its ability to interrupt the DNA synthesis when studied in human HT-29 cells.

5.4.2 Drug uptake studies

Theophylline displayed a concentration-dependent accumulation in-vitro when tested within the range of 0.14 – 27.8 μM (Figure 5.3).

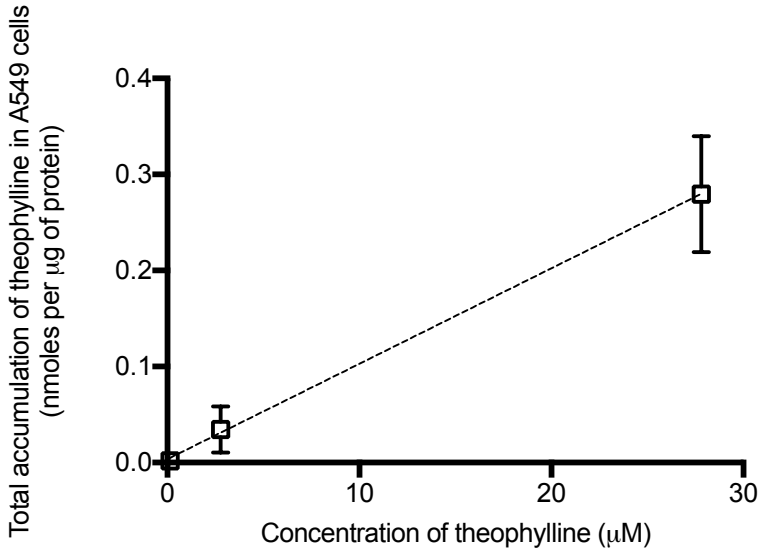

Figure 5.3 Total accumulation of theophylline in human lung epithelial A549 cells (nmoles per μg of protein) at 2-min, 37 °C after the application of theophylline solutions (0.14, 2.78, 27.8 μM) prepared in water at pH 9.6 to the HBSS-submerged cells (n = 3 $\pm$ SD).

It was anticipated that theophylline, due to its small molecular size (MW = 180.16 g moL^{-1}), could passively permeate through the cell membrane (Lipinski et al. 1997). This has been previously reported by Bellemann and Scholz (1974) when assessing the drug uptake in the guinea-pig heart. The low percentage of drug accumulation (ca. 0.2%) which was in line with the finding reported by Beanouda et al., (2018) indicated a very weak affinity of theophylline to the cells. The limited cell uptake of theophylline could be due to the molecules poor lipophilicity. The log D values of theophylline were previously determined in Chapter 2 of this thesis using the octanol/water partitioning experiments: log $D_{7.4}$ = -0.025 ± 0.008, log $D_{9.6}$ = -0.186 ± 0.015). To support this hypothesis, Arakawa and Kitazawa (1987) showed that the pulmonary absorption of theophylline was massively influenced by it lipophilicity when tested in rats. This was evidenced by a significant 11 % reduction of theophylline absorption when administered in a solution at pH 9.4 compared to its absorption at pH 7.4. The pK_a of theophylline is 8.6. At pH 9.4, theophylline was primarily existed ionized whilst at pH 7.4, the drug was presented uncharged in the solution which allowed better penetration of theophylline across the cell layers.

The total accumulation of theophylline in the lung epithelial cells did not increase as a function of time when tested up to 20-min, at 37 ^{o}C (Figure 5.4A). This suggested that theophylline quickly exited the cells once absorbed. A similar observation has been reported previously (Arakawa & Kitazawa 1987). In this study, ca. 90% of the theophylline was transferred into circulation following 1 min of pulmonary administration. Similarly, a similar observation was reported by Belleman and Scholz (1974) reported that theophylline uptake was rapid (>95% of drug absorption within 3 min), but after 5 min, >95% of the drug was washed out from the cells. In the current work it was thought that the poor accumulation of theophylline within the cells was mediated by active efflux. To test this hypothesis, the

accumulation experiment was repeated at 4 ^{o}C. It is known that the membrane transport at 4 ^{o}C suppresses the activity of active efflux tremendously due the depletion of the ATP production (Bratic & Trifunovic 2010). Interestingly, at 4 ^{o}C, the total accumulation of the drug increased as a function of time (Figure 5.4B). The total accumulation of theophylline was 2.6-fold higher after 20-min at 4 ^{o}C compared to its accumulation at 37 ^{o}C after 20 min incubation. This suggested that the poor accumulation of theophylline could be attributed to active efflux. This effect was further investigated.

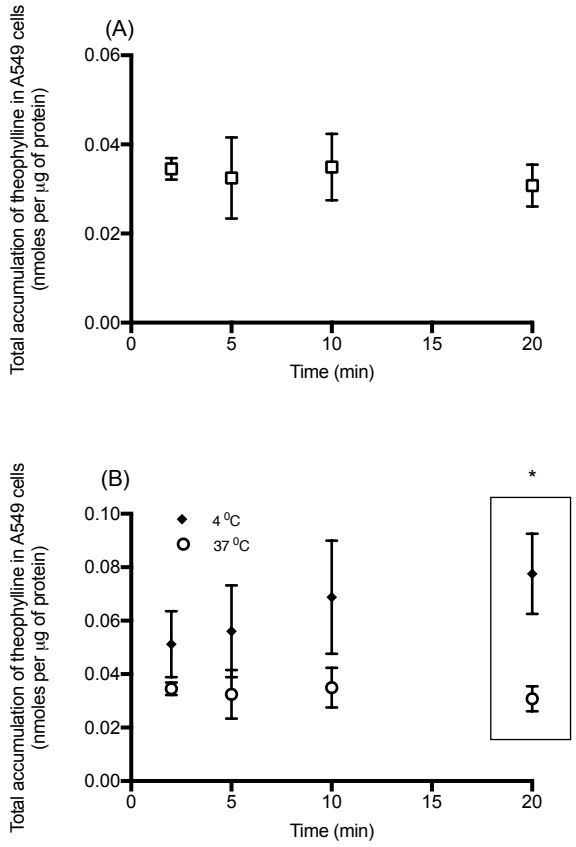

Figure 5.4 Total accumulation of theophylline in human lung epithelial A549 cells (nmoles per µg of protein) at 37 °C (*graph A*), 37 vs 4 °C (*graph B*) following the application of 2.78 µM theophylline to the HBSS-submerged cells at 2, 5, 10 and 20 minutes. All solutions were prepared in water at pH 9.6 and mixed with HBSS on the cell surface (n=3 $\pm$ SD). *statistically significant ($p<0.05$) when compared the total accumulation of theophylline between 4 and 37 ^{0}C at t=20 min (Student's t-test).

5.4.3 P-gp inhibition studies

A functionalized P-gp activity in A549 cells have been reported before (Xu et al. 2014; Hamilton et al. 2001). In this study, when the cells monolayer was pre-incubated with the specific P-gp inhibitors, elacridar and valspodar for 30-min, a significant 2-fold increment of total theophylline accumulation was achieved up to 20-min compared to the total accumulation when dosing the drug to the cells in the absence of the P-gp inhibitors (Figure 5.5). Both elacridar and valspodar are listed in the FDA list (last updated 26/9/2016) as specific inhibitor for P-gp transporter.

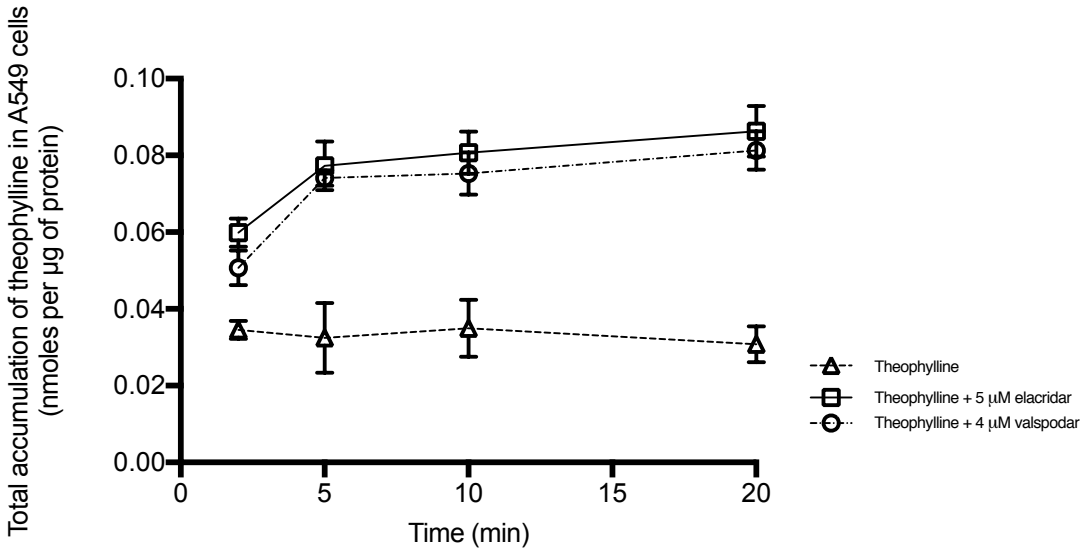

Figure 5.5 Effect of specific P-gp inhibitors (5 µM of elacridar and 4 µM of valspodar) on the total accumulation of theophylline in A549 cells at 37 ^{o}C at 2,5, 10 and 20-min. The figure shows the total accumulation of theophylline (nmoles per µg of protein) following the application of 2.78 µM of theophylline prepared in water pH 9.6 to HBSS submerged cells after 30 mins incubation with the inhibitors. Cells treated with theophylline without pre-incubation with P-gp inhibitor was used as control (n=3 $\pm$ SD).

5.4.4 Effect of polyamine ion-pairing on theophylline cell uptake

A significant increase ($p<0.05$) in theophylline accumulation in A549 cells was observed at t=2-min and 5-min when mixed with excess spermine counter-ion compared to the uptake of the drug alone (Figure 5.6). This relationship between the spermine concentration and its effects on the theophylline uptake was attributed to the ion-pairing effect where the presence of excess spermine in the medium forced the drug to bind to the counter-ion. However, over time, the percentage increase of drug uptake started to decrease significantly, which was thought to be induced by the dissociation of the ion-pair (as predicted in Chapter 4). The increase of theophylline ion-pair uptake by A549 cells was thought to be a consequence of the active PTS. Alternative mechanisms such as the ion-pair increasing cell uptake due to enhanced passive transport was unlikely to occur. This was due to a significant increase of theophylline polarity when mixed with spermine as mentioned previously. A similar trend of theophylline-spermine ion-pair (1:20 ratio) and free theophylline was observed at 4 ^{o}C (Figure 5.7). This again supported the idea that the theophylline-spermine ion-pair cell accumulation was enhanced through the active uptake via specific spermine-PTS binding.

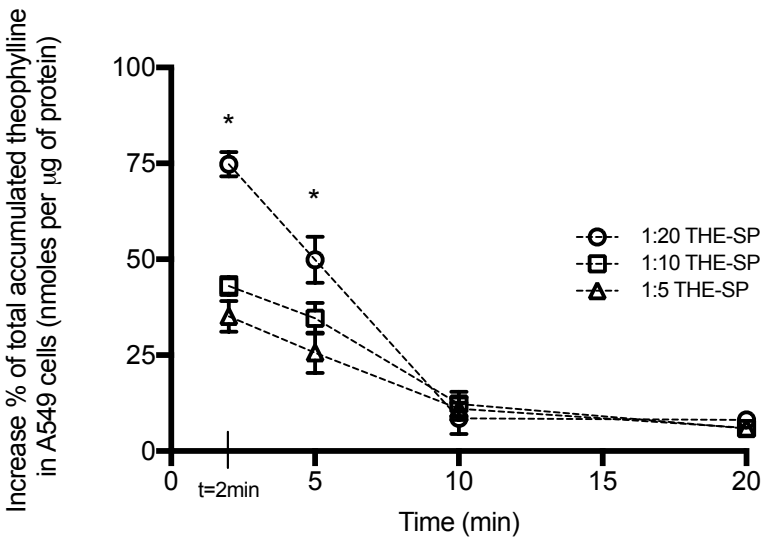

Figure 5.6 Increase percentage of the total accumulation of theophylline (nmoles per µg of protein) in lung epithelial A549 cells at 37 °C following the application of 2.78 µM free theophylline and theophylline mixed with spermine at different molar ratios (1:5, 1:10 and 1:20) to HBSS-submerged cells at 2, 5, 10 and 20-mins. All solutions were prepared in water pH adjusted to 9.6 (n=3 $\pm$ SD). Increase % of accumulated theophylline was calculated against the total accumulation of free theophylline. *statistically significant ($p<0.05$) when compared to the total accumulation of the free theophylline (Student's t-test).

Unfortunately, to-date, there is not a highly specific polyamine transporter inhibitor to test the hypothesis using inhibition studies. Furthermore, the concentration dependence, and hence saturation of the uptake process, could not be observed in the presence of the P-gp efflux. An additional complicating factor to the studies was that the spermine concentration (SP at 55.6 µM) applied to the cells, which exceeded the PTS K_m (at 0.5 µM) recorded for the spermidine uptake (Cullis et al. 1999) and hence the free unbound spermine, which is needed to force ion-pair formation, may have been competing for the PTS with the ion-paired theophylline-spermine.

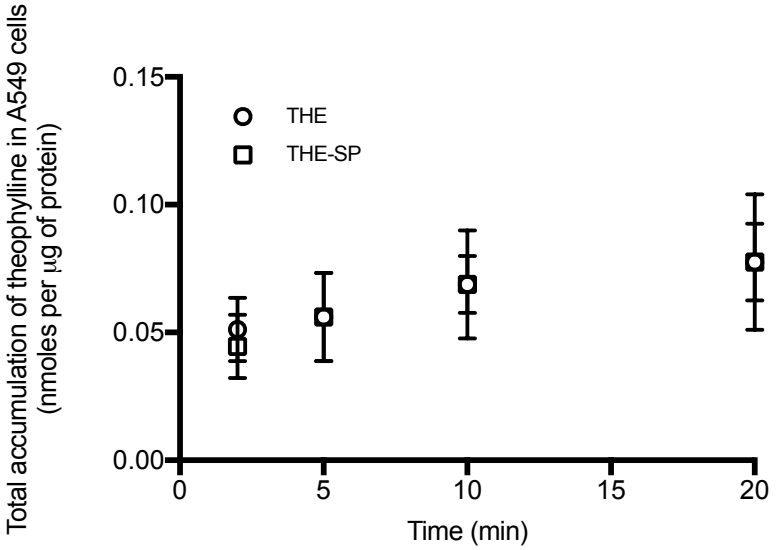

Figure 5.7 Total accumulation of theophylline (nmoles per μg of protein) in lung epithelial A549 cells at 4 °C following the application of free theophylline (2.78 μM) and theophylline mixed with spermine (2.78:55.6 μM; 1:20 molar ratio) to HBSS-submerged cells at 2, 5, 10 and 20-min. All solutions were prepared in water pH adjusted to 9.6 (n=3 ± SD).

The possibility of other active transporters increasing the uptake of the ion-pair was considered to be unlikely. The OCT transporter is known to sequester polyamines, but recent studies have shown that this active transport mechanism is 30-fold less efficient at moving amines into cells compared to the PTS (Sala-Rabanal, Li, et al. 2013). Thus, the conclusion that the PTS facilitated the theophylline ion-pair uptake into the A549 cells despite the potential complexities of how it achieved this was considered reasonable.

To further assess the effect of ion-pairing on the drug uptake into the cells, the theophylline-spermine (1:20) was prepared at pH 7.4 and 9.6 (Figure 5.8). The final pH of the accumulation medium when 0.5 mL of test solution (pH 9.6) was mixed with 0.5 mL HBSS (pH 7.4) was 8.31 ± 0.12. The percentage of uptake was significantly greater at t=2 min when

the mixture was prepared at pH 9.6 compared at pH 7.4. Using pK_a of theophylline (8.6), HySS predicted that ca. 30% of theophylline is deprotonated at pH 8.3 compared to only ca. 7% at pH 7.4 indicating a greater potential of ion-pairing effect when dosing the ion-pair formulation at pH 9.6 to the cells.

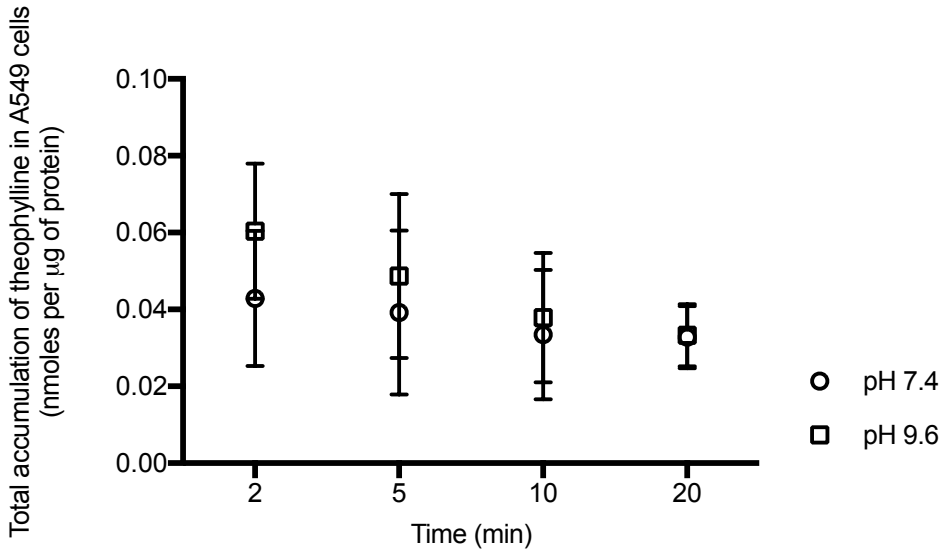

Figure 5.8 Total accumulation of theophylline (nmoles per μg of protein) in lung epithelial A549 cells at 37 °C following the application of theophylline mixed with spermine (2.78:55.6 μM; 1:20 molar ratio) to HBSS-submerged cells at 2, 5, 10 and 20-min. All solutions were prepared in water pH 7.4 or 9.6 (n=3 $\pm$ SD).

In the previous chapter, theophylline was found to exhibit greater affinity towards spermine when mixed in 70% PG-D_2O mixed solvent. However, no significant enhancement of drug uptake was seen when the theophylline-spermine mixture was prepared in 70% PG-H_2O and exposed to the cells compared when the formulation was made in H_2O (Figure 5.9). This could result from poor mixing of PG with the underlying HBSS due to high viscosity of PG.

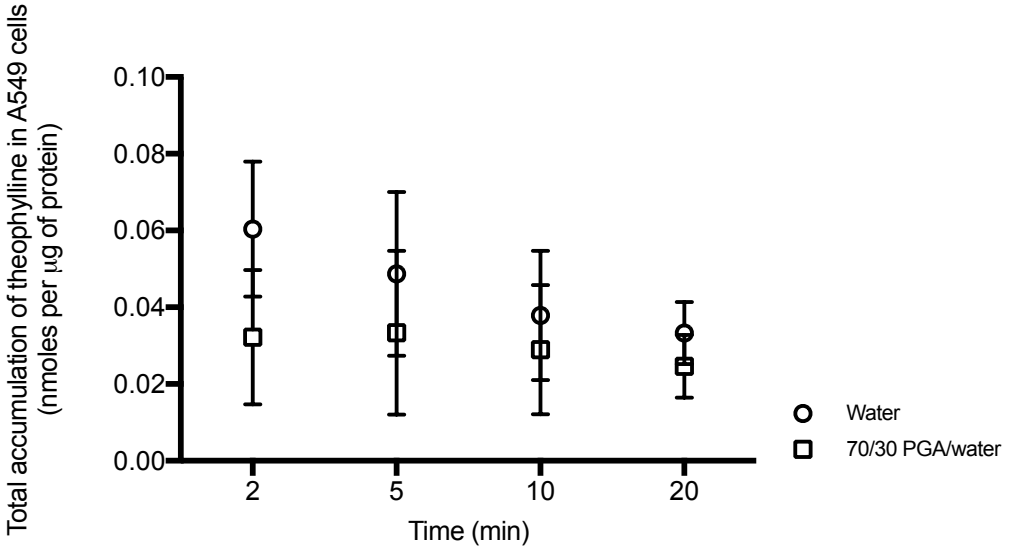

Figure 5.9 Total accumulation of theophylline (nmoles per µg of protein) in human lung epithelial A549 cells at 37 °C following the application of theophylline-spermine ion-pair (THE-SP) (2.78:55.6 µM; 1:20 molar ratio) prepared in water and 70/30 (v/v) propylene glycol/water pH 9.6 to HBSS-submerged cells at 2, 5, 10 and 20-min (n=3 $\pm$ SD).

The effect of vehicle viscosity on drug absorption has been studied before. Levy and Jusko (1964) assessed the absorption rate of ethanol and salicylic acid from the stomach of rats when administered in an aqueous solution containing increasing methylcellulose, which gave a viscosity range from 1 to 500 cps. In this study, the osmotic pressure was kept the same. The results showed an inverse correlation between viscosity and the molecules absorption rate. Levy and Jusko suggested that the decrease in drug absorption rate in a more viscous solution was due to the movement retardation of the molecules to the absorption site hence slowed the gastrointestinal transit. In another study by Furubayashi et al., (2007), they concluded that dosing solution with higher viscosity decreased drug i.e., acyclovir absorption whilst solution with moderate viscosity enhance drug permeation. This study was done in an

in-vitro Caco-2 system using dextran (DEX) as a dosing solution (Moderate viscosity = 20% DEX, High viscosity = 40% DEX).

A sustained retention of theophylline over time in the cells was achieved when dosing the ion-pair as complexed with cyclodextrins to the cells (Figure 5.10). This was seen up to 20-min. The ion-pair complexed with BCD exhibited a higher percentage of drug uptake compared when complexed with HPBCD and GCD. This could be associated to the higher binding capacity of BCD toward the ion-pair than HPBCD and GCD (as shown in Chapter 3). This suggested that the complexes formed between cyclodextrins and the ion-pair stabilized the weak association of the ion-pair resulted in a longer retention of the drug in the cells. The hydrophobic cavity of CDs was thought to provide a physical protection of the encapsulated fraction of the ion-pair from the extracellular medium, which resulted in improved of stability. The possible hydrogen bonding between the ion-pair with the hydroxyl group on the outer rim of CD enhanced the complex formation hence improved the overall stability of the ion-pair.

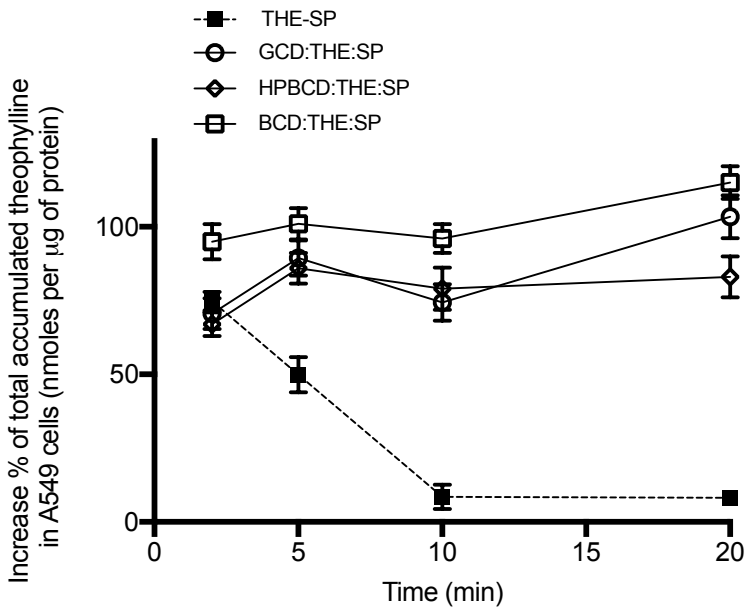

Figure 5.10 Percentage of increase of the total accumulated theophylline in human lung epithelial A549 cells at 37 °C following the application of (i) theophylline-spermine ion-pair (THE-SP) (2.78:55.6 μM; 1:20 molar ratio) and (ii) THE-SP complexed with gamma-cyclodextrin (GCD:THE:SP, 2.78:2.78:55.6 μM; 1:1:20 molar ratio), 2-hydroxypropyl-beta-cyclodextrin (HPBCD:THE:SP, 2.78:2.78:55.6 μM; 1:1:20 molar ratio) and beta-cyclodextrin (BCD:THE:SP, 2.78:2.78:55.6 μM; 1:1:20 molar ratio) to HBSS-submerged cells at 2, 5, 10 and 20-min. Increase % of accumulated theophylline was calculated against the total accumulation of free theophylline. All solutions were prepared in water pH adjusted to 9.6 (n=3 $\pm$ SD).

5.5 Conclusion

The free theophylline, spermine, cyclodextrin and their complexes were found to be well-tolerated to the HBSS submerged A549 cells when tested at the respective concentrations using a MTT assay. An improved accumulation of theophylline in A549 cells that was most likely to be mediated by PTS was achieved when dosing the drug as ion-pairing with excess spermine to the cells. Interestingly, a more sustained retention of the drug in the cells was seen when dosing the drug as ion-pair complexed with CDs suggested the ability of CDs to control the stability of the ion-pair. It was also found that the short retention time of theophylline within the A549 cell-line was mediated, at least in part, by P-gp efflux activity.

CHAPTER 6

General discussion and future studies

6.1 General discussion

The field of drug delivery has grown tremendously over the last few decades. Numerous new materials have been synthesized to be used in drug delivery and different approaches have been designed and tested with the ultimate aim to improve the treatment efficacy. One focus in this field is the development of a delivery system that can deliver bioactive agents specifically to target sites whilst minimizing harmful side-effects (Tian et al. 2017; Bashari et al. 2017; Papa et al. 2017). In this thesis, the polyamine ion-pairing approach was explored for lung-targeting delivery using theophylline as a model drug. It was hoped such targeting system could improve the nonspecific tissue distribution of theophylline when administered intravenously for anti-asthmatic treatment. The structure-activity studies have established that good PTS substrates require two or more N-containing moieties that are protonated at physiological pH. As very few therapeutic agents that require delivery into the lungs display these structural characteristics, the attempt to use a number of polyamine drug analogues and covalent polyamine drug conjugates to manipulate the PTS to target delivery to the lungs have had limited success because combining the molecular features required for effective active PTS transport and pharmacological action in a single molecule is problematic (Wang et al., 2003; Tomasi et al., 2010).

Secondary to that, since ion-pairs associations are temporary, they will almost certainly revert back into their parent ions and eliminated individually when enter the biological systems (W. Wang et al. 2017; Zhao et al. 2017b). Hence, forming a drug ion-pair not only offers simplicity in terms of sample preparation, but it also allows the active molecule to be presented in its original form upon dissociation hence bypassing any pharmacological and toxicological issues normally associated with covalently conjugated drug targeting. It seems

reasonable that drug ion-pairs that are formed through multiple hydrogen bonds could stay associated during the absorption process and this hypothesis has been supported by previous studies that show ion-pair formation influences absorption via the skin, GI tract and respiratory system. The spectroscopy data gathered for theophylline-amine mixtures suggested that ion-pairs were formed between theophylline and all of the counter-ions tested in the aqueous (Figures 2.3 and 2.4, Chapter 2), EtOH and PG-water co-solvents (Figures 4.2 and 4.3, Chapter 4) vehicles at pH 9.6. The differences in ion-pair affinities across the homologous series of amines were thought to be due to the differences in the hydrogen bonding capacity of amine counter-ions with the theophylline. The HPLC affinity coefficients were identical in rank order to the FT-IR measurements, but in all cases the absolute value was approximately 1 log unit higher. The HPLC studies analysed theophylline samples that were at least 1 order of magnitude lower in concentration (this value is probably > 1 order of magnitude due to dilution upon the HPLC column). As theophylline is prone to dimerization, it could be that at higher drug concentrations, when the theophylline is more likely to dimerise its affinity with the amine counter-ions is lower. Although the HPLC concentrations were closer to the cell uptake concentrations and more like those found in vivo, the FT-IR values were used in the calculations of percentage ion-pair formation in the cell culture work as this was more conservative and less likely to falsely inflate the impact of the results.

The effects of the co-solvent on the ion-pair association was only demonstrated using the strongest theophylline-spermine ion-pair. With this test system, the addition of an organic component to the solvent (PG and EtOH) showed a minimal impact on the ion-pair association in a similar manner to previous work (Table 4.2, Chapter 4). The changes of the

ion-pair interactions were most likely due to the weakening of the water's supramolecular structure in the organic mixed solvent systems (Benaouda et al. 2012). The ability to change the association strength of the complex, through modification of the solvent in which it was dissolved, provided a degree of flexibility in this drug targeting approach, as presumably a greater association of the complex would lead to slower release of the parent drug from the ion-pair upon administration, however the *in-vitro* dissociation experiments did provide support to this notion (Figures 4.6 and 4.7, Chapter 4). This may have been a consequence of the lack of sensitivity in the dissociation assay or it could have been that the small differences in association constants having little practical significance.

Drug ion-pair dissociation is driven by fluctuations in pH and the dilution effects experienced during the drug absorption process, but it is problematic to directly study this process using traditional analytical techniques during the process of drug absorption. One of the issues faced when trying to understand ion-pair cell uptake is defining the concentrations of the ion-pairs that are presented to the absorptive barrier. Simply adding an equal molar equivalent ratio of drug and counterion does not generate 100% of the 1:1 ion-paired system due to their relatively weak association strength. Previous work has measured the association constant, the relative concentrations of the parent drug and counterion and the pH to calculate the proportion of ion-paired drugs that were presented to cells in transport studies. From this work, it was discovered that for most ion-pairs to achieve a high degree of ion-pair formation an excess of counter-ion was required (Patel et al. 2016). A second issue faced when attempting to understand the ability of drug ion-pairs to influence absorption is the inability to predict or experimentally measure ion-pair dissociation during absorption. Currently the best way to determine if the ion-pair does stay intact during the cell uptake is to characterise the effect of ion-pairs on the process of absorption. Although ion-pairs are sensitive to both

changes in drug, counter-ion and competing ionised molecule presence, which can confound the sound interpretation of some experiments, it is possible using tightly controlled functional studies to investigate the effects of ion-pairs on absorption in-vitro, ex-vivo and in-vivo.

Mixing theophylline with increasing levels of the amine counter-ions diminished the drug's lipophilicity and significantly increased its aqueous solubility (Figure 2.9, Chapter 2). This effect was opposite to the traditional notion that ion-pair formation always results in an increase in lipophilicity. The results demonstrated that ion-pair properties are a function of both the drug and counter-ion properties and when these two elements are held together in a complex it can be more hydrophilic compared to the parent compound. The effects of ion-pair formation on solubility were more apparent at pH 9.6 compared to pH 7.4 presumable due to the greater proportion of ion-pairs formed at the more alkaline pH due to the theophylline's pKa. However, that fact that the significant effects was observed at physiological conditions meant that the ion-pairing of the drug was still consequential even when only a small proportion of it was ionised.

The uptake of theophylline into the lung epithelia cells was surprisingly low for a therapeutic agent that acts in the lung tissue (ca. 0.035 nmoles per g of tissue) (Figure 5.3, Chapter 5). However, previous theophylline bio-distribution studies support this low uptake. Although the A549 cells showed a dose dependant uptake at 2 min they failed to accumulate the drug over a 20-min period. It was unlikely that theophylline transport into the cells had reached its passive transport equilibration point after only 2 min given that only approximately 0.2 % of the drug have moved into the cells after 2 min and that the dose dependant uptake showed that the cells did have the capacity to accept more drug. It was more likely that the rapid

equilibration point in cell uptake was achieved as a result of the uptake and efflux processes finding equipoise. The increased of drug uptake when ion-paired with spermine was most likely to be mediated by the polyamine transporter system (PTS) because the more hydrophilic nature of the ion-pair compared to the parent drug was not likely to enhance passive cell drug accumulation (Figure 5.6, Chapter 5). The structure-activity studies have established that good PTS substrates require two or more N-containing moieties that are protonated at physiological pH. As very few therapeutic agents that require delivery into the lungs display these structural characteristics, a number of polyamine drug analogues and covalent polyamine drug conjugates have been developed in an attempt to use the PTS to target delivery to the lungs. However, these strategies have had limited success because combining the molecular features required for effective active PTS transport and pharmacological action in a single molecule is problematic. Since the specific gene responsible to modulate the PTS in animal cells is not known, the confirmation molecular biology techniques could not be used to confirm this PTS mediated theophylline-spermine ion-pair into cells. Functional studies, which increased the ion-pair, reduced the transport temperature all pointed to the PTS are the mechanism of active uptake, but it is possible that another transporter such as the OCT transporter could have been involved in this process (Sala-Rabanal et al. 2013). Apart from that, the increase in the cell uptake of theophylline when presented as ion-pair to the cells could also be facilitated by an advanced endocytosis process.

Cell pre-incubation with the P-gp inhibitors elacridar and valspodar suggested active drug efflux (Figure 5.5, Chapter 5). In addition to P-gp both BCRP and MRP2 could be inhibited by elacridar (BCRP) and valspodar (MRP2) , but unlike P-gp there is not studies confirming expression of these transporters in the alveolar epithelium cells (Bosquillon 2010). In the

literature, theophylline has not been reported to be a P-gp substrate. Wang et al. (2005), using an unsupervised machine learning approach based on the Kohonen self-organizing maps (SOM) (average accuracy of 82.3%) which incorporated a predefined set of physicochemical descriptors encoding the key molecular properties suggested that a theophylline-like molecule i.e., caffeine as an unfit molecule to be a P-gp substrate. However, until the gathering of more data it seemed reasonable to suggest that the ca. 2-fold increase of the total accumulated theophylline in the pre-incubated cells with the inhibitors owas a consequence of efflux and this could have been mediated by the P-gp as both elacridar and valspodar are both known P-gp inhibitors.

A sustained retention of theophylline over time in the cells was achieved when dosing the ion-pair as a cyclodextrin complex to the cells (Figure 5.10, Chapter 5). Our findings suggested that the hydrophobic cavity of cyclodextrin could provide a physical protection of the encapsulated lipophilic part of the ion-pair which resulted in a relatively stronger association of the theophylline-spermine ion-pair to withstand the corrosive environment at the extracellular level. Apparently more work is required to understand the relationship between drug ion-pair association strength, physical stability and their ability to influence absorption in-vivo. Further in-vivo work is obviously necessary to assess the influence of ion-pair formation on in-vivo bio-distribution which would help not only to understand the significance of the physical stability of the ion-pair on its whole body distribution but also aid designing new ion-pairs to target specific tissues after systemic administration.

6.2 Future studies

In this present study, in-vitro studies suggested that ion-pairing spermine with theophylline formulated using cyclodextrins improved the cell uptake of the drug into the lung cells. In order to prove that this strategy can improve theophylline lung-targeting delivery, in-vivo studies need to be carried out. The theophylline test formulations can be introduced to the animals using tail injection method. After 5-min and 60-min time points, the major organs (brain, liver, spleen, kidney, heart) should be harvested to trace the amount of theophylline in the respective tissue. The amount of theophylline in the blood should also be examined. The biodistribution studies should be performed with and without the presence of the polyamine and cyclodextrin to assess the impact of these molecules on the biological behavior of the drug.

The current work suggests that PTS will not only extract polyamines from the circulation into the lung, but can also transport therapeutic agents ion-paired to polyamines, in this case theophylline. This mechanism could also be utilized for other drugs that can ion-pair with polyamines. Since it is known that cancer cells overexpressed PTS, ion-pairing polyamine with an anti-cancer agent could provide a new means to improve the anti-cancer treatment. One agent which could benefit from this is 5-fluorouracil (5-Fu) which is currently used in the treatment of cancers. The drug has a pK_a of 8 which means that it is ionizable at physiological pH and hence has the potential to form an ion-pair with a polyamine. 5-Fu-based chemotherapy has been shown to improve overall and disease-free survival of patients but chemoresistance of 5-Fu is one of the major challenges (Zhao et al. 2014). Physicochemical characterization (binding, log D and solubility studies) of 5-Fu complexed with polyamine at physiological pH needs to be done to understand how the interactions

between these molecules occur in addition to in-vitro and in-vivo studies. Apart from using the known existence polyamine *e.g.,* spermine to form ion-pairing with drugs for targeting delivery, future studies can also explore the use of novel polyamine analog to form drug ion-pair as this could also provide a new strategy for anti-cancer treatments since a study by Alm et al., (2000) demonstrated significant disturbances in polyamine metabolism caused by treatment with the spermine analog DENSPM when tested in Chinese hamster ovary cells. However, since the instability of this association can cause major setback of this approach, future studies also need to focus on finding a strategy to overcome this issue. This can be done by evaluating different strategies (*e.g.,* using liposomes formulated using cylcodextrins to form a complex with the ion-pair) to engineer a physically stable drug-ion-pair complex in solution.

References

Adjei, A. & Gupta, P., 1994. Pulmonary delivery of therapeutic peptides and proteins. *Journal of Controlled Release*, 29(3), pp.361–373.

Agu, R.U. et al., 2001. The lung as a route for systemic delivery of therapeutic proteins and peptides. *Respiratory research*, 2(4), pp.198–209.

Akbarzadeh, A. et al., 2013. Liposome: classification, preparation, and applications. *Nanoscale Research Letters*, 8(1), p.102.

Aksamija, A. et al., 2016. The inclusion complex of rosmarinic acid into beta-cyclodextrin: A thermodynamic and structural analysis by NMR and capillary electrophoresis. *Food Chemistry*, 208, pp.258–263.

Alberti, E., Zampakou, M. & Donghi, D., 2016. Covalent and non-covalent binding of metal complexes to RNA. *Journal of Inorganic Biochemistry*, 163, pp.278–291.

Allen, T.M. & Cullis, P.R., 2013. Liposomal drug delivery systems: From concept to clinical applications. *Advanced Drug Delivery Reviews*, 65(1), pp.36–48.

Alves, C. et al., 2011. Stability of furosemide and aminophylline in parenteral solutions. *Brazilian Journal of Pharmaceutical Sciences*, 47, pp.89–96.

Amin, M.L., 2013. P-glycoprotein inhibition for optimal drug delivery. *Drug Target Insights*, 2013(7), pp.27–34.

Andres, A. et al., 2015. Setup and validation of shake-flask procedures for the determination of partition coefficients (log D) from low drug amounts. *European Journal of Pharmaceutical Sciences*, 76, pp.181–191.

Arakawa, E. & Kitazawa, S., 1987. Studies on the factors affecting pulmonary absorption of xanthine derivatives in the rat. *Chemical and pharmaceutical bulletin*, 35, pp.2038–2044.

Aszalos, A., 2004. P-glycoprotein-based drug-drug interactions: Preclinical methods and relevance to clinical observations. *Archives of Pharmacal Research*, 27(2), pp.127–135.

Averill-Bates, D.A. et al., 2008. Mechanism of cell death induced by spermine and amine oxidase in mouse melanoma cells. *International Journal of Oncology*, 32(1), pp.79–88.

Azarmi, S., Roa, W.H. & Löbenberg, R., 2008. Targeted delivery of nanoparticles for the treatment of lung diseases. *Advanced Drug Delivery Reviews*, 60(8), pp.863–875.

Baalousha, M., 2017. Effect of nanomaterial and media physicochemical properties on nanomaterial aggregation kinetics. *NanoImpact*, 6, pp.55–68.

Ballard, A.J. & Dellago, C., 2012. Toward the mechanism of ionic dissociation in water. *Journal of Physical Chemistry B*, 116(45), pp.13490–13497.

Banerjee, A. et al., 2017. Strategies for targeted drug delivery in treatment of colon cancer: current trends and future perspectives. *Drug Discovery Today*, 22(8), pp.1224–1232.

Barnes, P.J., 2010. Theophylline. *Pharmaceuticals*, 3, pp.725–747.

Bartyzel, A., 2017. Effect of molar ratios of reagents and solvent on the complexation process of nickel(II) ions by the N_2 O_3 -donor Schiff base. *Polyhedron*, 134, pp.30–40.

Bashari, O. et al., 2017. Discovery of peptide drug carrier candidates for targeted multi-drug delivery into prostate cancer cells. *Cancer Letters*, 408, pp.164–173.

Benaouda, F. et al., 2012. Discriminating the molecular identity and function of discrete supramolecular structures in topical pharmaceutical formulations. *Molecular Pharmaceutics*, 9(9), pp.2505–2512.

Benaouda, F. et al., 2018. Ion-pairing with spermine targets theophylline to the lungs via the polyamine transport system. *Molecular Pharmaceutics*, 15(3), pp.861-870.

Biesta, W. et al., 2012. Preparation, Characterization, and Surface Modification of Trifluoroethyl Ester-Terminated Silicon Nanoparticles. *Chemistry of Materials*, 24(22), pp.4311–4318.

Blessy, M. et al., 2014. Development of forced degradation and stability indicating studies of drugs — A review. *Journal of Pharmaceutical Analysis*, 4(3), pp.159–165.

Bosquillon, C., 2010. Drug transporters in the lung - Do they play a role in the biopharmaceutics of inhaled drugs? *Journal of Pharmaceutical Sciences*, 99(5), pp.2240–2255.

Boija, S. et al., 2014. Determination of conditional stability constants for some divalent transition metal ion-EDTA complexes by electrospray ionization mass spectrometry. *Journal of Mass Spectrometry*, 49(7), pp.550–556.

Borges-Walmsley, M.I., McKeegan, K.S. & Walmsley, A.R., 2003. Structure and function of efflux pumps that confer resistance to drugs. *The Biochemical journal*, 376(Pt 2), pp.313–38.

Bosch, F. & Rosich, L., 2008. The contributions of paul ehrlich to pharmacology: A tribute on the occasion of the centenary of his nobel prize. *Pharmacology*, 82(3), pp.171–179.

Boulmedarat, L. et al., 2005. Evaluation of buccal methyl-β-cyclodextrin toxicity on human oral epithelial cell culture model. *Journal of Pharmaceutical Sciences*, 94(6), pp.1300–1309.

Bratic, I. & Trifunovic, A., 2010. Mitochondrial energy metabolism and ageing. *Biochimica*

et Biophysica Acta - Bioenergetics, 1797(6–7), pp.961–967.

Brown, H.. & Wilkins, B.., 2003. Use of intravenous salbutamol in acute severe asthma. *Anaesthesia*, 58, pp.729–731.

Browne, M., Kugler, A. & Eldon, M., 1996. Pharmacology and Pharmacokinetics of Rituximab. *Neurology*, (46), pp.3–7.

Brune, K., Renner, B. & Tiegs, G., 2015. Acetaminophen/paracetamol: A history of errors, failures and false decisions. *European Journal of Pain*, 19(7), pp.953–965.

Bruni, R. et al., 2017. Ultrasmall polymeric nanocarriers for drug delivery to podocytes in kidney glomerulus. *Journal of Controlled Release*, 255(March), pp.94–107.

Buchner, R. et al., 2003. Hydration and ion pairing in aqueous sodium oxalate solutions. *ChemPhysChem*, 4(4), pp.373–378.

Cabeça, L.F. et al., 2011. Prilocaine-cyclodextrin-liposome: Effect of pH variations on the encapsulation and topology of a ternary complex using 1H NMR. *Magnetic Resonance in Chemistry*, 49(6), pp.295–300.

Chakraborty, S. et al., 2017. Zinc(II)-salphen complexes bearing long alkoxy side arms: Synthesis, solvent dependent aggregation, and spacer group substituent effect on mesomorphism and photophysical property. *Journal of Molecular Liquids*, 246, pp.290–301.

Cheng, H. et al., 2017. Development of nanomaterials for bone-targeted drug delivery. *Drug Discovery Today*, 22(9), pp.1336–1350.

Cirri, M. et al., 2009. Physical-chemical characterization of binary and ternary systems of ketoprofen with cyclodextrins and phospholipids. *Journal of Pharmaceutical and Biomedical Analysis*, 50(5), pp.683–689.

Cui, H. et al., 2015. Mechanism of Ion-Pair Strategy in Modulating Skin Permeability of Zaltoprofen: Insight from Molecular-Level Resolution Based on Molecular Modeling and Confocal Laser Scanning Microscopy. *Journal of Pharmaceutical Sciences*, 104(10), pp.3395–3403.

Cullis, P.M. et al., 1999. Probing the mechanism of transport and compartmentalisation of polyamines in mammalian cells. *Chemistry and Biology*, 6(10), pp.717–729.

Das, N. et al., 2010. Codrug: An efficient approach for drug optimization. *European Journal of Pharmaceutical Sciences*, 41(5), pp.571–588.

Dhand, C. et al., 2014. Role of size of drug delivery carriers for pulmonary and intravenous administration with emphasis on cancer therapeutics and lung-targeted drug delivery. *RSC Advances*, 4(62), pp.32673–32689.

Eisert, W.G. et al., 2010. Dabigatran: An oral novel potent reversible nonpeptide inhibitor of

thrombin. *Arteriosclerosis, Thrombosis, and Vascular Biology*, 30(10), pp.1885–1889.

Elshaer, A., Hanson, P. & Mohammed, A.R., 2014. European Journal of Pharmaceutical Sciences A novel concentration dependent amino acid ion pair strategy to mediate drug permeation using indomethacin as a model insoluble drug. *European Journal of Pharmaceutical Sciences*, 62, pp.124–131.

Ester, H. et al., 2012. Enabling the Intestinal Absorption of Highly Polar Anti-Viral Agents: Ion-Pair Facilitated Membrane Permeation of Zanamivir Heptyl Ester and Guanidino Oseltamivir. *Molecular Pharmaceutics*, 7(4), pp.1223–1234.

Frassineti, C. et al., 2003. Determination of protonation constants of some fluorinated polyamines by means of 13 C NMR data processed by the new computer program HypNMR2000 . Protonation sequence in polyamines. *Anal Bioanal Chem*, pp.1041–1052.

Gabizon, A. et al., 2002. Dose dependency of pharmacokinetics and therapeutic efficacy of pegylated liposomal doxorubicin (DOXIL) in murine models. *Journal of Drug Targeting*, 10(7), pp.539–548.

Gabrielsson, J.L., Paalzow, L.K. & Nordstrm, L., 1984. A Physiologically Based Pharmacokinetic Model for Theophylline Disposition in the Pregnant and Nonpregnant Rat. *Journal of Pharmacokinetics and Biopharmaceutics*, 12(2).

Gaidamauskas, E. et al., 2009. Deprotonation of β-cyclodextrin in alkaline solutions. *Carbohydrate Research*, 344(2), pp.250–254.

Geng, Y. & Romsted, L.S., 2005. Ion pair formation in water. Association constants of bolaform, bisquaternary ammonium, electrolytes by chemical trapping. *Journal of Physical Chemistry B*, 109(49), pp.23629–23637.

Giorgi, E.P. & Stein, W.D., 1981. The transport of steroids into animal cells in culture. *Endocrinology*, 108(2), pp.688–697.

Gottesman, M.M. & Pastan, I.H., 2015. The Role of Multidrug Resistance Efflux Pumps in Cancer: Revisiting a JNCI Publication Exploring Expression of the MDR1 (P-glycoprotein) Gene. *Journal of the National Cancer Institute*, 107(9), pp.4–6.

Granero, G.E. et al., 2008. Synthesis, characterization and in vitro release studies of a new acetazolamide-HP-β-CD-TEA inclusion complex. *European Journal of Medicinal Chemistry*, 43(3), pp.464–470.

Gromiha, M.M. & Yugandhar, K., 2017. Integrating computational methods and experimental data for understanding the recognition mechanism and binding affinity of protein-protein complexes. *Progress in Biophysics and Molecular Biology*, 128, pp.33–38.

Guminski, Y. et al., 2009. Synthesis of conjugated spermine derivatives with 7-nitrobenzoxadiazole (NBD), rhodamine and bodipy as new fluorescent probes for the

polyamine transport system. *Bioorganic and Medicinal Chemistry Letters*, 19(9), pp.2474–2477.

Haas, K.L. & Franz, K.J., 2010. Application of Metal Coordination Chemistry to Explore and Manipulate Cell Biology. *Chemical Reviews*, 109(10), pp.4921–4960.

Hamai, S., 2009. Ternary inclusion complexes of γ-cyclodextrin with sodium 1-pyrenesulfonate and cationic and anionic organic compounds having an alkyl chain in aqueous solution. *Journal of Inclusion Phenomena and Macrocyclic Chemistry*, 63(1–2), pp.77–86.

Hamilton, K. et al., 2001. P-glycoprotein efflux pump expression and activity in calu-3 cells. *Journal of Pharmaceutical Sciences*, 90(5), pp.599–606.

Hassan, S. et al., 2017. Evolution and clinical translation of drug delivery nanomaterials. *Nano Today*, 15, pp.91–106.

He, Z. et al., 2011. Doxycycline and hydroxypropyl-β-cyclodextrin complex in poloxamer thermal sensitive hydrogel for ophthalmic delivery. *Acta Pharmaceutica Sinica B*, 1(4), pp.254–260.

Higashi, K. et al., 2010. Simultaneous dissolution of naproxen and flurbiprofen from a novel ternary gamma-cyclodextrin complex. *Chemical & Pharmaceutical Bulletin*, 58(5), pp.769–72.

Hoet, P.H.M. & Nemery, B., 2000. Polyamines in the lung: polyamine uptake and polyamine-linked pathological or toxicological conditions. *American Journal Physiology and Lung Cell Molecular Physiology*.

Horiuchi, Y. et al., 1990. Release control of theophylline by beta-clodextrin derivatives : hybridizing effect of hydrophilic , hydrophobic and ionizable beta-cyclodextrin complexes. *Journal of Controlled Release*, 15, pp.1–7.

Hoshino, K. et al., 2005. Polyamine Transport by Mammalian Cells and Mitochondria. *The Journal of Biological Chemistry*, 280(52), pp.42801–42808.

Hughes, J.P. et al., 2011. Principles of early drug discovery. *British Journal of Pharmacology*, 162(6), pp.1239–1249.

Huttunen, K.M., Raunio, H. & Rautio, J., 2011. Prodrugs - from serendipity to rational design. *Pharmacological Reviews*, 63(3), pp.750–71.

Ivaturi, V.D. & Kim, S.K., 2009. Enhanced Permeation of Methotrexate In Vitro by Ion Pair Formation With L -Arginine. *Journal of Pharmaceutical Sciences*, 98(10), pp.3633–3639.

Iyire, A., Alayedi, M. & Mohammed, A.R., 2016. Pre-formulation and systematic evaluation of amino acid assisted permeability of insulin across in vitro buccal cell layers. *Scientific Reports*, 6(September), pp.1–15.

Jansook, P. & Loftsson, T., 2008. gCD/HPgCD: Synergistic solubilization. *International Journal of Pharmaceutics*, 363(1–2), pp.217–219.

Jesse V Jokerst, Tatsiana Lobovkina, R.N.Z. and S.S.G., 2012. Nanoparticle PEGylation for imaging and therapy. *Nanomedicine*, 6(4), pp.715–728.

Jornada, D.H. et al., 2016. The prodrug approach: A successful tool for improving drug solubility. *Molecules*, 21(1).

Jr. Casero, R. & Woster, P., 2010. Recent Advances in the Development of Polyamine Analogues as Antitumor Agents. *Journal of Medicine (Cincinnati)*, 52(15), pp.4551–4573.

Juluri, A. & Narasimha Murthy, S., 2014. Transdermal iontophoretic delivery of a liquid lipophilic drug by complexation with an anionic cyclodextrin. *Journal of Controlled Release*, 189, pp.11–18.

Jusko, J., 1984. Theophylline disposition in obese rats. *The Journal of Pharmacology and Experimental Therapeutics*, pp.380–386.

Kah, M. & Brown, C.D., 2008. Chemosphere Log D : Lipophilicity for ionisable compounds. *Chemosphere*, 72, pp.1401–1408.

Kell, D.B. & Oliver, S.G., 2014. How drugs get into cells: tested and testable predictions to help discriminate between transporter-mediated uptake and lipoidal bilayer diffusion. *Frontiers in Pharmacology*, 5(October), pp.1–32.

Khan, A.R. et al., 2017. Progress in brain targeting drug delivery system by nasal route. *Journal of Controlled Release*, 268(August), pp.364–389.

Kim, D., Friedman, A.D. & Liu, R., 2014. Tetraspecific ligand for tumor-targeted delivery of nanomaterials. *Biomaterials*, 35(23), pp.6026–6036.

Kim, J.W. & Cochran, J.R., 2017. Targeting ligand–receptor interactions for development of cancer therapeutics. *Current Opinion in Chemical Biology*, 38, pp.62–69.

Kim, R.B., 2002. Drugs as P-glycoprotein substrates, inhibitors, and inducers. *Drug Metabolism Reviews*, 34(1–2), pp.47–54.

Kim, S.K. et al., 2010. Infrared vibrational spectra as a structural probe of gaseous ions formed by caffeine and theophylline. *Physical Chemistry Chemical Physics*.

Kiss, T. et al., 2010. Evaluation of the cytotoxicity of β-cyclodextrin derivatives: Evidence for the role of cholesterol extraction. *European Journal of Pharmaceutical Sciences*, 40(4), pp.376–380.

Kocyła, A., Pomorski, A. & Krężel, A., 2015. Molar absorption coefficients and stability constants of metal complexes of 4-(2-pyridylazo)resorcinol (PAR): Revisiting common chelating probe for the study of metalloproteins. *Journal of Inorganic Biochemistry*,

152(May), pp.82–92.

Konášová, R., Dytrtová, J.J. & Kašička, V., 2016. Study of solvent effects on the stability constant and ionic mobility of the dibenzo-18-crown-6 complex with potassium ion by affinity capillary electrophoresis. *Journal of Separation Science*, 39(22), pp.4429–4438.

Korytkowska-Wałach, A. et al., 2017. Spectroscopic study on the inclusion complexes of β-cyclodextrin with selected metabolites of catecholamines. *Journal of Molecular Structure*, 1127, pp.532–538.

Kumar, B. et al., 2017. Recent advances in nanoparticle-mediated drug delivery. *Journal of Drug Delivery Science and Technology*, 41, pp.260–268.

Kumar, S. & Nussinov, R., 2002. Relationship between ion pair geometries and electrostatic strengths in proteins. *Biophysical Journal*, 83(3), pp.1595–1612.

Kundu, M., Saha, S. & Roy, M.N., 2017. Evidences for complexations of β-cyclodextrin with some amino acids by 1H NMR, surface tension, volumetric investigations and XRD. *Journal of Molecular Liquids*, 240, pp.570–577.

Kustin, B.K., Wolff, M.A. & Dalton, J.C.S., 1971. Complexes of the Nickel (II) Ion with Purine Bases : Relaxation Spectra with Theophylline. *Journal of Physical Chemistry*, pp.1971–1974.

Labiris, N.R. & Dolovich, M.B., 2003. Pulmonary drug delivery . Part I : Physiological factors affecting therapeutic effectiveness of aerosolized medications. *British Journal of Clinical Pharmacology*, 56, pp.588–599.

Li, W. et al., 2007. Effect of Water and Organic Solvents on the Ionic Dissociation of Ionic Liquids. *The Journal of Physical Chemistry B*, 111(23), pp.6452–6456.

Li, Z. et al., 2017. Cell-borne 2D nanomaterials for efficient cancer targeting and photothermal therapy. *Biomaterials*, 133, pp.37–48.

Lipinski, C.A. et al., 1997. Experimental and Computational Approaches to Estimate Solubility and Permeability in Drug Discovery and Develop ment Settings. *Advanced Drug Delivery Reviews*, 23, pp.3–25.

Liu, Q. et al., 2017. Targeted drug delivery to melanoma. *Advanced Drug Delivery Reviews*.

Liu, X., Testa, B. & Fahr, A., 2011. Lipophilicity and its relationship with passive drug permeation. *Pharmaceutical Research*, 28(5), pp.962–977.

Loftsson, T., Matthíasson, K. & Másson, M., 2003. The effects of organic salts on the cyclodextrin solubilization of drugs. *Journal of Drug Delivery and Science Technology*, 262(1–2), pp.101–107.

Longmire, M., Choyke, P.L. & Kobayashi, H., 2008. Clearance properties of nano-sized particles and molecules as imagin agents: consideration and caveats. *Nanomedicine*

(Lond), 3(5), pp.703–717.

Luk, B.T. & Zhang, L., 2015. Cell membrane-camouflaged nanoparticles for drug delivery. *Journal of Controlled Release*, 220, pp.600–607.

Malamatari, M. et al., 2016. Preparation of theophylline inhalable microcomposite particles by wet milling and spray drying : The in fl uence of mannitol as a co-milling agent. *International Journal of Pharmaceutics*, 514(1), pp.200–211.

Malathi, R., 2012. Spectral Analysis of Naturally Occurring Methylxanthines (Theophylline , Theobromine and Caffeine) Binding with DNA. *Plos One*, 7(12).

Marcus, Y. & Hefter, G., 2006. Ion pairing. *Chemical Reviews*, 106(11), pp.4585–4621.

Masoudipour, E., Kashanian, S. & Maleki, N., 2017. A targeted drug delivery system based on dopamine functionalized nano graphene oxide. *Chemical Physics Letters*, 668, pp.56–63.

Matilainen, L. et al., 2008. In vitro toxicity and permeation of cyclodextrins in Calu-3 cells. *Journal of Controlled Release*, 126(1), pp.10–16.

Miller-Fleming, L. et al., 2015. Remaining Mysteries of Molecular Biology: The Role of Polyamines in the Cell. *Journal of Molecular Biology*, 427(21), pp.3389–3406.

Miller, J.M. et al., 2010. Enabling the intestinal absorption of highly polar antiviral agents: Ion-pair facilitated membrane permeation of zanamivir heptyl ester and guanidino oseltamivir. *Molecular Pharmaceutics*, 7(4), pp.1223–1234.

Minois, N., Carmona-gutierrez, D. & Madeo, F., 2011. Polyamines in aging and disease. *Aging*, 3(8), pp.1–17.

Mobaraki, N. & Hemmateenejad, B., 2011. Chemometrics and Intelligent Laboratory Systems Structural characterization of carbonyl compounds by IR spectroscopy and chemometrics data analysis. *Chemometrics and Intelligent Laboratory Systems*, 109(2), pp.171–177.

Mu, C.-F. et al., 2018. Targeted drug delivery for tumor therapy inside the bone marrow. *Biomaterials*, 155, pp.191–202.

Muth, A. et al., 2013. Development of polyamine transport ligands with improved metabolic stability and selectivity against specific human cancers. *Journal of Medicinal Chemistry*, 56(14), pp.5819–5828.

Nafisi, S. et al., 2012. Interaction of Metal Ions with Caffeine and Theophylline : Stability and Structural Features Interaction of Metal Ions with Caffeine and Theophylline : Stability and Structural Features. *Journal of Biomolecular Structure and Dynamics*, 1102(August).

Nakura, H. et al., 1998. Comparative Study with Sprague-Dawley Rats and a Mutant

Sprague-Dawley Hyperlipidemic Strain with Hypoalbuminemia ABSTRACT : *Drug Metabolism and Disposition*, 26(6), pp.595–597.

Nam, S.H. et al., 2011. Ion pairs of risedronate for transdermal delivery and enhanced permeation rate on hairless mouse skin. *International Journal of Pharmaceutics*, 419(1–2), pp.114–120.

Northfelt, D.W. et al., 1996. Doxorubicin Encapsulated in Liposomes Containing Surface-Bound Polyethylene Glycol: Pharmacokinetics, Tumor Localization, and Safety in Patients with AIDS-Related Kaposi's Sarcoma. *The Journal of Clinical Pharmacology*, 36(1), pp.55–63.

Palmer, A.J. & Wallace, H.M., 2010. The polyamine transport system as a target for anticancer drug development. *Amino Acids*, 38(2), pp.415–422.

Papa, A.-L. et al., 2017. Ultrasound-sensitive nanoparticle aggregates for targeted drug delivery. *Biomaterials*, 139, pp.187–194.

Paranjpe, M. & Müller-Goymann, C.C., 2014. Nanoparticle-mediated pulmonary drug delivery: A review. *International Journal of Molecular Sciences*, 15(4), pp.5852–5873.

Patel, A. et al., 2016. Using Salt Counterions to Modify β2-Agonist Behavior in Vivo. *Molecular Pharmaceutics*, 13(10), pp.3439–3448.

Peng, X.X. et al., 2012. Overexpression of P-glycoprotein induces acquired resistance to imatinib in chronic myelogenous leukemia cells. *Chinese Journal of Cancer*, 31(2), pp.110–118.

Pey, A.L., 2014. PH-dependent relationship between thermodynamic and kinetic stability in the denaturation of human phosphoglycerate kinase 1. *Biochimie*, 103(1), pp.7–15.

Potter, M.J., Gilson, M.K. & Mccammont, J.A., 1994. Small Molecule pKa Prediction with Continuum Electrostatics Calculations Michael. *Journal of American Society*, 111(12), pp.10298–10299.

Poulin, R., Casero, R.A. & Soulet, D., 2012. Recent advances in the molecular biology of metazoan polyamine transport. *Amino Acids*, 42(2–3), pp.711–723.

Powell, J.R. et al., 1978. Theophylline Disposition in Acutely III Hospitalized Patients. *American Review of Respiratory Disease*, 118, pp.229–238.

Puri, A. et al., 2009. Lipid-based nanoparticles as pharmaceutical drug carriers: from concepts to clinic. *Critical reviews in therapeutic drug carrier systems*, 26(6), pp.523–80.

Qie, Y. et al., 2016. Surface modification of nanoparticles enables selective evasion of phagocytic clearance by distinct macrophage phenotypes. *Scientific Reports*, 6(January), pp.1–11.

Rajan, V.K. & Muraleedharan, K., 2017. International Journal of Greenhouse Gas Control

The pKa values of amine based solvents for CO 2 capture and its temperature dependence — An analysis by density functional theory. *International Journal of Greenhouse Gas Control*, 58, pp.62–70.

Rautio, J. et al., 2008. Prodrugs: Design and clinical applications. *Nature Reviews Drug Discovery*, 7(3), pp.255–270.

Rautio, J., Kärkkäinen, J. & Sloan, K.B., 2017. Prodrugs – Recent approvals and a glimpse of the pipeline. *European Journal of Pharmaceutical Sciences*, 109(May), pp.146–161.

Ross, P.D. & Rekharsky, M. V., 1996. Thermodynamics of hydrogen bond and hydrophobic interactions in cyclodextrin complexes. *Biophysical Journal*, 71(4), pp.2144–2154.

Roy, M.N. et al., 2016. Exploration of inclusion complexes of neurotransmitters with β-cyclodextrin by physicochemical techniques. *Chemical Physics Letters*, 655–656, pp.43–50.

Sahin-Yilmaz, A. & Naclerio, R.M., 2011. Anatomy and Physiology of the Upper Airway. *Proceedings of the American Thoracic Society*, 8(1), pp.31–39.

Sala-Rabanal, M., et al., 2013. Polyamine Transport by the Polyspecific Organic Cation Transporters OCT1, OCT2 and OCT3. *Molecular Pharmaceutics*, 10(4), pp.1450–1458.

Samiei, N. et al., 2017. An investigation into the ability of alendronate ion pairs to increase oral absorption. *International Journal of Pharmaceutics*, 527(1–2), pp.184–190.

Samiei, N. et al., 2014. European Journal of Pharmaceutical Sciences Enhancement and in vitro evaluation of amifostine permeation through artificial membrane (PAMPA) via ion pairing approach and mechanistic selection of its optimal counter ion. *European Journal of Pharmaceutical Sciences*, 51, pp.218–223.

Saunders, N.A., Ilett, K.F. & Minchin, A.N.D.R.F., 1989. Pulmonary Alveolar Macrophages Express a Pol yamine Transport System. *Journal of Cellular Physiology*, 631.

Scott, D.O. et al., 2017. Passive drug permeation through membranes and cellular distribution. *Pharmacological Research*, 117, pp.94–102.

Sercombe, L. et al., 2015. Advances and challenges of liposome assisted drug delivery. *Frontiers in Pharmacology*, 6(DEC), pp.1–13.

Shan, S. -o. & Herschlag, D., 1996. The change in hydrogen bond strength accompanying charge rearrangement: Implications for enzymatic catalysis. *Proceedings of the National Academy of Sciences*, 93(25), pp.14474–14479.

Sharmin, S. et al., 2001. Polyamine cytotoxicity in the presence of bovine serum amine oxidase. *Biochemical and Biophysical Research Communications*, 282(1), pp.228–235.

Singh, R. & W., L.J., 2009. Nanoparticle-based targeted drug delivery. *Experimental Molecular Phatology*, 86(3), pp.215–223.

Singh, V.B., 2015. RSC Advances Spectroscopic signatures and structural motifs in isolated and hydrated theophylline : a computational study. *RSC Advances*, 5, pp.11433–11444.

Smith, L.L. et al., 1990. The Importance of Epithelial Uptake Systems in Lung Toxicity. *Environmental Health Perspcectives*, 85(4), pp.25–30.

Song, I.S. et al., 2013. Transport of organic cationic drugs: Effect of ion-pair formation with bile salts on the biliary excretion and pharmacokinetics. *Pharmacology and Therapeutics*, 138(1), pp.142–154.

Stella, V.J. & He, Q., 2008. Cyclodextrins. *Toxicologic Pathology*, 36(1), pp.30–42.

Stone, K.C. et al., 1992. Allometric relationships of cell numbers and size in the mammalian lung. *American journal of respiratory cell and molecular biology*, 6(2), pp.235–243.

Stuart, B.O., 1976. Deposition and clearance of inhaled particles. *Environmental Health Perspectives*, 16(January), pp.41–53.

Sturm, R. et al., 2002. Particle clearance in human bronchial airways: Comparison of stochastic model predictions with experimental data. *Annals of Occupational Hygiene*, 46(December), pp.329–333.

Sugano, K. et al., 2010. Coexistence of passive and carrier-mediated processes in drug transport. *Nature reviews. Drug discovery*, 9(8), pp.597–614.

Suydam, F., 1963. The C = N Stretching Frequency in Azomethines. *Analytical Chemistry*, 35(2), pp.193–195.

Sykes, E.A. et al., 2014. Investigating the impact of nanoparticle size on active and passive tumor targeting efficiency. *ACS Nano*, 8(6), pp.5696–5706.

Szczepanowicz, K. et al., 2016. Pegylated polyelectrolyte nanoparticles containing paclitaxel as a promising candidate for drug carriers for passive targeting. *Colloids and Surfaces B: Biointerfaces*, 143, pp.463–471.

Szejtli, J., 1998. Introduction and General Overview of Cyclodextrin Chemistry. *Chemical Reviews*, 98(5), pp.1743–1754.

Takjoo, R. & Magué, J.T., 2017. Effect of solvents in mixed-ligand supramolecular self-assembly architectures. *Polyhedron*, 134, pp.41–49.

Tantishaiyakul, V., Phadoongsombut, N. & Wongpuwarak, W., 2004. ATR-FTIR characterization of transport properties of benzoic acid ion-pairs in silicone membranes. *International Journal of Pharmaceutics*, 283, pp.111–116.

Taulier, N. & Chalikian, T. V., 2006. Hydrophobic hydration in cyclodextrin complexation. *Journal of Physical Chemistry B*, 110(25), pp.12222–12224.

Terekhova, I. V., Volkova, T. V. & Perlovich, G.L., 2007. Interactions of theophylline with cyclodextrins in water. *Mendeleev Communications*, 17(4), pp.244–246.

Thackaberry, E.A. et al., 2014. Solvent-based formulations for intravenous mouse pharmacokinetic studies: tolerability and recommended solvent dose limits. *Xenobiotica*, 44(3), pp.235–241.

Tian, T. et al., 2017. Surface functionalized exosomes as targeted drug delivery vehicles for cerebral ischemia therapy. *Biomaterials*, 150, pp.137–149.

Tomasi, S. et al., 2010. Targeting the polyamine transport system with benzazepine- and azepine-polyamine conjugates. *Journal of Medicinal Chemistry*, 53, pp. 7647-7663.

Turner, B.A., 1948. The Spectrophotometric Determination of the Dissociation Constants of Theophylline, Theobromine and Caffeine. *Journal of American Pharmaceutical Association*, pp.158–161.

Ulloth, J.E. et al., 2007. Characterization of methyl-beta-cyclodextrin toxicity in NGF-differentiated PC12 cell death. *Neurotoxicology*, 28(3), pp.613–21.

Wang, G. & Cole, R.B., 1996. Effects of solvent and counterion on ion pairing and observed charge states of diquaternary ammonium salts in electrospray ionization mass spectrometry. *Journal of the American Society for Mass Spectrometry*, 7(10), pp.1050–1058.

Wang, C.J. et al., 2003. Defining the molecular requirements for the selective delivery of polyamine conjugates into cells containing active polyamine transporters. *Journal of Medicinal Chemistry*, 24, 5129-5138.

Wang, H. et al., 2017. Facile encapsulation of hydroxycamptothecin nanocrystals into zein-based nanocomplexes for active targeting in drug delivery and cell imaging. *Acta Biomaterialia*, 61, pp.88–100.

Wang, M. et al., 2008. Effect of ion-pairing and enhancers on scutellarin skin permeability. *Journal of Pharmacy and Pharmacology*, pp.429–435.

Wang, W. et al., 2017. Investigate the control release effect of ion-pair in the development of escitalopram transdermal patch using FT-IR spectroscopy , molecular modeling and thermal analysis. *International Journal of Pharmaceutics*, 529(1–2), pp.391–400.

Wang, Z. et al., 2017. Mechanisms of drug release in pH-sensitive micelles for tumour targeted drug delivery system: A review. *International Journal of Pharmaceutics*, 535(1–2), pp.253–260.

Wei, Y. et al., 2017. Characterization of glabridin/hydroxypropyl-ß-cyclodextrin inclusion complex with robust solubility and enhanced bioactivity. *Carbohydrate Polymers*, 159, pp.152–160.

Weiss-Errico, M.J. & O'Shea, K.E., 2017. Detailed NMR investigation of cyclodextrin-perfluorinated surfactant interactions in aqueous media. *Journal of Hazardous Materials*, 329, pp.57–65.

Wilczewska, A.Z. et al., 2012. Nanoparticles as drug delivery systems. *Pharmacological Reports*, 64(5), pp.1020–1037.

Wouessidjewe, D., Ponchel, G. & Duchene, D., 1999. Cyclodextrins and carrier systems. *Journal of Controlled Release*, 62, pp.263–268.

Wu, K.M., 2009. A new classification of prodrugs: Regulatory perspectives. *Pharmaceuticals*, 2(3), pp.77–81.

Xu, L. et al., 2014. Enhanced activity of doxorubicin in drug resistant A549 tumor cells by encapsulation of P-glycoprotein inhibitor in PLGA-based nanovectors. *Oncology Letters*, 7(2), pp.387–392.

Xue, Y., Traina, S.J. & Hille, R., 1996. Stability of metal-organic complexes in acetone- and methanol-water mixtures. *Environmental Science and Technology*, 30(11), pp.3177–3183.

Yang, L. et al., 2017. Luminescence of Au(I)-thiolate complex affected by solvent. *Radiation Physics and Chemistry*, 137, pp.68–71.

Yin, F. et al., 2017. Functionalized 2D nanomaterials for gene delivery applications. *Coordination Chemistry Reviews*, 347, pp.77–97.

Young, B.K., 1981. Stabilityof Theophylilne In Serum , Influenceof Bilirubinon Determinationof Angiotensln- ConvertIngEnzyme. *Clinical Chemistry*, 27(12), pp.2071–2072.

Zawilska, J.B., Wojcieszak, J. & Olejniczak, A.B., 2013. Prodrugs: A challenge for the drug development. *Pharmacological Reports*, 65(1), pp.1–14.

Zhang, X. et al., 2017. Prodrug strategy for cancer cell-specific targeting: A recent overview. *European Journal of Medicinal Chemistry*, 139, pp.542–563.

Zhao, H. et al., 2017. Mechanism study on ion-pair complexes controlling skin permeability : Effect of ion-pair dissociation in the viable epidermis on transdermal permeation of bisoprolol. *International Journal of Pharmaceutics*, 532(1), pp.29–36.

Zhao, J., Ren, K. & Tang, J., 2014. Overcoming 5-Fu resistance in human non-small cell lung cancer cells by the combination of 5-Fu and cisplatin through the inhibition of glucose metabolism. *Tumor Biology*, 35(12), pp.12305–12315.